HIGHWAY RESEARCH BOARD

Bulletin 307

Prestressed Concrete Structures

Creep, Shrinkage, Deflection Studies

1961

National Academy of Sciences—
National Research Council

publication 937

HIGHWAY RESEARCH BOARD

Officers and Members of the Executive Committee

1961

OFFICERS

W. A. BUGGE, *Chairman* R. R. BARTLESMEYER, *First Vice Chairman*

C. D. CURTISS, *Second Vice Chairman*

FRED BURGGRAF, *Director* ELMER M. WARD, *Assistant Director*

Executive Committee

REX M. WHITTON, *Federal Highway Administrator, Bureau of Public Roads* (ex officio)

A. E. JOHNSON, *Executive Secretary, American Association of State Highway Officials* (ex officio)

LOUIS JORDAN, *Executive Secretary, Division of Engineering and Industrial Research, National Research Council* (ex officio)

HARMER E. DAVIS, *Director, Institute of Transportation and Traffic Engineering, University of California* (ex officio, Past Chairman 1959)

PYKE JOHNSON, *Consultant, Automotive Safety Foundation* (ex officio, Past Chairman 1960)

R. R. BARTELSMEYER, *Chief Highway Engineer, Illinois Division of Highways*

E. W. BAUMAN, *Director, National Slag Association, Washington, D. C.*

W. A. BUGGE, *Director of Highways, Washington State Highway Commission*

MASON A. BUTCHER, *County Manager, Montgomery County, Md.*

C. D. CURTISS, *Special Assistant to the Executive Vice President, American Road Builders' Association*

DUKE W. DUNBAR, *Attorney General of Colorado*

H. S. FAIRBANK, *Consultant, Baltimore, Md.*

MICHAEL FERENCE, JR., *Executive Director, Scientific Laboratory, Ford Motor Company.*

D. C. GREER, *State Highway Engineer, Texas State Highway Department.*

BURTON W. MARSH, *Director, Traffic Engineering and Safety Department, American Automobile Association*

J. B. MCMORRAN, *Superintendent of Public Works, New York State Department of Public Works, Albany*

CLIFFORD F. RASSWEILER, *Vice-President, Johns-Manville Corp., New York, N. Y.*

GLENN C. RICHARDS, *Commissioner, Detroit Department of Public Works*

C. H. SCHOLER, *Applied Mechanics Department, Kansas State University*

WILBUR S. SMITH, *Wilbur Smith and Associates, New Haven, Conn.*

K. B. WOODS, *Head, School of Civil Engineering, and Director, Joint Highway Research Project, Purdue University*

Editorial Staff

FRED BURGGRAF ELMER M. WARD HERBERT P. ORLAND

2101 Constitution Avenue Washington 25, D. C.

HIGHWAY RESEARCH BOARD

Bulletin 307

Prestressed Concrete Structures

Creep, Shrinkage, Deflection Studies

1961

Presented at the
40th ANNUAL MEETING
January 9-13, 1961

National Academy of Sciences —
National Research Council
Washington, D.C.
1962

Department of Design

T. E. Shelburne, Chairman
Director of Research, Virginia Department of Highways
University of Virginia, Charlottesville

COMMITTEE ON BRIDGES

G. S. Paxson, Chairman
Assistant State Highway Engineer
Oregon State Highway Commission, Salem

Raymond Archibald, State Bridge Engineer, Alaska Division of Highways, Juneau

J. N. Clary, Engineer of Bridges, Virginia Department of Highways, Richmond

E. M. Cummings, Manager of Sales, Bethlehem Steel Company, Bethlehem, Pennsylvania

Frederick H. Dill, Assistant to Vice-President, Engineering, American Bridge Division, United States Steel Corporation, Pittsburgh, Penn.

Arthur L. Elliott, Bridge Engineer Planning, California Division of Highways, Sacramento

Eric L. Erickson, Chief, Bridge Division, Office of Engineering, Bureau of Public Roads, Washington, D. C.

R. S. Fountain, Bridge Engineer, Portland Cement Association, Chicago, Illinois

F. M. Fuller, Assistant Vice-President, Raymond International, Inc., New York, N. Y.

H. deR. Gibbons, The Union Metal Manufacturing Company, Canton, Ohio

John J. Hogan, Consulting Structural Engineer, Portland Cement Association, New York, N. Y.

W. T. Lankford, Applied Research Laboratory, Unites States Steel Corporation, Monroeville, Pennsylvania

Adrian Pauw, Professor of Civil Engineering, University of Missouri, Columbia

M. N. Quade, Consulting Engineer, Parsons, Brinckerhoff, Quade & Douglas, New York, N. Y.

William H. Rabe, Columbus, Ohio

C. P. Siess, Department of Civil Engineering, University of Illinois, Urbana

Charles B. Trueblood, Armco Drainage and Metal Products, Inc., Middletown, Ohio

Contents

Time-Dependent Deflections of Prestressed Concrete Beams

W. G. CORLEY, M. A. SOZEN, and C. P. SIESS, respectively, Graduate Assistant, Associate Professor, and Professor, Department of Civil Engineering, University of Illinois, Urbana

Two procedures, the "rate-of-creep" and the "superpositon" methods, are used for computing creep of concrete under variable stress from known relations for creep under constant stress and routine numerical procedures are presented for these methods.

These numerical methods are applied to two series of sustained load tests on prestressed concrete beams carried out under laboratory conditions. Measured deflections are compared with computed deflections and found to be in good agreement. The rate-of-creep method is then applied to a full size bridge beam and measured and computed deflections are again compared.

In the final section, the methods presented in the first part of the paper are used to investigate the possible ranges of time deflections in five representative composite highway bridges. A procedure is outlined for investigating the time-dependent deflections of prestressed concrete beams.

●ALL MATERIALS deform with time, although at different rates. The time-dependent deformation of concrete, which is ascribed classically to two different phenomena, creep and shrinkage, is such that the resulting dimensional changes within the life span of a structural member are usually appreciable. Consequently, prestressed concrete members undergo time-dependent deformations primarily as a result of the dimensional instability of the concrete. In addition, the relaxation of the prestressing reinforcement, the time-dependent loss of stress at constant strain which occurs when steel is subjected to a high sustained stress, results as an "elastic" change in the deformation.

Both practical experience and laboratory experiments have shown the need for being able to predict the time-dependent deformations of prestressed concrete members. Creep and shrinkage of the concrete combined with relaxation of the reinforcement cause loss of prestress, deflection of flexural members, and secondary stresses in continuous structures; and none of these can be ignored completely. In the early phases of the development of prestressed concrete as a building material, much emphasis was placed on the time-dependent loss of prestress which was considered to be the Achilles' Heel of prestressed concrete. The availability of high strength steel and the development of a better understanding of the behavior of prestressed reinforced concrete has put this problem in its proper perspective; partial loss of prestress is not necessarily accompanied by a loss in flexural strength, although the cracking moment may be reduced. More recently, interest in time-dependent effects has shifted towards the analysis of the deflections of flexural members, a consideration which has little to do with strength but which is frequently critical for serviceability.

A loaded prestressed concrete beam deflects with time under the influence of two effects: the nearly constant stresses caused by the load which tend to make it deflect in one direction, and the changing stresses caused by the prestress which tend to make it deflect in the other direction. By judicious design, these two opposing effects may be used by the engineer in such a manner that they offset each other. The primary

objective of this paper is to present methods for the computation of time-dependent deflections so that the designer may use this concept to control such deflections, or, at least, to obtain a reasonable estimate of the maximum deflection.

No pretensions are made in the paper regarding the precise prediction of the qualitative or quantitative characteristics of creep, shrinkage, or relaxation as a function of time. In the analyses presented, these are assumed to be known. Because the sensitivity of these relationships, especially for creep and shrinkage, to various factors which are practically uncontrollable in engineering works is well-known, the adoption or admission of any expression giving the magnitude of creep and shrinkage would curtail unnecessarily the applicability of the analyses. Therefore, it is strongly recommended that, whenever the basic creep shrinkage and relaxation versus time relationships are not established under conditions similar to those imposed on the structure in question, deflections be computed for the possible upper and lower bounds of these relationships.

The stresses in prestressed concrete beams vary with time inasmuch as the prestress varies. Consequently, a knowledge of the relationship between creep strain and time under constant stress is not sufficient for the analysis of time-dependent deflections of prestressed concrete beams. It is necessary to know this relationship for varying stress. Because it is not practical to obtain creep strain relationships under every possible rate of varying stress, a hurdle in the analysis is the construction of a creep strain curve for a given "program" of stress variation from a creep strain curve obtained under constant stress. Two methods can be used to accomplish this, the "rate-of-creep" and the "superposition" methods. The first part of this paper is devoted essentially to a discussion of the relative merits of these two methods in view of the results of laboratory tests on beams under sustained load in a controlled environment. In addition, the applicability of the commonly used "reduced modulus" method is also considered, not because the writers feel it has possibilities but because of its time-honored place among methods of analysis for time-dependent deflections of reinforced concrete members. (These methods are described in this paper primarily from the point of view of their application in the analysis of deflections of prestressed beams. Ross (1) gives an excellent general discussion of these methods.)

A study of time-dependent deflections measured in eight laboratory tests on beams and in one highway bridge under actual working conditions constitutes the second part of the paper.

To give the reader some "feel" for the magitude of time-dependent deflections to be expected in highway bridges, and also to outline a routine method of analysis, deflections for a group of representative composite highway bridge girders are studied in the final part of the paper.

ANALYSIS

General Remarks

Time-dependent deformations in prestressed concrete are attributed to creep and shrinkage of the concrete and relaxation of the steel. Each of these is a function of numerous other effects. Creep and shrinkage are affected by almost every variable involved in the fabrication and loading of a member. In addition, exposure to different atmospheric conditions results in different rates and magnitudes of time-dependent deformations in the concrete. Relaxation of the steel may be affected by the composition of the steel and the manufacturing process as well as by the loading conditions.

In general, creep of the concrete is the predominant variable insofar as time-dependent deformations of prestressed concrete beams are concerned. It has been observed generally that creep strain is approximately proportional to stress for stresses up to about 50 percent of the concrete strength. Assuming that this relationship holds, time deformations of a member under a given constant stress can be computed by proportions if the time deformation relationship is known for a member under a different constant stress. In prestressed concrete members, the concrete stresses are varying continuously with time; consequently, the problem becomes more complicated. If the relation for creep strain versus time has not been determined for similarly vary-

ing conditions of stress, time deformations of a prestressed concrete member cannot be found by simple proportion but must be modified to take into account the variation of stress.

In the following paragraphs, three methods of computing time deformations are discussed. Two of the procedures, the "rate-of-creep" and the "superposition" methods, use a known relationship between creep strain and time at constant stress to predict the relationship under varying stress. The third method, the "reduced modulus" method, involves simply a reduction of the value of modulus of elasticity for the concrete.

Each of the three methods of analysis has advantages over the others under certain conditions. The reduced modulus method is often applied to reinforced concrete. If the stresses remain nearly constant, this method is a convenient one-step procedure for computing deformations. Because there are often large stress changes in prestressed concrete members, however, a one-step method is not reliable for computing time-dependent deformations, and either the "rate-of-creep" method or the "superposition" method should be used.

Reduced Modulus Method

This method uses a reduced modulus of elasticity for predicting creep strains in members. In order for it to be applicable, it is necessary that the creep strain versus time relationship for the concrete be obtained for the same variation of stresses as that which occurs in the member. If this is done, the reduced modulus method provides a convenient one-step method of predicting deformations. The reduced modulus is defined as:

$$E' = \frac{1}{\epsilon + c} \qquad (1)$$

in which

E' = reduced modulus of elasticity of the concrete;
ϵ = instantaneous strain of concrete under 1.0 psi stress; and
c = unit creep (creep strain per unit stress) at the time when strain is computed.

Once the reduced modulus has been determined, deformations are computed by ordinary methods.

The major disadvantage of this method lies in determining the proper relationship between strain and time. Even if the stress variation in a given member could be predetermined, the evaluation of the correct reduced modulus would involve a special test. Consequently the reduced modulus method is not convenient for predicting time-dependent deformations in prestressed concrete.

The Rate-of-Creep Method

The rate-of-creep method takes into account the fact that concrete stresses in a prestressed concrete member change with time. The relationship between creep strain and time is expressed as follows:

$$\frac{dC}{dt} = f_c \frac{dc}{dt} \qquad (2)$$

The total creep is then given by the expression:

$$C = \int_{t_1}^{t_2} f_c \frac{dc}{dt}\, dt \qquad (3)$$

in which

C = total creep strain between times t_1 and t_2;
c = unit creep strain (creep strain per unit stress), a function of time; and
f_c = concrete stress, a function of time.

Although this method does take into account changing stress, it does not consider the entire stress history of the member. Eq. 2 states that the concrete will creep at the same rate dc/dt regardless of whether stresses are increasing or decreasing. McHenry (2) found that changes in applied stress cause changes in the rate of creep which are not proportional to the change in stress. His findings indicated that if stresses are increased the unit rate of creep is increased, and if stresses are decreased the unit rate of creep decreases. For this reason the rate-of-creep method results in an overestimation of creep strains where concrete stresses are decreasing and an underestimation of creep strain where concrete stresses are increasing.

Although the rate-of-creep method can be expressed by Eq. 2, the solution of this equation is accomplished with ease only in the simplest problems. For this reason, it is convenient to use a numerical integration for the solution of most problems encountered in engineering. A simple numerical integration method for the analysis of beam deflections can be developed with the following assumptions:

1. The initial stress conditions are known for the member considered.
2. The unit creep (strain per unit stress) versus time relationship for constant stress is known and may be considered as a step function. (A step function is defined as a function which is represented graphically by a set of horizontal line segments with abrupt rise or fall from one segment to the next.)
3. The shrinkage strain versus time relationship is known for each fiber of the beams and may be considered as a step function.
4. The relaxation versus time relationship is known and may be considered as a step function.
5. Creep strain is proportional to stress up to a stress of 50 percent of the concrete strength.
6. Strains are linearly distributed over the depth of the cross-section.
7. Concrete has a linear stress-strain relationship up to 50 percent of the concrete strength under short-time loading.
8. Steel has a linear stress-strain relationship under short-time loading.

With these assumptions, the time-dependent deflection of a simply-supported prestressed beam can be computed in the following steps:

1. The gross increase in creep strain in the extreme fibers is computed by multiplying the stress in each fiber at the beginning of the time interval considered by the increment of unit creep strain for that interval.
2. The change in creep strain at the level of the steel is found on the basis of the assumption that strains are linearly distributed over the depth of the cross-section.
3. The total change in strain at the level of the steel is found by adding the creep strain (step 2) to the shrinkage strain increment for the corresponding time interval.
4. The loss in steel stress caused by creep and shrinkage is determined by multiplying the change in strain at the level of the steel (step 3) by the modulus of elasticity of the steel.
5. The total loss in steel stress for the interval considered is found by adding the loss due to creep and shrinkage (step 4) to the relaxation loss for the corresponding time interval.
6. The change in stress in the extreme fibers is found by considering the loss of steel stress as a load applied at the center of gravity of the steel and computing the corresponding "elastic" change in stress in the extreme fibers.
7. The "elastic" change in strain in the extreme fibers is computed by dividing the change in stress (step 6) by the "instantaneous modulus" of the concrete.
8. The net change in strain in the extreme fibers is found by finding the algebraic difference between the gross change in strain found in step 1 and the "elastic" change in strain found in step 7.
9. The stress in the extreme fibers at the end of the time interval is determined by finding the algebraic difference between the initial stress and the change in stress found in step 6.

Once the strain versus time relationship has been determined for a given member,

curvatures can be computed and deflections found from the distribution of curvature along the span. Because most structures experience deformations from causes which can be separated conveniently, deformations can be computed for fictitious beams subjected to the separate stresses and the resulting deflections added algebraically. For example, in a highway bridge beam, separate calculations of deflections due to prestress, beam dead load, and slab dead load can be made and their results added algebraically at the appropriate times.

Because it is convenient to compute time-dependent deformations caused by "external" effects such as load and prestress separately, it is a simple matter to use different time versus unit creep relationships for loads applied at different times. In this way it is possible to eliminate a portion of the error inherent in this method. If the unit creep curve corresponding to the age at loading is used, a portion of the change in rate of creep caused by the external load is taken into account.

Superposition Method

The superposition method was first applied to time deformations of concrete by McHenry (2). He found that if stresses in concrete are changed, the increase or decrease in stress has the same effect as applying a stress of the same magnitude to an unloaded cylinder. Although it is not possible to express this method with a simple relationship as in the case of the rate-of-creep method, a numerical procedure can be used to superpose the effects of increasing or decreasing stresses.

The superposition method does take into account the entire stress history of the member. Because each incremental change in stress follows a new creep versus time curve, changes in the rate of creep are accounted for. To be able to use the method, it is necessary to know the creep strain versus time relationship measured from the time of application of any large change in stress. For small changes in stress, such as internally caused changes in prestressed concrete members, good results can be obtained by using the creep strain versus time relationship measured from the date of prestressing.

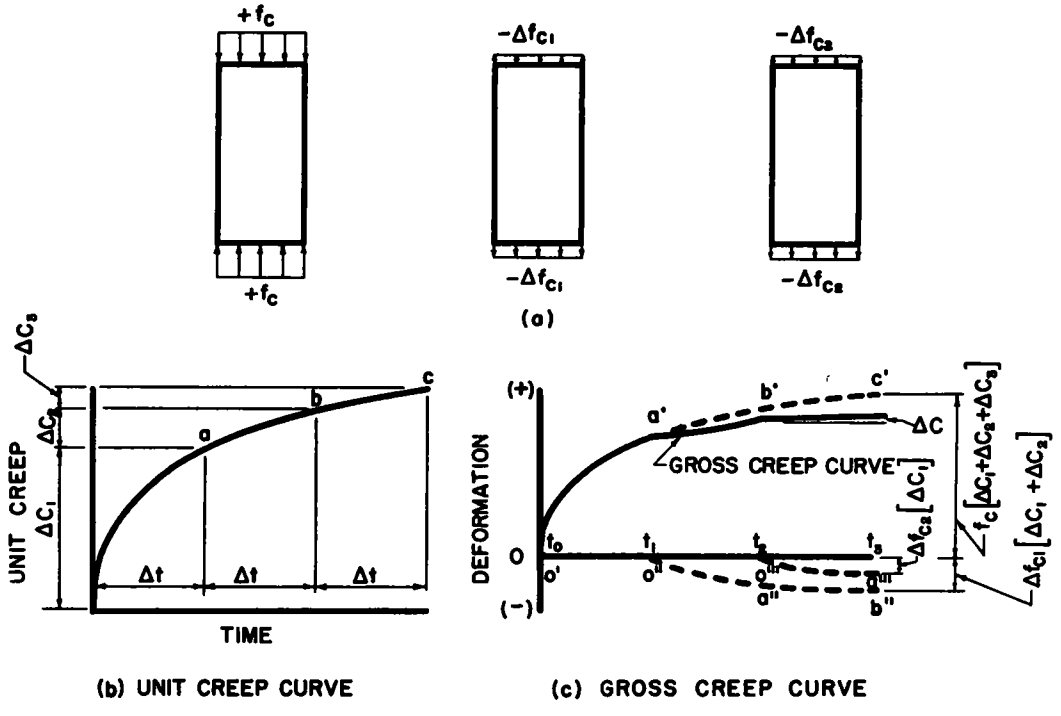

Figure 1. Illustration of gross creep computation by superposition method.

To illustrate the superposition method for computing gross creep, consider a concrete cylinder which has three different stress increments applied as shown in Figure 1(a). Stress $+f_c$ is applied at time t_o and remains on the cylinder, an additional stress, $-\Delta f_{c_1}$ is applied at time t_1, and still another stress $-\Delta f_{c_1}$ is applied at time t_2. The final stress is $[f_c - \Delta f_{c_1} - \Delta f_{c_2}]$. The time intervals t_o to t_1, t_1 to t_2, and t_2 to t_3 are each equal to the interval Δt shown in Figure 1(b). The unit creep curve for the cylinder is shown by line oabc in Figure 1(b).

The gross creep for each stress increment is found by multiplying the ordinates of the unit creep curve by the magnitude of the stress. The gross creep curve for the stress $+f_c$ is represented by line o'a'b'c' in Figure 1(c). At time t_3 the ordinate to this curve is $+f_c [\Delta C_1 + \Delta C_2 + \Delta C_3]$. In a similar manner, the gross creep curves for the stress increments $-\Delta f_{c_1}$ and $-\Delta f_{c_2}$ are shown by lines o" a" b" and o''' a''', respectively, in Figure 1(c). The ordinate to curve o" a" b" at time t_3 is $-\Delta f_{c_1} [\Delta c_1 + \Delta C_2]$ and the ordinate to curve o''' a''' at time t_3 is $-Af_{c_2} [\Delta C_1]$.

The gross creep curve for the total stress on the cylinder at any time is shown by the solid line in Figure 1(c). The ordinates to the gross creep curve are the algebraic sum of the ordinates to curves o' a' b' c', o" a" b", and o''' a'''. From this it can be seen that the gross creep for the cylinder from time t_2 to time t_3 is the difference between the ordinates to the gross creep curve at times t_2 and t_3 and may be expressed by the quantity:

$$\Delta C = f_c (\Delta C_3) - \Delta f_{c_1} (\Delta C_2) - \Delta f_{c_2} (\Delta C_1)$$

The gross creep for other time increments can be computed in a similar manner.

To develop a numerical procedure for the superposition method, it is again necessary to make some assumptions regarding the behavior of the materials involved. The first eight assumptions are identical to those necessary for a solution by the rate-of-creep method. In addition, it is necessary to assume that deformations due to the separate stresses can be superposed and that the shape of the curve for creep strain versus time is known for loads applied at any time and may be considered a step function.

With these assumptions, the numerical procedure for the superposition method involves the following steps:

1. The gross increase in creep strain in the extreme fibers is computed by the method illustrated in Figure 1.
2. The change in creep strain at the level of the steel is found from the assumption that strains are linearly distributed over the depth of the cross-section.
3. The total change in strain at the level of the steel is found by adding the creep strain (step 2) to the shrinkage for the corresponding time interval.
4. The loss in steel stress due to creep and shrinkage is determined by multiplying the change in strain at the level of the steel (step 3) by the modulus of elasticity of the steel.
5. The total loss in steel stress for the interval considered is found by adding the loss due to creep and shrinkage (step 4) to the relaxation loss for the corresponding time interval.
6. The change in stress in the extreme fibers is found by considering the loss of steel stress as a load applied at the center of gravity of the steel and computing the corresponding "elastic" change in stress in the extreme fibers. This change in stress is considered as a newly applied stress in the next cycle of computations.
7. The "elastic" change in strains in the extreme fibers is computed by dividing the changes in stress (step 6) by the "instantaneous modulus" of the the concrete.
8. The net change in strain in the extreme fibers is found by finding the algebraic difference between the gross change in strain found in step 1 and the "elastic" change in strain found in step 7.

Although the assumption that the creep strain versus time curve has the same shape regardless of the time of loading is not correct, the assumption gives good results when the rate of change in stress is small. The method can be improved by determining separate curves for the time of loading corresponding to each change in stress. Be-

cause this involves either questionable assumptions or a great deal of laboratory work, it is practical only on extremely large projects.

Computations of deflections are made in the same manner as described for the rate-of-creep method. Separate computations are made for deflections caused by prestress and by individual externally applied loads. These separate effects are then superposed at the pertinent times and the net deflections obtained.

RESULTS OF TESTS AT THE UNIVERSITY OF ILLINOIS

Description of Specimens

Four prestressed concrete beams were subjected to sustained loads for a period of 2 yr. The beams were 4 by 6 in. in cross-section and had a clear span of 6 ft. Six 0.196-in. diameter prestressing wires were placed in each beam so that the center of gravity of the steel coincided with the kern limit of the cross-section (Fig. 2).

Type III portland cement was used in all specimens. The coarse aggregate had a maximum size of $\frac{3}{8}$ in. and the sand had a fineness modulus of 3.30. Table 1 contains proportions of the mixes, slumps, 7-day compressive strengths, and moduli of elasticity for the concrete in each beam. Compressive strengths are based on 6- by 12-in. control cylinders.

The beams and cylinders were cured in the forms in laboratory air until the concrete had gained sufficient strength to allow release of the prestress wires. The wires were released when the computed bottom fiber stress in the beams was from 50 to 55 percent of the cylinder strength. The variation in concrete strength with time, as obtained

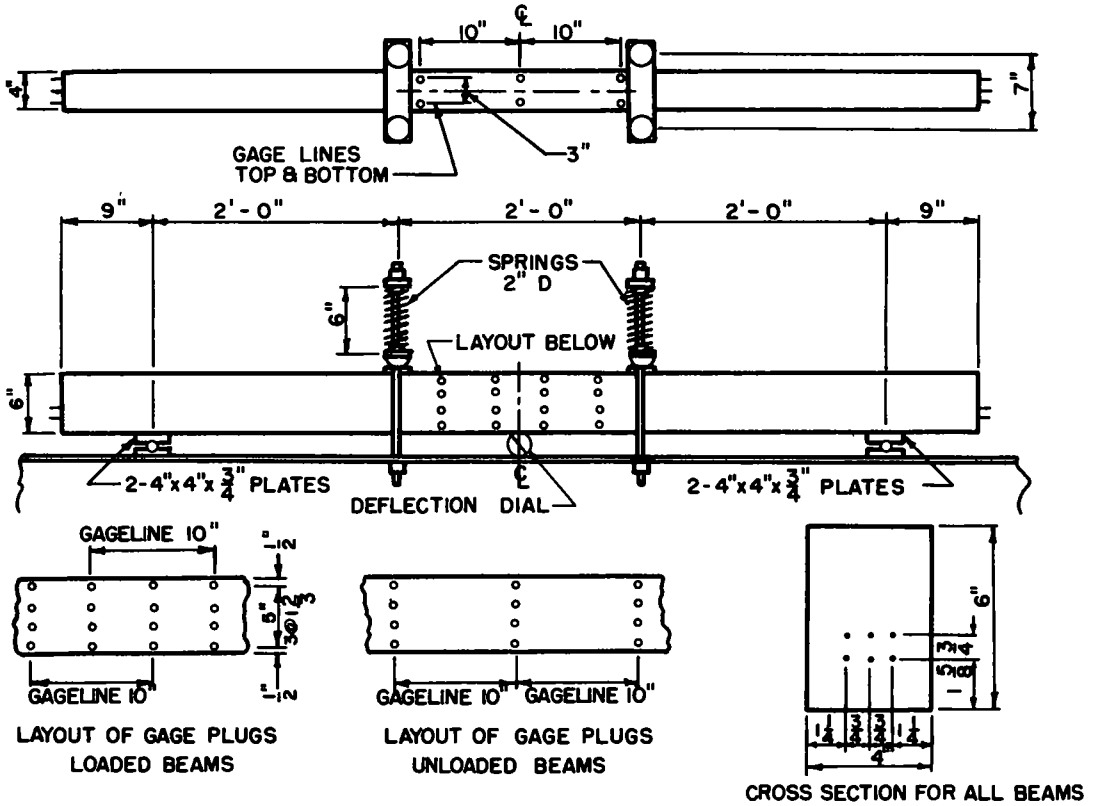

Figure 2. Dimensions and loading arrangement for beams, University of Illinois tests.

TABLE 1

PROPERTIES OF CONCRETE MIXES FOR UNIVERSITY OF ILLINOIS TESTS

Beam	Cement:Sand:Gravel (by wt)	Water:Cement (by wt)	Slump (in.)	7-Day Compressive Strength, f'_c (psi)	Modulus of Elasticity, E_c (psi x 10^6)	Cement Type
MU-1	1:2.98:3.35	0.76	3	4,070	3.08	III
MU-2	1:2.97:3.32	0.74	3	4,300	3.18	III
ML-1	1:2.97:3.36	0.75	2½	4,170	3.08	III
ML-2	1:2.96:3.33	0.80	5	3,500	2.70	III

from compressive tests of ten concrete cylinders over a period of 28 days, is shown in Figure 3. Table 2 gives the chronology of the various operations involved in the preparation of the test specimens.

Two samples of the prestressing wire used in the beams were used to determine the stress-strain curve shown in Figure 4. Two other lengths of the same wire were placed in steel frames at stress levels of approximately 51 to 55 percent of the ultimate strength to determine their relaxation properties (3). Plots of relaxation versus time for the two specimens are shown in Figure 5.

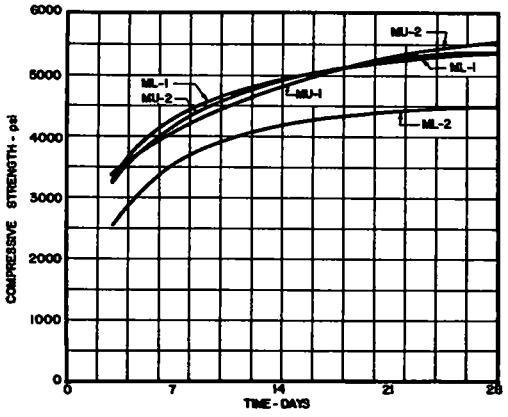

Figure 3. Concrete strength vs time based on 6- by 12-in. cylinders.

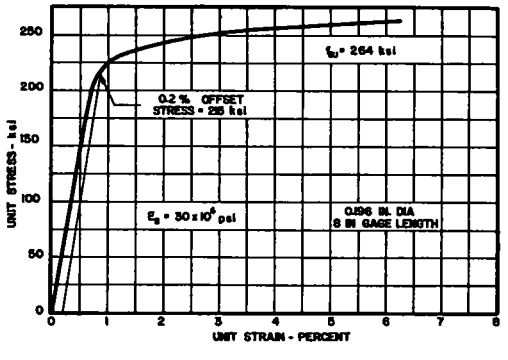

Figure 4. Stress-strain relationship for prestressing wire.

Four 4- by 16-in. control cylinders were also cast for each beam. One of the 4- by 16-in. cylinders from each batch was loaded to a stress of 2,000 psi in the sustained-loading rig shown in Figure 6. This stress was maintained throughout the duration of the beam tests to determine time-dependent strains of the concrete under constant stress. Because 30 to 40 min were required to load the cylinders in the special rigs, companion specimens were loaded rapidly to 2,000 psi in a screw-type testing machine and kept under constant load for one week so that early strain readings of the cylinders in the special testing rigs could be compared with those for the cylinders loaded "instantaneously". No significant difference was found for the two methods of loading. Figure 7 shows the relationship between time and total measured strain for each of the cylinders loaded in the special frames.

The remaining two 4- by 16-in. cylinders cast from each batch were left unloaded in order to measure time-dependent strains under zero applied stress. The time-strain relationship for the unloaded cylinders for each beam is shown in Figure 7.

The four test beams were placed in the special loading frame shown in Figure 8. Two of the beams, MU-1 and MU-2, were placed in the lower berths and had no externally applied loads. These beams were designed for a nominal prestress of 2,000 psi in the bottom fiber and zero in the top fiber. Computed stress distributions based on the measured effective prestress are shown in Figure 9.

TABLE 2

TEST CHRONOLOGY FOR UNIVERSITY OF ILLINOIS TESTS

Beam	Date of Tensioning of Wires	Date of Casting Beams and Cylinders	Date of Release of Prestress in Beam	Beam Installed[a] on Storage Frame	Beam Loaded[a] at Third Points	4 by 16-in.[a] Cylinder Loaded in Testing Machine	Initial[a] Reading on Shrinkage Cylinder	4- by 16-in.[a] Cylinder Loaded in Frame
MU-1	4-11-57	4-12-57	4-17-57	+3.0	-	+44.5	- 4.0	+19.0
MU-2	4-18-57	4-19-57	4-24-57	+3.5	-	- 3.5	+ 6.5	+28.5
ML-1	5-1-57	5-2-57	5-7-57	+3.0	+4.5	- 4.5	+ 7.0	+22.0
ML-2	5-9-57	5-10-57	5-17-57	+5.5	+6.0	- 1.5	+15.0	+14.0

[a] Hours after release of prestress (+).
Hours before release of prestress (-).

Beams ML-1 and ML-2 were placed in the two upper berths of the special frame and were loaded by means of four 2-in. diameter steel springs. Spring deflections were measured with a direct reading compressometer equipped with a 0.001-in. dial indicator. Load was applied by tightening the nuts on ½-in. diameter rods bolted to the frame angles.

Beam ML-1 was designed so that the net stress under load would be 2,000 psi in the top fiber in the middle third of the span. Beam ML-2 was designed for a constant stress under load of 1,000 psi throughout the depth of the cross-section in the mid-

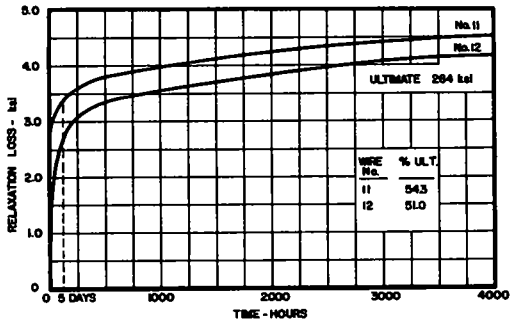

Figure 5. Plot of relaxation loss vs time for prestressing wire.

dle third of the span. The computed stresses based on the measured effective prestresses are shown in Figure 9.

After the prestress was released, the forms were removed from the beam and the cylinders removed from their molds. The beams and cylinders, except the cylinders loaded for one week in the screw-type testing machine, were moved into a controlled temperature and humidity room within 24 hr after the release of prestress. This room is kept at a constant 50 percent relative humidity and 75 F temperature by means of automatic equipment.

The tensioning force in each prestress wire was determined by measuring electrically the compressive strain in aluminum dynamometers placed on the wire between the nut and the bearing plate at the end of the beam opposite that at which tension was applied.

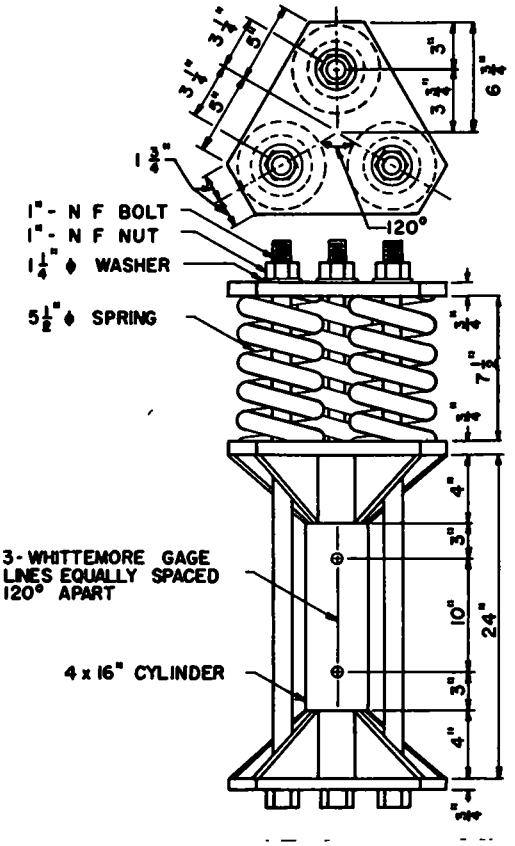

Figure 6. Dimensions and loading arrangement for the 4- by 16-in. cylinders.

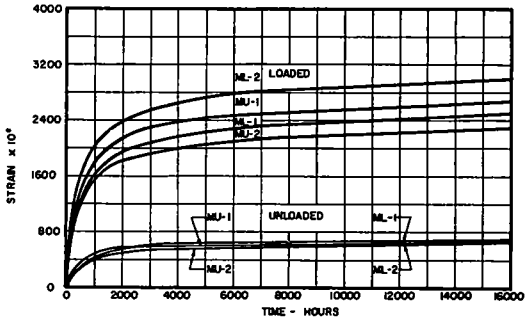

Figure 7. Measured total strains in 4- by 16-in. cylinders.

All concrete strains were measured with a 10-in. Whittemore strain gage. Each beam had four gage lines on each side, as shown in Figure 2. The unloaded beams had one set of four gage lines on each side of the centerline while the loaded beams had two sets of gage lines overlapping the centerline 5 in. The gage plugs were embedded in a high-strength gypsum plaster flush with the surface of the concrete.

Instantaneous and long-time deflections were measured at midspan of each beam with a 0.001-in. dial indicator.

For measuring strains in the 4- by 16-in. control cylinders, three sets of gage lines were arranged symmetrically about the circumference as shown in Figure 6. Holes were drilled in the cylinders and gage plugs were set in the same manner as those in the beams. For the 4- by 16-in. cylinders which were put in the special loading rigs, applied loads were measured by the deflection of the three railroad car springs (Fig. 6). Type A-7 SR-4 strain gages applied to opposite sides of the steel tie rods were used to measure loads during their initial application.

After the beams and cylinders were placed in the loading frame, deflection and strain readings were taken at time intervals corresponding to approximately equal increments of deflection. On the average, readings were taken every day for the first four days, every two days for the next four days, every week for the next two weeks, every three weeks for the next nine weeks, and every six months thereafter. Strains in the unloaded cylinders were read less frequently because of the relatively small strains involved.

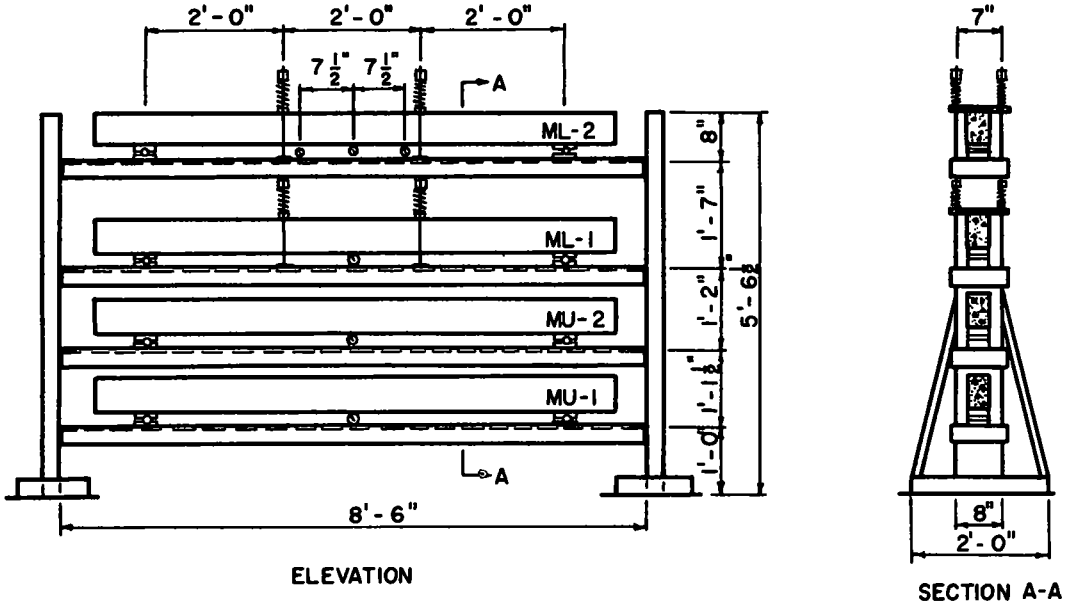

Figure 8. Beams in place on storage frame, University of Illinois tests.

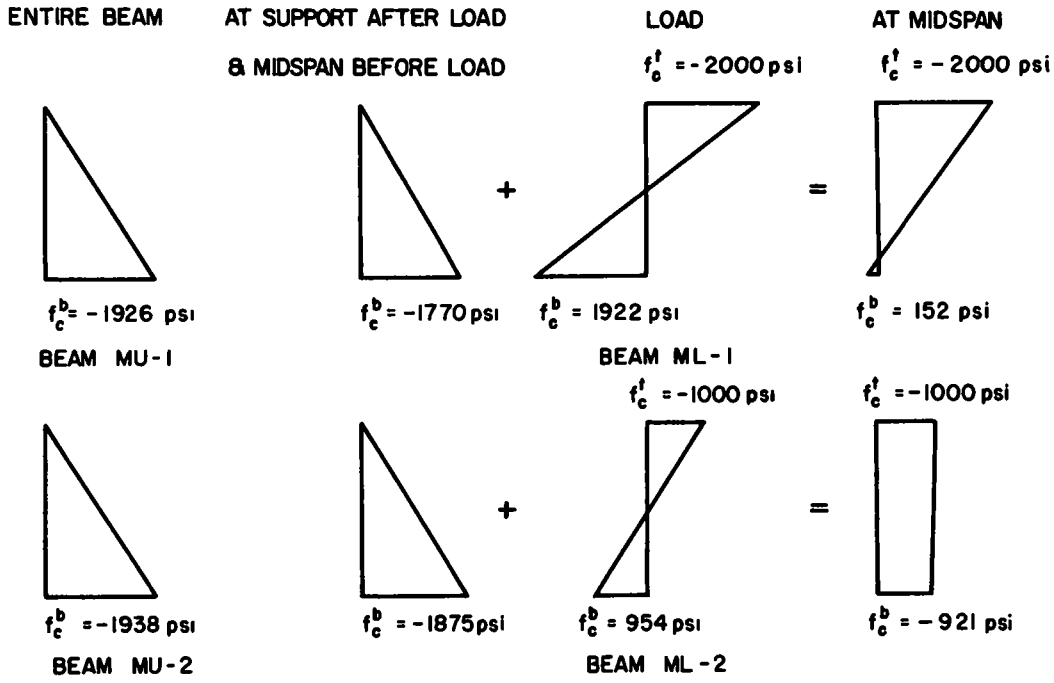

Figure 9. Computed stress distributions in beams.

Comparison of Measured and Computed Results

Figure 7 shows the measured strains in the 4- by 16-in. control cylinders. The origin of the curves for the loaded cylinders refers to the time of loading of the cylinders (Table 2). The ordinates to these curves do not include the "instantaneous" strains caused by the application of load, but represent the sum of creep and shrinkage strains. The origin of the curves for the unloaded cylinders is referred to the time immediately after the beams were placed in the loading frame.

Unit creep curves for the cylinders corresponding to each beam are shown in Figure 10. These curves were obtained by subtracting the measured strain in the unloaded cylinders at a given time from the measured strain in the loaded cylinders at the corresponding time and dividing the result by the applied stress. The origin of the unit creep curves refers to the time immediately after the cylinders were loaded (Table 2).

Distributions of beam strains at given time intervals are shown in Figure 11. The strain at each level is the average of readings from four gage lines, two on each side of the beam. The strains "before prestress" are represented by the vertical zero strain line. All other strain distribution lines represent the difference in readings after the wires were released and the readings "before prestress." For beams MU-1 and MU-2, time is measured from the release of prestress. Zero time for the loaded beams, ML-1 and ML-2, is the time at which the load was applied. Although some variation from a straight line was found in individual rows of gages, the average strain distribution was linear throughout the depth of the cross-section.

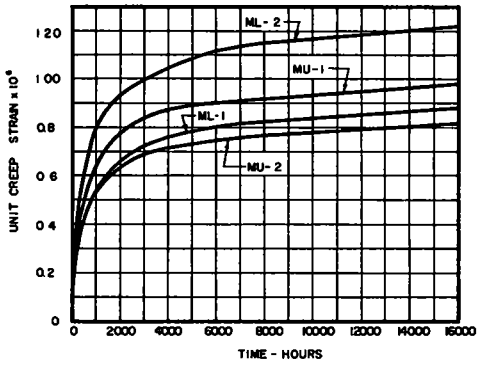

Figure 10. Unit creep relationships for University of Illinois tests.

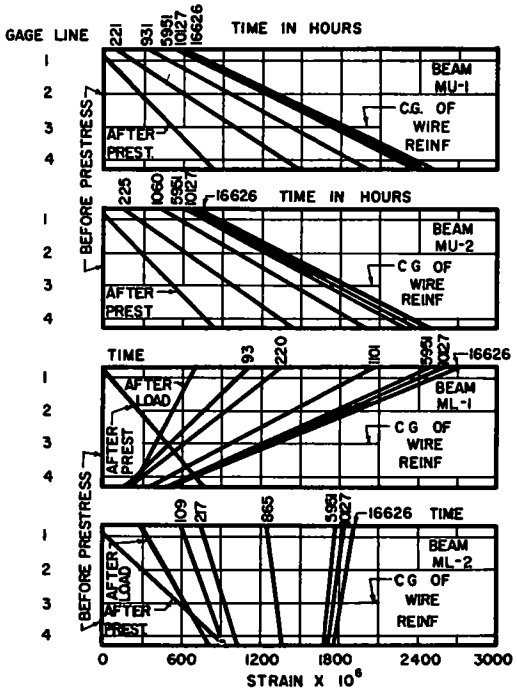

Figure 11. Successive strain distributions for University of Illinois tests.

Figures 12, 13, 14, and 15 show plots of midspan deflection versus time for beams MU-1, MU-2, ML-1, and ML-2, respectively. In all of these figures, the origin corresponds to the position of the beam before release of the prestress. Upon release, there was an instantaneous upward deflection which is indicated by the ordinate at zero time marked "after prestress." Three hours were required to transfer each beam to the loading frame. During this time, deflections were not recorded. Time-dependent deflections for the unloaded beams, MU-1 and MU-2, are referred to the reading taken immediately after positioning the beam in the loading frame. For the loaded beams, time-dependent deflections are referred to the ordinate at zero time marked "after load." This ordinate corresponds to the deflection after the load had been applied.

Time-dependent deflections of the four beams were computed by both the rate-of-creep and superposition methods. The computations were made in accordance with the methods described previously. Initial stress conditions for the beams were assumed to be as shown in Figure 9. The unit creep, shrinkage, and relaxation relationships used were those shown in Figures 10, 7, and 5, respectively. Other properties of the beams used in the computations are given in Table 3.

It was assumed that the curvature caused by the prestress was constant along the span of the beam. Curvature caused by the load was assumed to be constant in the middle third of the span and to vary linearly from the value at the load points to zero at the supports.

For both methods of computation, deflections of the loaded beams were computed for the beam under prestress alone and under load alone, and the total deflection taken as the algebraic sum of these two effects. Dead load of the beam was not considered in any of the computations. Deflections computed by the rate-of-creep and superposition methods are shown with the measured deflections in Figures 12-15.

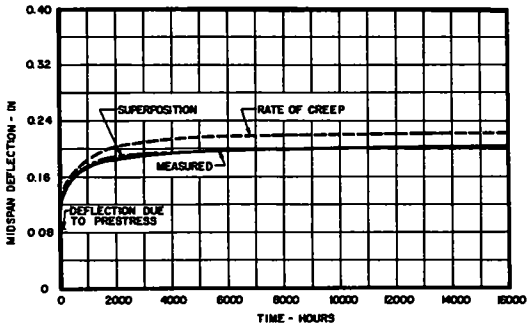

Figure 12. Measured and computed deflections for beam MU-1.

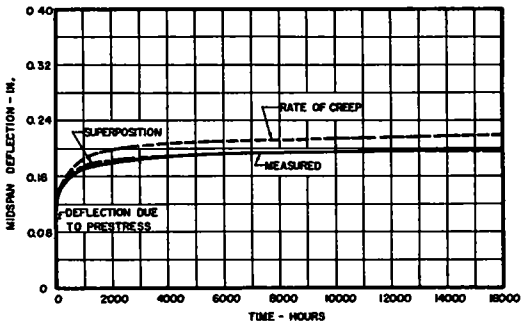

Figure 13. Measured and computed deflections for beam MU-2.

TABLE 3

PROPERTIES OF BEAMS FOR UNIVERSITY OF ILLINOIS TESTS

Beam	Width, b (in.)	Over-all Depth h (in.)	Effective Depth d (in.)	Number of Wires	Area of Steel A_s (sq in.)	Clear Span (ft)	Cylinder Strength at Release (psi)	Initial Prestress (ksi)	Total Load (lb)
MU-1	3.96	5.94	4.00	6	0.181	6	3,760	149.4	0
MU-2	3.96	5.94	4.00	6	0.181	6	3,930	149.4	0
ML-1	3.96	5.94	4.00	6	0.181	6	3,800	137.4	4,000
ML-2	3.96	5.94	4.00	6	0.181	6	3,550	149.4	2,000

Comparison of Computed and Measured Deflections

Figures 12 and 13 show that the rate-of-creep method overestimated the deflection of the unloaded prestressed concrete beams. This may be ascribed to the fact that the rate-of-creep method does not consider the entire stress history of the member. As pointed out previously, this method predicts that the concrete will creep at the rate dc/dt regardless of the stress level during the previous increment. Because decreasing stresses decrease the rate of creep, the rate-of-creep method predicts a deflection greater than that which actually occurs.

The superposition method, which considers the stress history of the concrete, gave a better prediction of the deflection of the unloaded beams.

Figures 14 and 15 show that both the rate-of-creep and superposition methods underestimated the downward deflection of the loaded beams. Because time deflections for the loaded beams were computed by first finding the upward deflections of the beam due to prestress alone and adding to these the downward deflections of a fictitious beam under external load alone, the differences between measured and computed final deflections are a combination of errors in the computations for upward and downward deflections. The rate-of-creep method overestimates the amount of deflection in a member with decreasing stress; therefore, error in computations made by this method will depend partially on the relative magnitudes of the upward and downward deflections. Because the stresses are decreasing both in the beam subjected only to prestress and in the fictitious beam subjected only to external load, the rate-of-creep method overestimates the magnitude of both the upward and downward deflection. These errors tend to cancel each other in the loaded beams; consequently, the inherent errors should have a relatively small effect on the net deflections.

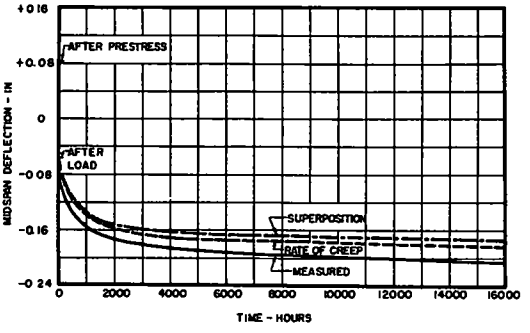

Figure 14. Measured and computed deflections for beam ML-1.

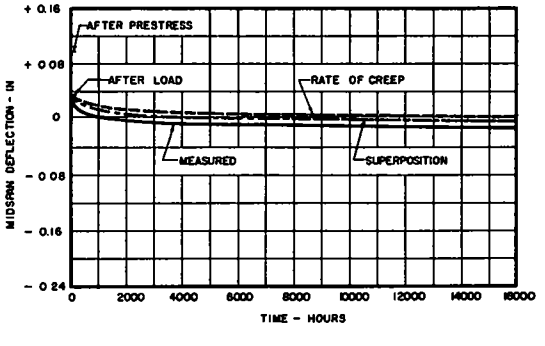

Figure 15. Measured and computed deflections for beam ML-2.

Because the net deflection of the loaded beams was downward, it would be expected that the rate-of-creep method would overestimate the downward deflection. Because both methods of computation actually underestimated the deflection, it is possible that there is another source of error. One

possibility is that the applied load was in error. However, the decrease in spring load caused by deflection of the beams was measured and taken into account in the computations. The unit creep and shrinkage curves are another possible source of error. However, the agreement of measured and predicted deflections for the unloaded beams indicates that the methods used to determine these curves were sufficiently accurate. If this is true, then it can be inferred that the computation of the upward deflections is probably correct, but some source of error is present in the computation of the downward deflections.

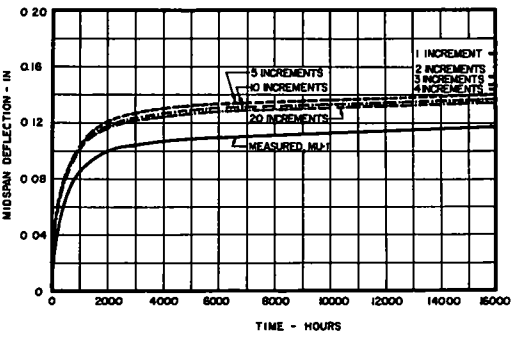

Figure 16. Effect of variation of strain increments for rate of creep method.

The deflections computed by the superposition method stand in the expected relation to those computed by the rate-of-creep method. Considering the many variables concerned, it is believed that either method gives as good a prediction of the time deflections of the test beams as can be expected.

The total deflection of a member may be found by the rate-of-creep method without knowing the shape of the unit creep curve, if the relations between the unit creep curve and the shrinkage and relaxation curves are known. Consequently, computations can be made using equal increments of unit creep and corresponding increments of shrinkage and relaxation.

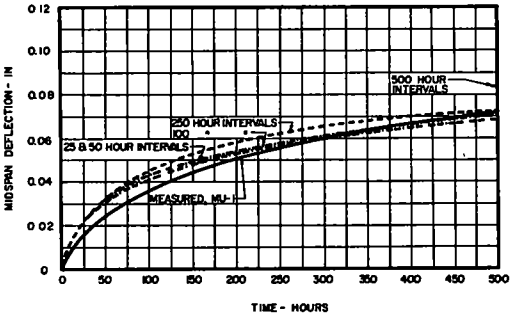

Figure 17. Effect of variation of time intervals for superposition method.

Once the computations are made, the deflection history of the beam can be obtained, if desired, by plotting the points in accordance with an assumed shape of the unit creep curve.

To determine the effect of the number of increments on the accuracy of the rate-of-creep method, several sets of computations were made using various numbers of increments. Figure 16 shows a comparison of measured deflections for beam MU-1 and deflections computed by the rate-of-creep method using various numbers of strain increments. From this comparison it can be seen that increments equal to about

TABLE 4

PROPERTIES OF BEAMS FOR UNIVERSITY OF FLORIDA TESTS

Beam	Width, b (in.)	Over-all Depth, h (in.)	Effective Depth, h (in.)	Area of Steel, A_s (sq in.)	Clear Span (ft)	Concrete Strength, f'_c (psi)	Modulus of Elasticity, E_c (psi x 10^6)	Initial Bottom Fiber Stress[a] (psi)
1	10	12	8	1.32	25	6,500	5.20	-2,400
2	10	12	8	1.32	25	6,500	5.20	-2,400
3	10	12	8	1.32	25	6,500	5.20	-1,500
4	10	12	8	1.32	25	6,500	5.20	-1,500

[a]Compressive stress (-).
Tensile stress (+).

one-tenth or less of the total unit strain will give answers with little error. Good results can be obtained from as few as three increments but the errors become relatively large when only one or two increments are used.

Computations for deflections are more easily made by taking time increments rather than strain increments when using the superposition method. In this method, the shape of the unit creep curve has a direct effect on the deflection computations; therefore, there is no advantage in taking equal strain increments as a basis for computation intervals. A comparison of measured deflections with those computed from the superposition method using various magnitudes of time intervals is shown in Figure 17. The curves are shown only for the first 500 hr of the test. These curves indicate that time increments up to 250 hr will give satisfactory results. This corresponds to a strain increment of about one-fifth the total. For larger time increments, the errors again become large.

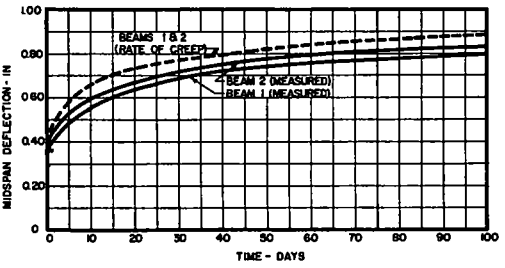

Figure 18. Measured and computed deflections for beams 1 and 2 of University of Florida tests.

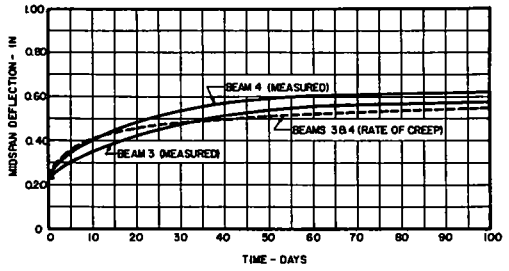

Figure 19. Measured and computed deflections for beams 3 and 4 of University of Florida tests.

RESULTS OF TESTS AT THE UNIVERSITY OF FLORIDA

Description of Tests

The results of a series of tests investigating time-dependent deformations of prestressed concrete beams have been reported by Ozell and Lofroos (4). This series consisted of four post-tensioned beams with a span of 25 ft. Each beam was 10 by 12 in. in cross-section and was post-tensioned by three straight, unbonded, "Stressteel" bars. The reinforcement was arranged so that its center of gravity coincided with the lower kern limit of the cross-section. In addition to the four beams, two shrinkage speciments, 10 by 12 in. in cross-section and 5 ft long, and thirty 6- by 12-in. cylinders were cast. Ordinary stone with a maximum size of 1 in. was used for coarse aggregate. All specimens were cured 5 days under wet burlap. After 5 days, the forms were stripped and the beams remained in the open laboratory for the rest of the test period. The duration of the test period was in excess of 100 days.

Beams 1 and 2 were post-tensioned 20 days after casting and beams 3 and 4 were post-tensioned 34 days after casting. Computed bottom fiber stresses were 2,400 psi in beams 1 and 2 and 1,500 psi in beams 3 and 4. The beams were tested under the effect of post-tensioning forces and beam dead load only. The only difference between beams 1 and 2 and beams 3 and 4 was the magnitude of the post-tensioning force.

Comparison of Measured and Computed Results

The rate-of-creep method has been used to predict the deflections of these beams. To use this method, unit creep, shrinkage, and relaxation properties of the materials must be known or assumed. Because the tests did not include the determination of all of these properties, it was necessary to estimate them.

At the University of California, tests of up to 30 yr duration have been made on a large number of concrete specimens subjected to varied conditions of load and storage and having widely different properties (5). The envelope of unit creep curves for these tests fell within a very small range. It was found that the curve for the first 720 days under load had the shape:

$$\epsilon = K \log_e (t + 1) \qquad (4)$$

in which

ϵ = fraction of total creep;
K = "creep coefficient," or slope of curve on semilogarithmic plot; and
t = time in days.

These tests also indicated that it took an additional 18 yr to add 15 percent to the creep at the end of 2 yr. Because the increase in creep after 2 yr is small, it appears acceptable to assume that all of the creep takes place in the first 720 days. The shape of the unit creep curve can be then described by the following expression:

$$\epsilon = 0.152 \log_e (t + 1) \qquad (5)$$

Although the shape of the shrinkage and relaxation curves does not have as large an effect on the calculated deflections as the shape of the unit creep curve, it is still necessary to use some reasonable method of approximating their shapes. In view of the many variables involved and the small effects these shapes have on computed deflections, the assumption can be made that the shrinkage and relaxation curves have the same shape as the unit creep curve.

After the shapes of the curves have been assumed, it is necessary to estimate the magnitudes of the unit creep, shrinkage, and relaxation. Troxell, Raphael, and Davis (5) point out that creep strain at 90 days may range between 40 and 70 percent of the 20-yr creep, and that the 90-day shrinkage strain may range between 40 and 80 percent of the 20-yr shrinkage. Using this as a guide to extrapolate the test results, it appears that a creep strain of two times the elastic strain and a shrinkage strain of 0.0003 would be reasonable values. A value of 4 percent was assumed for relaxation loss. The instantaneous modulus of the concrete as measured from 6- by 12-in. cylinders in the Florida tests was about 5.2×10^6 psi when the beams were loaded. Measured deflections of the beams indicated a slightly lower value, but these deflections included a small amount of creep. The higher value of "instantaneous" modulus was used in the rate-of-creep computations.

Using these assumptions, the time-dependent deflections were computed and plotted with the test results. The results for beams 1 and 2 are shown in Figure 18 and the results for beams 3 and 4 are shown in Figure 19.

Comparison of Computed and Measured Deflections

Lofroos and Ozell concluded that for beams containing the same concrete at different stress levels, large variations can occur in the "apparent modulus of elasticity" (4). Figures 18 and 19 show that the time-dependent deflections computed, by the rate-of-creep method compare closely with the measured deflections. Moreover, consistent results were obtained with only one set of assumptions for the time-dependent properties of the materials.

This comparison shows that time-dependent deflections which are computed by simply using a reduced modulus of elasticity can lead to inconsistent results for members in which stresses vary. Because the rate-of-creep method does consider the stress history of the member, more consistent results can be obtained.

MEASURED DEFLECTIONS OF A HIGHWAY BRIDGE

Description of the Bridge and Measurements

The time-dependent deformations of one beam of a highway bridge in North Africa have been reported by J. Delarue (6). This beam was a post-tensioned T-section, 28 m long and 2 m deep. The cross-sectional properties of the beam at midspan and at the supports are shown in Figure 20. The post-tensioning reinforcement consisted of seven cables each of which contained 20 wires 8 mm in diameter. The cables were draped in the shape of a parabola and had an initial tension of 140,000 psi. The concrete strength at 28 days was 8,200 psi. In addition to the test beam, several control specimens were cast from the same concrete mix. The control specimens were one

meter long and were 12, 15, or 17 cm square in cross-section. One-half of these specimens were loaded axially to a compressive stress of 120 kg/cm^2 (1,710 psi) and were kept at this stress for the duration of the test. The remaining prisms were left unloaded and were used to determine the shrinkage of the concrete under zero external load. The concrete in all specimens was made with ordinary aggregate.

Post-tensioning operations were begun 60 days after the beam was cast, and required seven days to complete. After post-tensioning, the beam was supported on a clear span of 27.6 m. The beam remained on these supports for 12 months after which it was moved to the bridge site and placed in its final position. During the transportation of the beam to the bridge site, the beam was prestressed externally to prevent cracking at the top. The move was completed in one day. After the beam was put in place, 9-in. thick slab strips were cast beween the beams. Casting and curing of the slab were completed in two months. Construction equipment was then placed on the bridge to simulate a sustained live load. After three days, the construction equipment was removed and the bridge was opened to traffic approximately 500 days after the beam was cast. Observations made for the first 650 days were reported by Delarue (6). This paper reports the deflection data for 1,000 days (10). The observations are still being continued.

Computation of Deflections

The numerical procedure for the rate-of-creep method was used to analyze this beam. Because laboratory tests were made to determine the shrinkage and creep properties of the concrete, the results of these tests were used in the computations. The laboratory results obtained from control specimens of different sizes were in good agreement. Consequently, measured deformations of the control specimens which were 15 cm square in cross-section were taken as representative of the time-dependent properties of the concrete.

The curves for time versus shrinkage and time versus unit creep used in the compu-

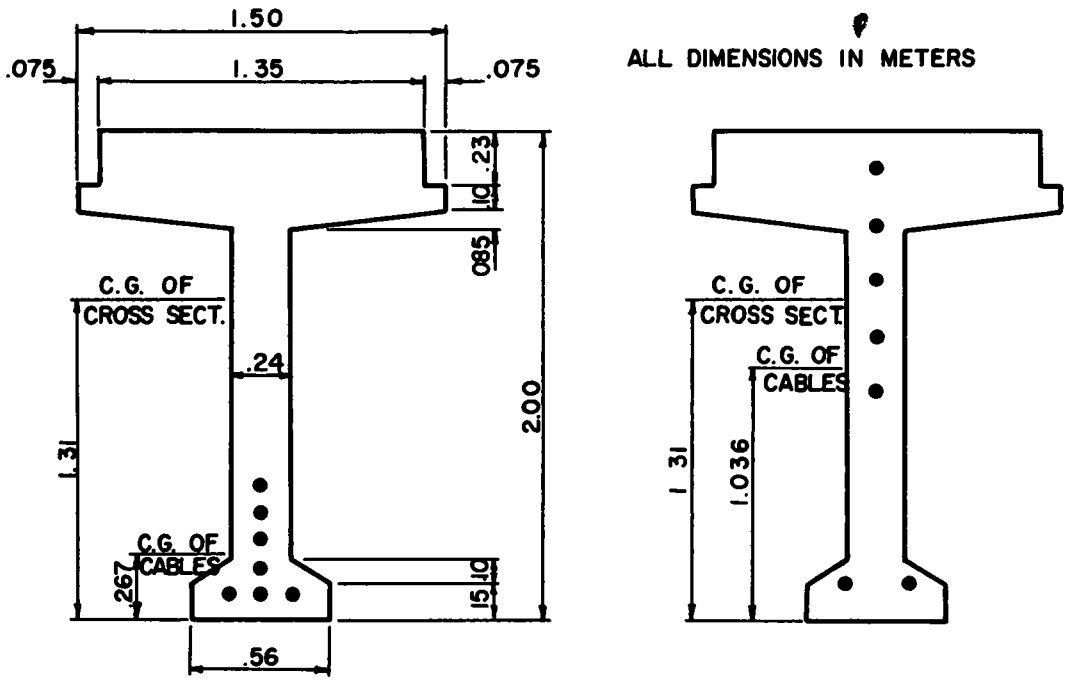

Figure 20. Cross-sectional properties of Rabat bridge test beam.

tations are shown in Figures 21 and 22, respectively. The unit creep curve was obtained by dividing the ordinates to the curve of time versus strain for the specimen under the sustained load by the magnitude of the sustained load. For simplicity, the unit creep curve was assumed to have this shape regardless of the age of the concrete at the time of loading. Relaxation of the steel was assumed to be two percent of the initial steel stress and was assumed to have the same shape as the unit creep curve. The elastic modulus of the steel was taken as 30×10^6 psi and the "instantaneous" modulus of the concrete was taken to be 6×10^6 psi as determined from the control prisms. Computed initial stresses in the concrete caused by prestress, beam dead load, and slab dead load, are given separately in Table 5. Deflections caused by temporary loads were neglected in the computations.

Time-dependent deflections due to prestress only were found by computing the curvatures at the reactions and at midspan and assuming the curvature between these

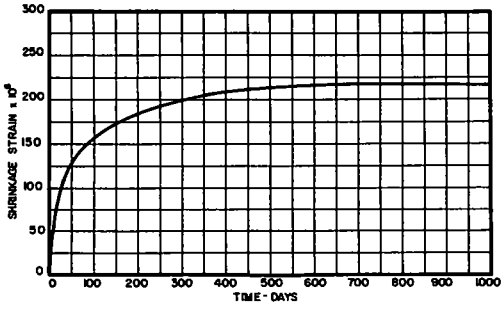

Figure 21. Shrinkage strain vs time relationship for Rabat bridge test beam.

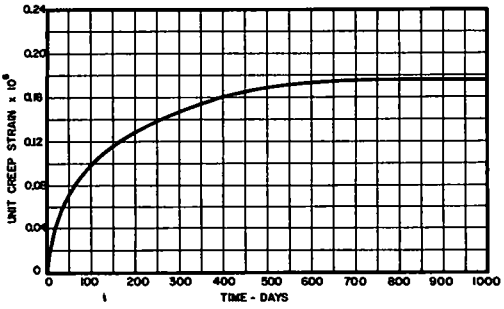

Figure 22. Unit creep relationship for Rabat bridge test beam.

points to have a parabolic distribution. For deflections due to beam dead load and slab dead load, a parabolic distribution of curvature varying from a maximum at midspan to zero at the reactions was assumed in accordance with the moment distribution. After determining the time versus deflection relationships for the separate load effects, the ordinates to the individual curves were added at the appropriate times to the "instantaneous" deflections, and the time versus total deflection relationship was obtained.

Comparisons of Computed and Measured Deflections

Figure 23 shows measured and computed deflections for the bridge beam. It can be seen that deflections computed by the rate-of-creep method are in good agreement with the measured deflections up to about 700 days. In the early stages, the rate-of-creep method tends to overestimate the upward deflection, as would be expected. Later, however, the upward deflection of the bridge beam becomes greater than that computed.

Delarue has pointed out that the deflections of the bridge appear to vary with the seasons. During the summer, deflections were found to increase, whereas during the

TABLE 5

INITIAL STRESSES IN EXTREME FIBERS OF FULL SIZE BEAM TEST

	Stress in Top Fiber of Beam[a] (psi)		Stress in Bottom Fiber of Beam[a] (psi)	
Cause of Stress	Midspan	End	Midspan	End
Post-tensioning	+720	-570	-4,230	-1,870
Beam dead load	-530	0	+980	0
Slab dead load	-290	0	+540	0

[a]Compressive stress (-)
Tensile stress (+)

winter they decreased. The seasonal variations are due in part to the effect of moisture content on the creep and shrinkage properties of the concrete. Because the bridge was exposed to large variations in temperature and humidity, whereas the laboratory control specimens were stored under nearly constant atmospheric conditions, the shrinkage and creep characteristics of the laboratory specimens were not the same as those of the concrete in the beam. As the beam grows older, the differences in the behavior of the concrete in the laboratory and that in the beam appear to increase. At present, there is not enough information available to determine if this increase will continue. If the time versus deformation properties had been determined for the concrete under the same variations of temperature and humidity as the concrete in the beam, the rate-of-creep method would probably give a good indication of the complete deformation history of the beam including the seasonal effects which evidently can cause variations in deflection of the same magnitude as those occurring under nearly constant atmosphere conditions.

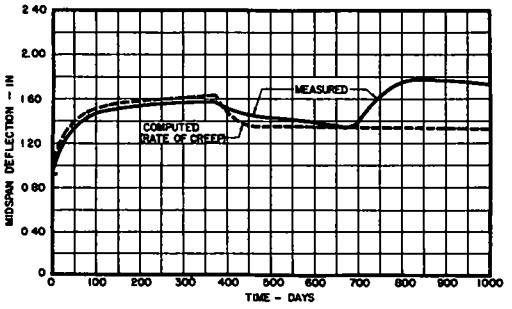

Figure 23. Measured and computed deflection for Rabat bridge test beam.

COMPUTED TIME-DEPENDENT DEFLECTIONS OF STANDARD PRESTRESSED CONCRETE BRIDGE SECTIONS

Properties of Sections

The studies of test results described in the preceding sections indicate that the basic time-dependent properties of concrete and steel can be used to compute the deflection of flexural members in which the concrete is subjected to variable stress. On the basis of these correlations of the unit creep, shrinkage, and relaxation under constant conditions with the deflection of prestressed concrete beams, it can be assumed that either the rate-of-creep or the superposition methods will provide a satisfactory basis for predicting the time-dependent deflections of prestressed concrete highway girders. However, it is necessary that the time-dependent properties be known for the materials used in the particular structure. Unfortunately, it is difficult to obtain these properties precisely. Even when laboratory tests are conducted on the materials used for a given structure, differences between laboratory and field conditions may be large enough to make the results unreliable. Laboratory tests are often conducted under constant or nearly constant conditions of temperature and humidity whereas a structure such as a highway bridge is subjected to a wide range of temperature and humidity. Quality of workmanship may also differ in the laboratory and field, thereby adding to the variation.

Any of the differences between laboratory and field conditions may cause a notable difference in the behavior of the control specimens and the structure. For this reason, it is preferable to work with reasonable approximations to the unit creep, shrinkage, and relaxation curves, unless circumstances warrant special tests. A guide to the ranges of the time-dependent parameters can be obtained from the literature. Any of the parameters which have a large effect on the results should be thoroughly investigated by using extreme values of their magnitudes.

The time-dependent deformations of several standard prestressed concrete bridge beams were analyzed by the rate-of-creep method to determine the effects of some of the many variables. For these computations it was again assumed that the deformations which occurred after about 2 yr (720 days) could be neglected and that the shape of the unit creep curve could be described by the relation:

$$\epsilon = 0.152 \log_e (t + 1) \qquad (6)$$

Although the shapes of the shrinkage and relaxation curves do not have as large an effect on the calculated deflections as the shape of the unit creep curve, it is still necessary to use some reasonable method of approximating them. In view of the many

variables involved and the small effects these shapes have on the final deflections, the shrinkage and relaxation curves have been assumed to have the same shape as the unit creep curve.

Tests indicate that the magnitude of unit creep may range from 1 to 8 times the "instantaneous" deformation, depending on the properties of the material and conditions of temperature and humidity (5). For most conditions, a good estimate of creep deformation is 2 to 4 times the instantaneous deformations. More extreme values may be indicated for structures under severe atmospheric conditions or for concrete mixes of unusual proportions. For these computations, each beam was analyzed for unit creep under constant load of 2 and 4 times the instantaneous deformation.

Shrinkage strains have been found to vary in magnitude from zero, for concrete stored under very wet conditions, to more than 0.0012, for concrete stored under dry conditions (5). For highway bridges or other structures in open air, a reasonable value for shrinkage strain is 0.0003. This value was used in the analysis. Extreme values should be investigated for structures subjected to very wet or very dry conditions as well as for concrete of unusual consistency.

Relaxation losses after release of prestress may range from 1 to 8 percent of the initial stress (3). For these computations a rather high value of 8 percent was assumed.

Deflection calculations were made only for the dead load. Live loads were considered to be of such short duration that their effects on time deflections would be negligible.

The loads were divided into three categories: (a) the dead load of the beam, which was considered to act at all times; (b) the prestressing force, which was considered to act at all times; and (c) the dead load of the slab, which was considered to act from the time the slab was cast. The instantaneous modulus of the concrete and the magnitude of unit creep for the effects of prestress and beam dead load were based on a concrete strength of 4,000 psi, whereas those for the effect of slab dead load were based on a concrete strength or 5,000 psi.

Instantaneous deflections were computed on the basis of an elastic uncracked plain section. Time deflections were computed for the separate loading conditions and the time versus deflection relationships were found by plotting these deflections in accordance with the shape of the unit creep curve. The instantaneous deflections were then combined with the time deflections at the appropriate times to obtain the net time versus deflection relationship.

The concrete in the beams was assumed to have a strength of 4,000 psi at release

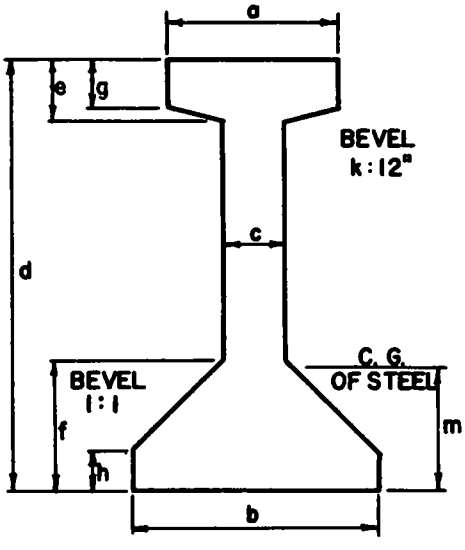

SPAN	a	b	c	d	e	f	g	h	k	m	NO. OF WIRES
40'-0"	16	18	6	36	5 1/2	10	4 1/4	4	3	9 3/4	30
45'-0"	17	18	6	40	5 1/2	10	4 1/8	4	3	10	32
50'-0"	18	18	6	44	5 1/2	10	4	4	3	11 7/8	36
60'-0"	20	24	6	48	6 1/2	14	5 1/2	5	2 1/4	9	43
70'-0"	22	26	6	56	6 1/2	14	5	4	2 1/4	10 3/4	52

DIMENSIONS IN INCHES

Figure 24. Cross-sectional properties of pretensioned standard prestressed concrete bridge sections.

of the prestress and a strength of 5,000 psi at the time the slab was cast. The instantaneous modulus for the concrete was obtained from the expression recommended by the ACI-ACE Joint Committee 332 (7):

$$E_c = 1,800,000 + 500\, f'_c \qquad (7)$$

in which

E_c = instantaneous modulus, and
f'_c = concrete strength in psi.

The steel was assumed to have a prestress of 175,000 psi prior to release. The modulus of elasticity of the steel was taken as 30×10^6 psi.

The beams analyzed were for 40-, 45-, 50-, 60-, and 70-ft spans with 28-ft roadways. These are the pre-tensioned standard prestressed concrete bridges listed by the Bureau of Public Roads (8). They are designed for H20-S16-55 loading. Cross-sectional dimensions for these beams are shown in Figure 24.

Method of Computation

The numerical procedure for the rate-of-creep method described previously was used for the computation of deflections. The problem of time deflection in prestressed concrete highway bridges is well suited to analysis by this method because it involves nearly every possible variable. The beams for a typical bridge may be cast at a factory, and stored for 60 days or more before the slab is cast on them. In such a case, some of the time deflections will take place in the beam before the slab is cast. If a period of 60 days or more elapses between the release of prestress and casting of the slab, shrinkage strains in the slab will usually be greater than combined shrinkage and creep strains in the top fiber of the beams. This will result in forces tending to shorten the top fibers of each beam. These forces may be handled easily by the numerical

TABLE 6

CREEP PARAMETERS USED FOR PRE-TENSIONED, STANDARD PRESTRESSED CONCRETE BRIDGES

Span Length (ft)	Beam No.	Days From Prestressing to Casting of Slab	Modulus of Elasticity, E_c, at Prestressing (psi x 10^6)	Modulus of Elasticity, E_c, at Casting of Slab (psi x 10^6)	Relaxation (ksi)	ϵ_c/ϵ_i
40	1	30	3.80	4.30	12.96	2
	2	60	3.80	4.30	12.96	2
	3	30	3.80	4.30	12.96	4
	4	60	3.80	4.30	12.96	4
45	1	30	3.80	4.30	12.96	2
	2	60	3.80	4.30	12.96	2
	3	30	3.80	4.30	12.96	4
	4	60	3.80	4.30	12.96	4
50	1	30	3.80	4.30	12.96	2
	2	60	3.80	4.30	12.96	2
	3	30	3.80	4.30	12.96	4
	4	60	3.80	4.30	12.96	4
60	1	30	3.80	4.30	12.96	2
	2	60	3.80	4.30	12.96	2
	3	30	3.80	4.30	12.96	4
	4	60	3.80	4.30	12.96	4
70	1	30	3.80	4.30	12.96	2
	2	60	3.80	4.30	12.96	2
	3	30	3.80	4.30	12.96	4
	4	60	3.80	4.30	12.96	4

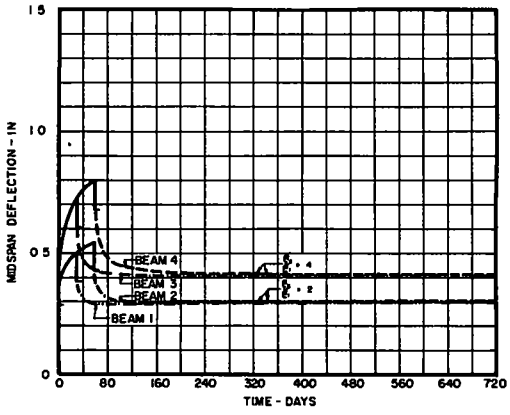

Figure 25. Computed deflection of 40-ft composite highway bridge beam.

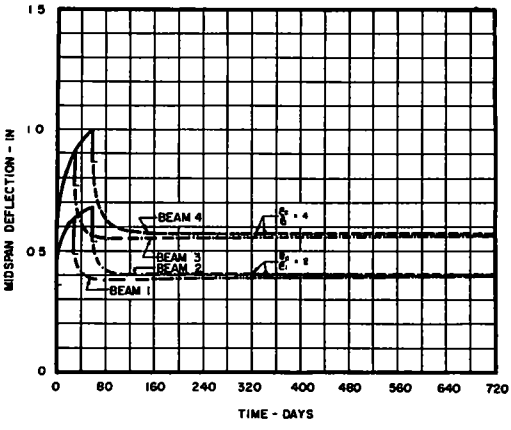

Figure 26. Computed deflection of 45-ft composite highway bridge beam.

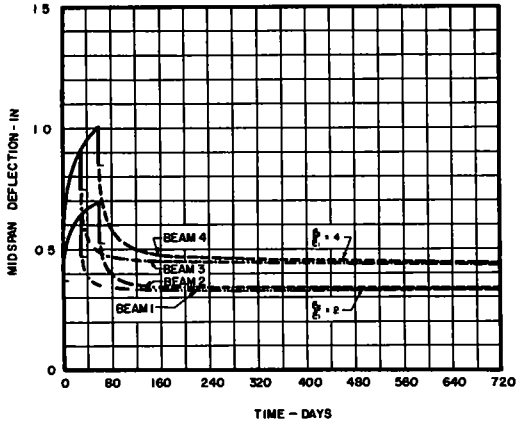

Figure 27. Computed deflection of 50-ft composite highway bridge beam.

procedure; however, they are usually small enough to be neglected. In the beams analyzed, the computed strain increments in the top fiber of the girder were almost equal to the expected shrinkage strain increments in the slab. Consequently, the forces exerted on the beams because of shrinkage of the slab were ignored.

Computed Deflections for Prestressed Bridges

Figures 25 through 29 show the time versus deflection relationships for five Pre-Tensioned Standard Prestressed Concrete Bridges with slabs cast at 30 or 60 days. Table 6 gives the parameters used in the computations for each curve. The curves include both instantaneous and time deflections.

If the girders are assumed to be straight before prestressing, it can be seen that the net camber after all deflections have taken place is quite small in every case. Final cambers range from about $\frac{5}{8}$ in. in the 45-ft span to less than $\frac{1}{4}$ in. in the 60-ft span. It can also be seen that a variation in creep strain from two times the instantaneous strain to four times the instantaneous strain has only a small effect on the net deflection due to dead load. One reason for the small computed deflection is the fact that the dead load stress gradient over the depth of the cross-section is small in all beams considered. In addition, the l/d ratio is nearly constant for all beams. These two effects combine to keep computed net upward deflections small and also nearly equal for all of the beams considered.

In general, time deflections will be relatively small if the stress gradient corresponding to the combined effects of dead load and prestress is small. The critical stress gradient is that corresponding to the dead load and any part of the live load which may remain on the structure for long periods of time.

The curves shown in Figures 25 through 29 also indicate that loading at 30 or 60 days results in a little difference in the final deflection of the structures. This is a result of the assumption made for the time-dependent characteristics of the concrete. If the concrete exhibited a greater change in magnitude of unit creep in relation to the age at loading than that assumed, there would be a larger difference in final deflection for different dates of loading. The comparison of measured and

computed deflections for the beam in Figure 23 shows that the effects of humidity and temperature may be greater than the effect of age of concrete at loading. Hajnal-Konyi has found the same effect in a number of reinforced concrete beam tests (9). In these tests, the beams were stored under shelters which were open on all four sides. A definite change in the rate and even in the sense of the deflection increase was noted during different seasons of the year. This rate was considerably lower during autumn (Great Britain). In view of these results, a more refined method of estimating the total unit creep does not appear to be justified unless the time-dependent parameters for the concrete are known for environmental conditions very similar to those for the structure.

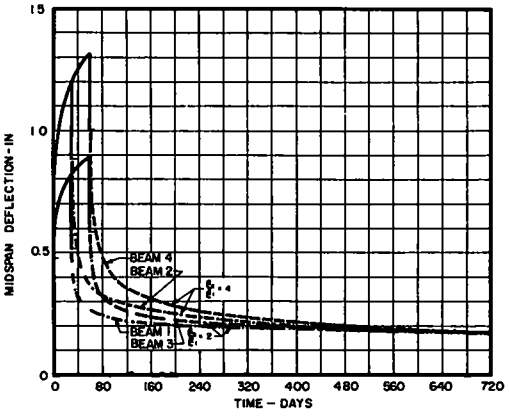

Figure 28. Computed deflection of 60-ft composite highway bridge beam.

In many cases, the important portion of the time-dependent deflection is that which occurs after the slab is cast. Figures 25 through 29 show that this deflection may range from as little as $\frac{1}{10}$ in. for the 40-ft span to as much as $\frac{7}{8}$ in. for the 70-ft span. Although this change in deflection can be larger than the net deflection, it is interesting to note that most of it occurs within the first 100 days after the slab is cast. This phenomenon is chiefly a function of the shape of the unit creep curve; consequently, errors in estimation of the magnitude of unit creep do not greatly affect the time at which the deflections nearly stabilize.

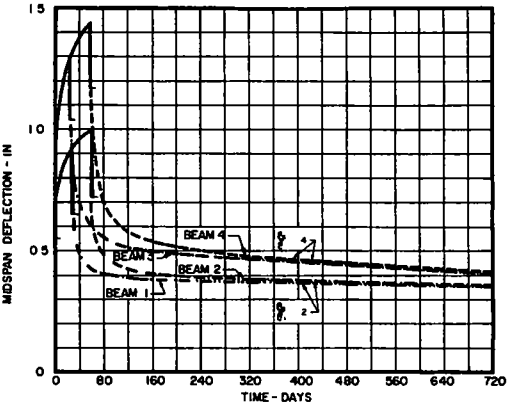

Figure 29. Computed deflection of 70-ft composite highway bridge beam.

Although this method of analysis of time-dependent deflections does not predict precisely the behavior of the beam, it is useful in determining the range in deflection. Comparison with test results indicates that either the rate-of-creep or the superposition method can be used to predict deflections if the time-dependent properties of the materials are known. Consequently, the method of analysis used for these examples can be used as a guide for determining the effects of time-dependent deformations.

SUMMARY

The objective of this paper has been to present and discuss various methods for computing the time-dependent deflections of prestressed concrete beams, to compare the deflections computed on the basis of these methods with results of tests, and to estimate the possible magnitudes of time-dependent deflections in representative prestressed concrete highway bridges.

The time-dependent deflection of prestressed concrete beams is attributed to three effects: creep and shrinkage of the concrete, and relaxation of the reinforcement. Ordinarily, creep of the concrete is the dominant factor. Because concrete is subjected to a stress which varies with time primarily as a result of the changes in the prestress level, its creep characteristics will be different from those determined under a constant

stress. To analyze the time-dependent deflections of prestressed concrete beams having various proportions using only one consistent set of assumptions regarding the material properties, it is necessary to recognize this variation in stress and its possible effects on the creep characteristics. The "rate-of-creep" method recognizes the stress variation but ignores the possible changes in the creep characteristics. The "superposition" method recognizes the stress variation and also modifies the creep characteristics according to the stress variation. Both methods involve a numerical integration procedure; the second requires more numerical work.

The measured deflections from four laboratory tests on beams were compared with deflections computed using creep strains evaluated according to these two methods. The shrinkage, relaxation, and the basic creep (creep under sustained stress) relationships were determined from control tests. All specimens were kept under conditions of controlled temperature and humidity. The agreement between the measured and computed curves (Figs. 12-15) was good. Although the superposition method gave better results, the rate-of-creep method was deemed preferable for general application in view of its relative simplicity.

The measured deflections of four beams tested by Lofroos and Ozell (4) were analyzed using the rate-of-creep method, primarily to show that the deflection of beams having different levels of prestresses could be predicted on the basis of the same basic creep curve.

The time-dependent deflections of a prestressed highway bridge in Morocco have been reported by J. Delarue (6). The measured deflections were compared with values computed using the material properties determined from laboratory tests (Fig. 23). The seasonal deflections of this bridge, which may be attributed to changes in relative humidity and possibly in temperature, were of nearly the same magnitude as the computed maximum time-dependent deflection. Such a seasonal variation can be predicted only on the basis of basic properties determined at the site.

Although the precise relationships for basic creep, shrinkage, and relaxation cannot be obtained without undue expense, it is possible to obtain a fairly good estimate of the time-dependent deflections of prestressed concrete girders by computations based on reasonable maximum and minimum values of the critical variables. This was done for five representative composite highway bridges with spans ranging from 40 to 70 ft. It was found that under ordinary conditions, the deflections under dead load for these bridges should not exceed ¾ in. and could be less than ¼ in. It should be pointed out, however, that the time-dependent deflections of prestressed concrete beams can be objectionably high, especially if there is a high stress gradient in the beam under permanent load.

ACKNOWLEDGMENTS

This study was carried out in the Structural Research Laboratory of the Department of Civil Engineering at the University of Illinois as part of an investigation of prestressed reinforced concrete for highway bridges. The investigation was sponsored by the Illinois Division of Highways as part of the Illinois Cooperative Highway Research Program. The U.S. Department of Commerce, Bureau of Public Roads participated through grants of Federal-aid funds.

Thanks are extended to P. E. Murphy, formerly Research Assistant in Civil Engineering, for his conscientious work in connection with the tests at the University of Illinois. The writers would like to acknowledge the cooperation of J. Delarue, Director, State Laboratory for Material Testing and Research, Casablanca, Morocco, in supplying unpublished data on the deflections of the Rabat bridge.

REFERENCES

1. Ross, A. D., "Creep of Concrete Under Variable Stress." Jour. ACI, Proc., Vol. 54, p. 739 (March 1958).
2. McHenry, D., "A New Aspect of Creep in Concrete and Its Application to Design." Proc., ASTM, 5:43, 1069 (1943).

3. McLean, G., "Study of the Time-Dependent Variables in Prestressed Concrete." M.S. Thesis, Univ. of Illinois (June 1954). Issued as part of Third Progress Report of the Investigation of Prestressed Concrete for Highway Bridges.
4. Lofroos, W.N., and Ozell, A.M., "The Apparent Modulus of Elasticity of Prestressed Concrete Beams Under Different Stress Levels." Jour., PIC, p. 23 (Sept. 1959).
5. Troxell, G.E., Raphael, I.M., and Davis, R.E., "Long-Time Creep and Shrinkage Tests of Plain and Reinforced Concrete." Proc., ASTM, Vol. 58, p. 1101 (1958).
6. Delarue, J., "Fluage et Beton Precontraint." RILEM Colloquim, Munich (Nov. 1958).
7. ACI-ASCE Joint Committee 323, "Tentative Recommendations for Prestressed Concrete." Jour., ACI, Proc., Vol. 54 (Jan. 1958).
8. "Standard Plans for Highway Bridge Superstructures." U.S. Department of Commerce, Bureau of Public Roads, U.S. Gov. Print. Office, Washington, D.C., pp. SL-1-56 to SL-3-56 (1956).
9. Hajnal-Konyi, K., "Special Reinforcements for Reinforced Concrete." Final Report, RILEM Symposium on Special Reinforcement, Wires, and Bars, Liege, p. 146 (1958).
10. Delarue, J., Private communication.

Creep and Shrinkage of Two Lightweight Aggregate Concretes

GORDON W. BEECROFT, Assistant Professor of Civil Engineering, Oregon State College

This report discusses a research project being conducted by the Oregon State Highway Department in cooperation with the U.S. Bureau of Public Roads to determine the creep and shrinkage characteristics of two expanded shale aggregate concretes. In the current phase of the project, measurements have been made for a period of about 1½ yr on concrete specimens. The shrinkage measurements were made on prisms having gage points 24 in. center to center, and the creep measurements were made on prestressed prisms having sufficient length to provide gage points 100 in. center to center. The creep specimens were stressed to provide an initial concrete stress of 1,820 psi. To more nearly parallel conditions as they exist in typical prestressed members, this stress has been permitted to diminish as creep and shrinkage occur. The loss of prestress force resulting from the plastic deformation of the specimens has been measured by means of pressure cells installed in connection with the prestressing steel.

To provide a basis for comparison, identical specimens were cast from one normal-weight concrete mixture, using sand and gravel aggregates. The magnitudes of creep, shrinkage, and loss of prestress measured on the lightweight prisms are compared with the values measured on the normal-weight prisms.

Curves showing the time deformations in prisms from an earlier phase of the research are also presented. These prisms, which were subjected to a constant stress, are now more than 4 yr old.

The various measurements are discussed and compared with typical allowances contained in literature on prestressed concrete design.

For specimens subjected to a relaxing stress, it is estimated the ultimate loss of prestress will be approximately 60 percent greater in the lightweight prisms than in the normal-weight prisms.

●THE principal purpose of this project is to evaluate the suitability of two expanded shale aggregates, processed in Oregon, for use in prestressed concrete bridge members. The present phase of the project is directed toward obtaining a comparison between the time deformation of prisms under a relaxing prestress force and the time deformations previously measured in similar prisms subjected to a constant stress intensity. In an attempt to maintain the conditions of stress as the only significant variable, the same design mixtures and the same curing conditions were used for both the relaxing stress conditions and the previous study of lightweight concrete prisms subjected to a constant stress.

In addition to the studies on lightweight aggregates, the current phase of the research includes identical specimens cast from sand and gravel aggregates to provide a further

comparison between the time deformations of lightweight and normal-weight concretes.

BACKGROUND

The engineering profession has long recognized the fact that in some structures employing prestressed concrete members, the weight reduction made possible by using lightweight aggregates would be highly advantageous. However, lightweight aggregates have not received widespread acceptance because of the limited knowledge of the physical properties of the lightweight concretes, particularly with regard to creep and shrinkage. During the past few years a number of projects have been undertaken to broaden the engineer's knowledge of the physical characteristics of structural quality lightweight concretes.

During 1955 the Oregon State Highway Department initiated a research project to gather information on the various properties of concrete made from locally available lightweight aggregates. The two principal aspects of this project were the development of lightweight concrete mixtures having suitable workability and strength for use in prestressed concrete members, and the study of time deformations in concrete prisms cast from selected mixes developed under the earlier phase. After curing, these prisms were subjected to an almost constant, axial compressive stress. A report covering a period of about 1½ yr of measurements on the prisms has been published (1). Portions of the information presented in the prior report, as well as current data on the prisms, are included in this paper.

In most prestressed concrete applications, the prestress force is applied by tensioning high strength steel tendons; either before or after the concrete has cured. In these applications, the initial stress is gradually reduced as creep and shrinkage of the concrete occurs. To more nearly approximate conditions as they commonly exist in prestressed members, it was deemed desirable to measure the creep of specimens subjected to a gradually relaxing stress. The current phase of the research was initiated during 1958 with these measurements as a principal objective. Additional prisms were cast which permitted the measurement of creep and loss of prestress. To permit comparisons between the constant stress condition and the relaxing stress condition, the same nominal concrete mixes were used in both phases and the specimens in each case were approximately the same size and were treated in the same manner. In addition to the creep measurements, specimens of the different mixtures were cast to permit measurements of shrinkage of the concrete.

AGGREGATES

The lightweight aggregates employed in this study were both expanded shales processed in Oregon and marketed under trade names. For this project, they have been designated as aggregate A and aggregate B.

Both of these aggregates are produced by crushing and burning Keasey shales. In each case, the materials are heated in a rotary horizontal kiln to temperatures in the vicinity of 2,000 F. Prior to burning, aggregate A is crushed to a 2-in. maximum size and aggregate B to a 3-in. maximum size. Following the burning process, the aggregates are crushed to the desired sizes for marketing. For this project, the sizes used were ⅜ in. to $^3/_{16}$ in. and $^3/_{16}$ in. to 0.

The aggregate used in the normal-weight concrete was Santiam River sand and gravel. The maximum particle size used in the test specimens was ¾ in. The materials from this source are generally sound and durable and have a good service record as concrete aggregates.

A sieve analysis for each of the aggregates used in the present phase of the study is given in Table 1.

CONCRETE MIXTURES

To enable comparisons to be made between the time deformations under constant stress with those under a relaxing stress, approximately the same lightweight concrete mixtures were used in each phase of the study. Inherent variations in the aggregates

TABLE 1

SIEVE ANALYSIS OF AGGREGATES

Sieve No.	Percent by Weight Retained on Sieve					
	Aggregate A		Aggregate B		Natural Aggregates	
	Fine	Coarse	Fine	Coarse	Fine	Coarse
3/4	-	-	-	-	-	0
1/2	-	-	-	-	-	32.1
3/8	-	0	-	0	-	59.0
1/4	-	7.2	0	23.2	0	81.0
4	0	48.8	0.8	70.8	6.4	100.0
8	22.6	96.0	42.2	94.8	22.4	100.0
16	42.6	97.4	66.8	95.8	35.3	100.0
30	54.8	97.8	77.8	96.0	50.2	100.0
50	63.2	98.0	83.2	96.2	80.1	100.0
100	70.4	98.2	87.6	96.4	95.7	100.0
Fineness modulus	2.54	5.36	3.58	5.50	2.90	6.59
Unit wt., pcf	49.8	33.4	57.2	54.4	101.3	111.0
Moisture content, %	0.5	0.4	7.2	19.7	-	-

caused some difference to exist between the mixes used previously and those used in the current phase. The same volumes of fine and coarse aggregates were used in each case; however, the gradation, unit weights, and moisture content of the aggregates varied somewhat from those used in the earlier studies. These differences caused some change in the unit weight, yield, modulus of elasticity, and ultimate strength of the concrete mixes made from the aggregates. The significance of these variations on the creep and shrinkage characteristics of the test specimens cannot be evaluated; but because the mixtures are essentially the same, the differences are assumed to be of minor importance. Details of the mixes used in the current test specimens are given in Table 2.

In making the concrete, about two-thirds of the mixing water was added to the aggregates and mixed for 4 or 5 min prior to the addition of cement and admixture. After the cement was combined with the aggregates, the mixing was continued and water was added until the desired consistency was obtained. Type I cement was used for all concrete in the investigation. After casting, the various specimens were moist cured at room temperature.

In the experimentation preceding the selection of the concrete mixtures to be used in time-deformation studies, sample batches of concrete were mixed with various proportions of the different components. Variations were made in proportioning the aggregates as to gradation, and the cement content was varied between values of 6 and 9½ sacks per cu yd for the various mixes. Six standard cylinders were cast from each of the trial mixes which were tested for ultimate strength, three each at ages of 28 and 60 days. In addition to the tests for ultimate strength, the various mixtures were judged for workability and the slump and wet weights were measured.

To obtain high strength concrete with the expanded shale aggregates used in this study, it was found that a rather high cement factor was required. An objective of the project was to devise and study mixtures having both high ultimate strength and suitable workability to make the placing of the concrete feasible using conventional field techniques. By using lower water-cement ratios or higher percentages of coarse aggregate in relation to the amount of fine aggregate, concrete mixtures having satisfactory strengths can be produced with lower cement factors; however, these mixtures did not

seem suitable for field placement. Under plant-type manufacture, operating under rigid controls and employing external vibration, the drier, harsher mixtures can be used to economical advantage.

Because the absorption of water by lightweight aggregates fluctuates widely, depending on the porosity and the moisture content of the particles, it was found impractical to design a mixture with a rigid water-cement ratio. A more satisfactory design results from a specified slump. For comparable workability, the lightweight concretes will have appreciably less slump than corresponding sand and gravel concretes. In the initial phase of this study, it was found that expanded shale concretes having a slump of 1½ in. were easily placed and tended to flow readily under the action of a vibrator. Although no direct comparisons were made, it was estimated that the consistency of this concrete was similar to sand and gravel concrete having a slump of about 3 in.

PROCEDURE FOR CREEP AND SHRINKAGE STUDIES

To determine the total time deformation in the concrete mixtures selected for these tests, rectangular prisms 5 in. by 6 in. by 107 in. were cast. A flexible metal conduit was cast into the prisms along the longitudinal axis to permit the introduction of reinforcement for prestressing. Near each end of each prism, bars were cast into the concrete perpendicular to the axis to provide gage points 100 in. center to center. These bars were placed 1 in. from the top and bottom faces of the prisms. Small holes were drilled and countersunk in the sides of the bars to provide four pairs of gage points for each prism. The gages used to measure the change of length consist of a ½-in. diameter Invar rod with a fixed 60-deg point at one end and a dial indicator graduated to 0.001 in. at the other end. The dial indicator is provided with a 60-deg contact point and the indicator is mounted so the stem is on the extended axis of the Invar bar. During the measurement of length, the gage is supported at the ends and at four intermediate points so the deflection of the Invar bar is practically eliminated.

The six creep prisms involved in the currect phase of the project were cast one above another in a timber rack. To minimize the resistance to creep and shrinkage, the bottom forms were covered with sheet aluminum which was coated with a parting compound before the prisms were cast. During the study, the prisms have remained fully supported by the bottom form. The side forms, of plywood, were removed 24 hr

TABLE 2

CONCRETE MIXTURES USED IN TIME DEFORMATION STUDIES

Property	Aggregate A	Aggregate B	Sand & Gravel
Prism numbers	7, 8	9, 10	11, 12
Coarse aggregate, ⅜ in -3/16 in., lb per cu yd	307	431	0
Coarse aggregate, cu ft per cu yd	9.2	7.9	0
Fine aggregate, 3/16 in. -0 lb per cu yd	1,056	1,183	0
Fine aggregate, cu ft per cu yd	21.2	20.7	0
Gravel, ¾ in. -3/16 in. lb per cu yd	0	0	2,220
Gravel, cu ft per cu yd	0	0	20.0
Natural sand, lb per cu yd	173	0	907
Natural sand, cu ft per cu yd	2.0	0	9.0
Cement factor, sacks per cu yd	9.5	8.6	7.5
Admixture, lb per sack	0.25	0.25	0.25
Water/cement ratio, total water, gal per sack	6.4	7.5	4.7
Wet wt, pcf	108	104	153
Slump, in., average	1¾	1½	2¼
28-day compressive strength, psi	6,260	5,880	6,420
Secant modulus of elasticity at 28 days, psi	2,244,000	2,233,000	5,010,000

after casting. The ends of the prisms are provided with load distributing plates 1¼ in. thick having the same areal dimensions as the prism cross-section. These plates served as the end forms in casting the prisms.

In addition to the 107-in. prisms previously described, six shorter prisms were cast to provide shrinkage specimens. These prisms have the same cross-sectional dimensions as the longer prisms, and to maintain the same area-perimeter ratio, they also contain flexible conduit at the longitudinal axis. They are provided with the same arrangement of gage points as the longer prisms, but the gage length is 24 in. To obtain adequate sensitivity, the dial indicators used for these measurements are graduated to 0.0001 in. Other than the length and least reading of the dial indicator, the gages are similar to the ones used on the longer prisms. To minimize the resistance to shrinkage, the prisms are supported by planks that were covered with aluminum and coated with a parting compound. The ends of these prisms are sealed from the air by metal plates to simulate conditions of curing in the long prisms which have steel load distributing plates at the ends.

Two of the longer prisms and two shrinkage prisms were cast from each of the mixtures given in Table 2. In addition to the prisms, 12 standard cylinders were cast from each mixture to provide data on strength and modulus of elasticity. All concrete for the project was mixed in a Lancaster laboratory mixer in batches of about 1.3 cu ft. Consistency was controlled by a slump test on each batch. A slump of 1½ in. was

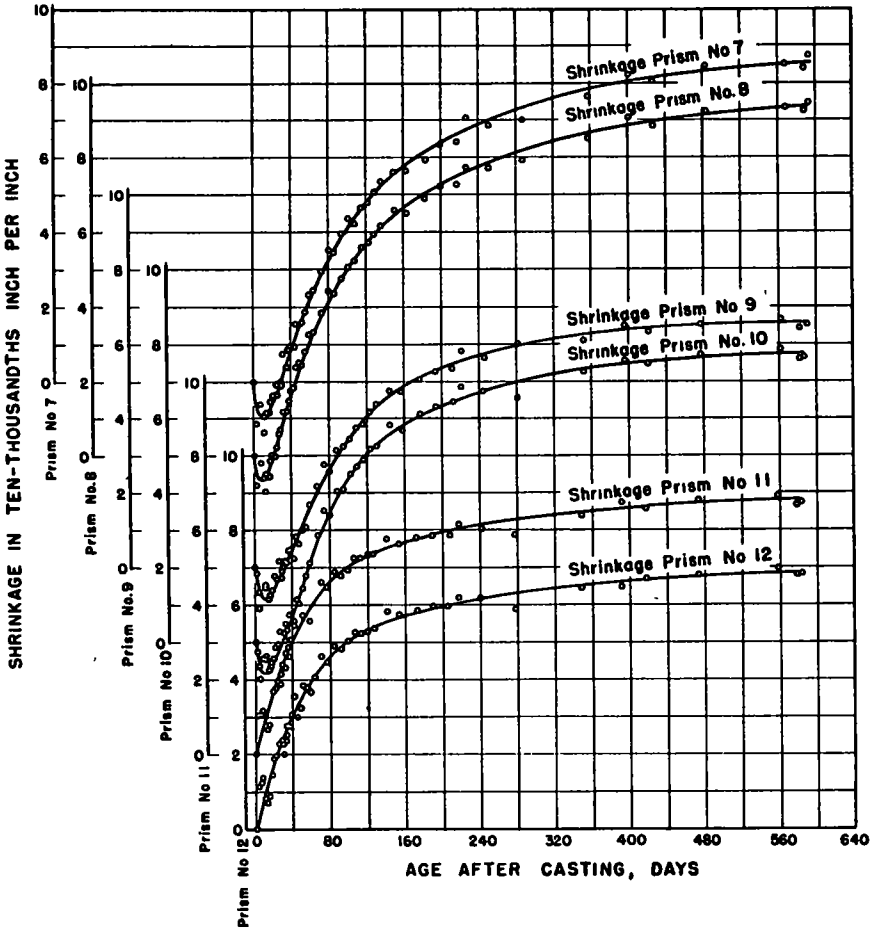

Figure 1. Shrinkage of test prisms.

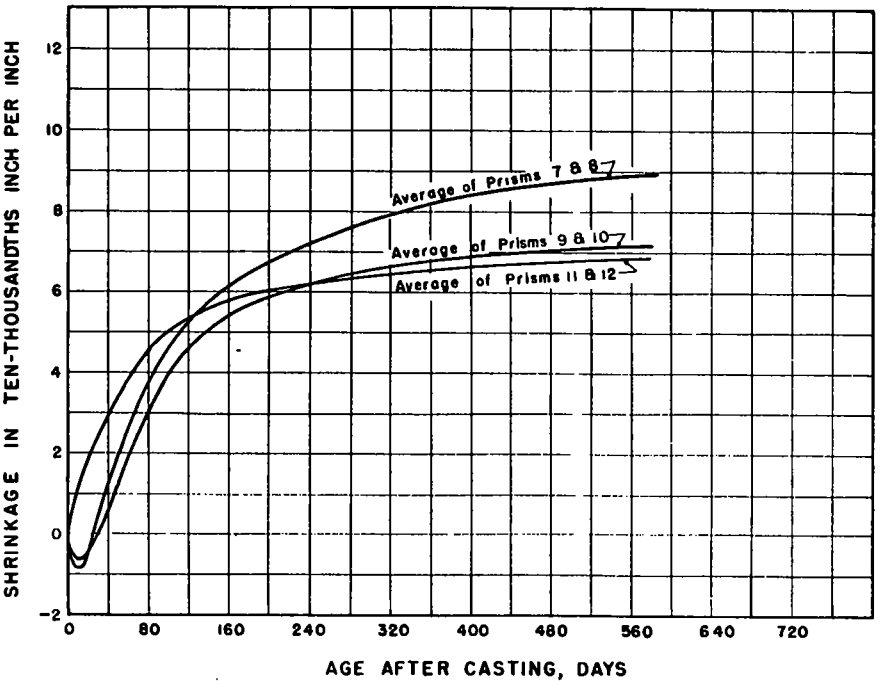

Figure 2. Average shrinkage of prisms.

chosen for the lightweight aggregates, and to obtain comparable workability, a slump of 2 to 3 in. was chosen for the normal-weight concrete. The average slumps are given in Table 2. The concrete was consolidated in the forms by means of hand rodding and tamping with wooden blocks. After the concrete had set, a wet burlap covering was maintained over the prisms for a 2-wk period. The cylinders were stored in a moist room from the time the molds were removed until they were tested. Three cylinders of each mix were tested at 28 days, 60 days, 180 days, and 1 yr.

Approximately 24 hr after casting the prisms, the side forms were removed and initial measurements of the prism lengths were made. To detect any differential shrinkage or creep, measurements were always made at each of the four gage positions on each prism. Periodic measurements were made on both sets of prisms during a 28-day curing period preceding the stressing of the longer prisms.

RESULTS OF SHRINKAGE MEASUREMENTS

During the 2-wk period the prisms were kept moist, some swelling occurred in those cast from expanded shale aggregates, whereas the prisms cast from sand and gravel showed shrinkage during this period. Measurements made on the longer creep specimens during the initial 28-day curing period showed some deviation from the values measured on the shrinkage prisms. The longer prisms indicated less change during this period than the shorter, shrinkage prisms. The creep prisms show a very slight shrinkage for the normal-weight concrete during the initial 2-wk period and the lightweight prisms show less growth than the shorter prisms of the same concrete. It is assumed that differences occurred in the moisture available to the prisms from the moist burlap used in curing; however, within the limit of the procedures used, all prisms recieved identical treatment. Figure 1 shows the shrinkage of each of the shrinkage prisms from the date of casting to the date of preparation of this report. Prisms 7 and 8 are from aggregate A, prisms 9 and 10 are from aggregate B, and prisms 11 and 12 are from natural aggregates. Each prism of these various pairs

was cast, cured, and stored under the same conditions as each of the others. The difference in shrinkage between individual prisms of the pairs of lightweight prisms cannot be attributed to any specific treatment. One possible cause of this difference is in mixing the concrete, because different batches of concrete were used in each prism. Other factors that might contribute to the difference are unknown variations that might have occurred in the placement or curing of the concrete or variations in the resistance of the prisms to sliding on the supports.

To compare better the shrinkage characteristics of concretes from the different aggregates, the average of each pair has been plotted in Figure 2. At an age of about 580 days, the shrinkage of prisms cast from aggregate B is 4 percent higher than the shrinkage of the normal-weight concrete, and the shrinkage of prisms cast from aggregate A exceeds that of the normal-weight prisms by almost 29 percent. Aside from this greater shrinkage of the prisms from aggregate A, the difference in shape of the normal-weight concrete curve from those of the lightweight concretes is significant. In considering the loss of prestress due to shrinkage, the shrinkage concerned is that which occurs subsequent to stressing the tendons. If, as was done on this project, the post-tensioned system is applied after a 28-day curing period, comparison of the curves of Figure 2 shows that the shrinkage of the sand and gravel concrete occurring after 28 days is appreciably less than that of either of the lightweight concretes. At the present time it is not possible to make precise estimates of the total shrinkage that will occur in the various mixtures; however, the general magnitude can be estimated with reasonable confidence. The average ultimate shrinkage for the specimens containing aggregate A will probably approach 0.0010 in. per in.; for specimens containing aggregate B, the ultimate value will probably be near 0.0008 in. per in.; and for the specimens using sand and gravel aggregates, the value will probably be between 0.0007 and 0.00075 in. per in.

These estimated values for ultimate shrinkage exceed by a wide margin the usual allowance contained in recommendations for the design of prestressed concrete members. Equations presented by the Bureau of Public Roads (9) can be reduced to an allowance for shrinkage of 0.0002 in. per in. for pretensioned members and 0.0001 in. per in. for post-tensioned members. Guyon (3) states that shrinkage may amount to 0.003 in. per in. for normal-weight concrete of a quality commonly used in prestressed construction. Lin (5) states that an average value of shrinkage strain would be about 0.0002 to 0.0004 in. per in. All of these references are for normal-weight concrete. No recommended allowances are presented for lightweight concrete.

Several other investigators have measured shrinkage amounts in various mixtures of structural quality concrete that are comparable in magnitude to the shrinkage values measured on this project. A paper by Raymond E. Davis and Harmer E. Davis (2) reports that unstressed specimens stored at 50 percent relative humidity showed a shrinkage of 0.00061 in. per in. at an age of one year. Shideler (6) reports ultimate shrinkage values for normal-weight concrete ranging from 0.000730 in. per in. for a 4,500-psi mixture to 0.000534 in. per in. for a 7,000-psi mixture. For corresponding lightweight concretes, Shideler found shrinkage values ranged from 6 to 38 percent higher than those for normal-weight concrete. These tests were conducted at 50 percent relative humidity. In a paper by Staley and Peabody (7) a shrinkage of 0.00087 in. per in. is reported for bars stored at 70 F and 50 percent relative humidity. Shrinkage values for various lightweight concretes ranging from a high of about 0.0009 in. per in. to a low of about 0.0004 in. per in. are reported by Jones and Hirsch (4) for specimens stored at an average relative humidity of 60 percent. The higher values were for the richer concrete mixtures.

On this project, no control of temperature and relative humidity was maintained. Temperatures were recorded each time measurements were made. The recorded values indicate the average temperature was about 72 F. From occasional measurements of relative humidity, it is estimated this value averaged around 50 percent. The average relative humidity of the storage area would be somewhat lower than that which would be expected in a typical outdoor installation in Oregon. This lower relative humidity would accelerate the time rate of shrinkage and probably increase the total amount. The paper by Jones and Hirsch (4) compares the shrinkage of specimens

stored inside with identical specimens stored in the field and exposed directly to precipitation and condensation. The average relative humidities were almost the same in each case and still the shrinkage of the outdoor specimens averaged only about one-third the amount measured on the indoor specimens.

The swelling characteristics of the lightweight concretes during the moist curing period raise a question concerning the effect of other curing methods on the total shrinkage and the time rate of shrinkage. The time rate of shrinkage would undoubtedly be appreciably different for steam-cured concrete. Other variations in method or duration of curing might produce significant changes in the time rate of shrinkage. The effect of these variations in curing methods is worthy of study because the time rate of shrinkage could be very significant in post-tensioned applications. For pretensioned applications, the usual method of curing would be by steam and the total shrinkage would be involved in creating stress loss in the prestressing steel.

PRESTRESSING DETAILS

To study creep, an initial stress of approximately 1,820 psi was applied to the concrete in the longer prisms after a 28-day curing period. To provide this stress, a standard "Prestressing Incorporated" unit having six 0.25-in. diameter wires was inserted at the longitudinal axis of each prism through the metal conduit cast into the prism. The wires in these units have double buttons at the ends — an outer button for stressing and an inner one for anchoring. The standard anchorage and stressing hardware was used.

In an effort to measure the difference in stress of various wires in a given wire group, type A-12, SR-4 resistance strain gages were installed on each wire. These gages have a 1-in. gage length and a trim width of $\frac{1}{8}$ in. Some difficulty was encountered in installing the gages on the small-diameter wires. The gages were sensitive to strain and in most cases reasonable readings were obtained from them; however, the variation in readings was large enough that the difference in stress in individual wires of a group was more or less obscured by the experimental errors in measurement. These data are not considered reliable.

To measure the total loss of stress in the wires caused by the creep and shrinkage of the concrete and the relaxation in the steel, pressure cells were installed between the end anchorage assembly and the bearing plate on each creep prism. Each pressure cell consisted of a 12-in. section of $2\frac{1}{2}$-in. outside diameter, 11-gage Shelby tubing of AISI 4130 steel. On opposite sides of each cell, dial indicators graduated to 0.0001 in. were installed near one end. The indicator stems rested on rods originating near the opposite end of the cell, providing measurements of elastic strain over a 10-in. gage length. One division on the dial indicators represents a change in load of about 280 lb. This sensitivity is equal to approximately $\frac{1}{2}$ of 1 percent of the initial applied force.

Immediately prior to stressing the steel tendons in a given prism, initial readings of the pressure cell indicators were recorded. Also, the prism length was measured at each of the four pairs of gage points, and the SR-4 gage readings were recorded for each of the six wires in the group.

To apply the prestress force to the prisms, a calibrated, center-hole hydraulic ram and pump was used. A 12-in. diameter pressure gage was used to measure the tensioning force during stressing. When the design load was reached, anchorage of the stressing unit was accomplished by an adjustable bearing collar. These threaded collars were used instead of shims to eliminate any slack that might exist in using shims. After the collar was brought into trim contact with the anchorage, the pressure in the ram was released, placing the load on the inner buttons on the wires. Because some seating deformation of these buttons was anticipated, the design load was reapplied, the slack was eliminated by adjusting the threaded bearing collar, and the pressure in the ram released again. The initial stress intensity in the wires was 170,000 psi, approximately 70 percent of the ultimate strength.

Immediately after the stressing operation was completed on a given prism, all measurements were repeated and gage readings recorded so the initial force and the elastic deformation of the prisms could be evaluated.

From the various measurements that were made, the initial force was evaluated by three different relatively direct means: (a) the design load was applied by a calibrated hydraulic ram; (b) after the hydraulic pressure was released, the deformation of the calibrated pressure cells gave an indication of the initial force; and (c) the total initial prestress force in the strands was obtained by summation of the indicated forces in the wires as obtained from the SR-4 gages. Except for one prism, the values obtained from the hydraulic ram and from the pressure cells agreed within about 1 percent. The pressure indicated by the SR-4 gages varied appreciably from that indicated by the other methods.

On the one prism having a significant discrepancy between the pressure indicated hydraulically and by pressure cell, it appears that an erroneous zero reading was obtained from the pressure cell. During the stressing operation, some slight damage may have occurred which caused a shift in the zero readings for the cell. The elastic shortening of the two prisms from this aggregate are almost identical, indicating the applied load was the same for each prism. For the one prism, the pressure cell indicated an initial stress about 8 percent higher than the stress corresponding to the hydraulic pressure recorded during the stressing operation.

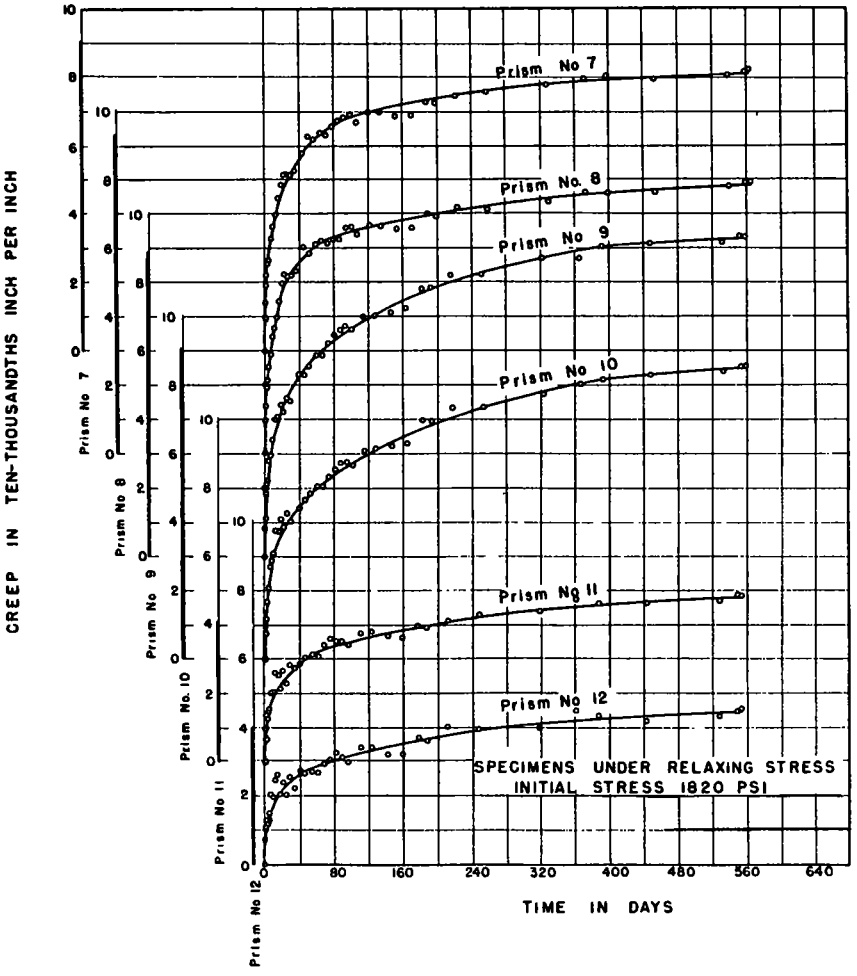

Figure 3. Creep deformation of prisms.

CREEP MEASUREMENTS

Immediately after the stressing operation was completed on an individual prism, the prism length was measured to obtain an initial reading for the time deformation measurements. The measurements of time deformation and the corresponding loss in prestress were repeated frequently at first and at gradually increasing increments of time as the rate of deformation diminished.

The change in length measured on the stressed prisms is, of course, the total time deformation resulting from the combination of shrinkage and creep. To obtain the deformation due to the application of stress, the average unit shrinkage measured on the two short prisms of a given aggregate was subtracted from the measurements on the stressed prisms of the same aggregate. Figure 3 shows the creep deformation for each of the six prisms subjected to stress. The origin of the ordinate on these curves is based on the length measured immediately after stressing and the abscissa originates from the date of stressing. To permit comparison, the elastic shortening of the prisms occurring during stressing is shown as a bar on the ordinate scale for each prism. Prisms 7 and 8 are from aggregate A, prisms 9 and 10 from aggregate B, and prisms 11 and 12 from natural aggregates.

The plotted points shown in Figure 3 represent the average of the four measurements made on each prism. The curves indicate the deformation attributable only to the application of stress because shrinkage effects have been deducted. The plotted points were not corrected for temperature fluctuations, but the smooth curves tend to make these corrections. The total creep is fairly similar for the four prisms cast from expanded shale aggregates although the average for the prisms from aggregate B is 11 percent higher than the average for aggregate A. The normal-weight concrete specimens show appreciably less creep than those of light-weight concrete. The average creep after 1½ yr for the normal-weight prisms is approximately 55 percent of the average of the four lightweight specimens. It is too early to predict with assurance what the ultimate creep will be for the various concrete mixtures, but from the slope of the curves, it would appear that the present value is from 85 to 90 percent of the ultimate creep to be anticipated. In studies conducted by other investigators (5, 8) it has been found that roughly 50 to 75 percent of the ultimate creep occurs during the first year; however, the studies leading to this determination were conducted under conditions of constant stress. In the present study, the relaxation of stress as the creep and shrinkage of the concrete occurs would encourage an equilibrium condition to exist at an earlier age than for specimens under constant stress. The present slope of the curves indicates the likelihood of this occurrence. Two factors exist to cause the reduced rate of creep demonstrated by the curves of Figure 3 in comparison to the rate of creep that would exist for specimens under constant stress. The first of these is that within the normal range of working stress of the concrete, the amount of creep is nearly proportional to the applied stress. By reducing the applied stress, the rate of creep would thus be reduced. The second factor is that as the applied stress is reduced, a portion of the initial elastic deformation is recovered. Actually, the curves shown in Figure 3 give the difference between the creep deformation and the recovered portion of the elastic deformation. Inasmuch as this difference is the quantity affecting the change in stress in the tensioning steel, separation of the items would needlessly complicate the determination of loss of prestress.

Creep in concrete is often discussed in terms of unit strain per unit applied load. This factor, sometimes called a "creep coefficient," assumes that the creep strain is directly proportional to the stress intensity. Many investigators have found an approximate proportionality to exist within the usual range of working stresses of the concrete. Because creep is a function of time, the creep coefficient is also a function of time—reaching an ultimate value after a period of several years.

For the current study, an exact expression of this type is not readily obtainable because of the diminishing stress intensity; however, a close approximation can be obtained by using a time-weighted mean between initial and final stress values. This was done in obtaining the values that follow. At the end of 1½ yr, the average creep coefficient was 0.56 microinches per in. per psi for prisms from aggregate A; 0.63 micro-

inches per in. per psi for prisms from aggregate B; and 0.30 microinches per in. per psi for prisms from sand and gravel. These values will be considered in more detail after the following discussion of loss of prestress.

LOSS OF PRESTRESS

The designer of prestressed concrete members must estimate the magnitude of the initial prestressing force required to assure the retention of some minimum design value after the ultimate creep and shrinkage of the concrete and the ultimate relaxation of the steel have occurred. The decrease in prestress from all causes can be estimated with reasonable accuracy if sufficient information about the physical characteristics of the concrete and steel is available. On this project, pressure cells were installed to measure the loss of prestress directly. Figure 4 shows the change in prestress for the various prisms expressed in terms of the initial prestress remaining. At the end of

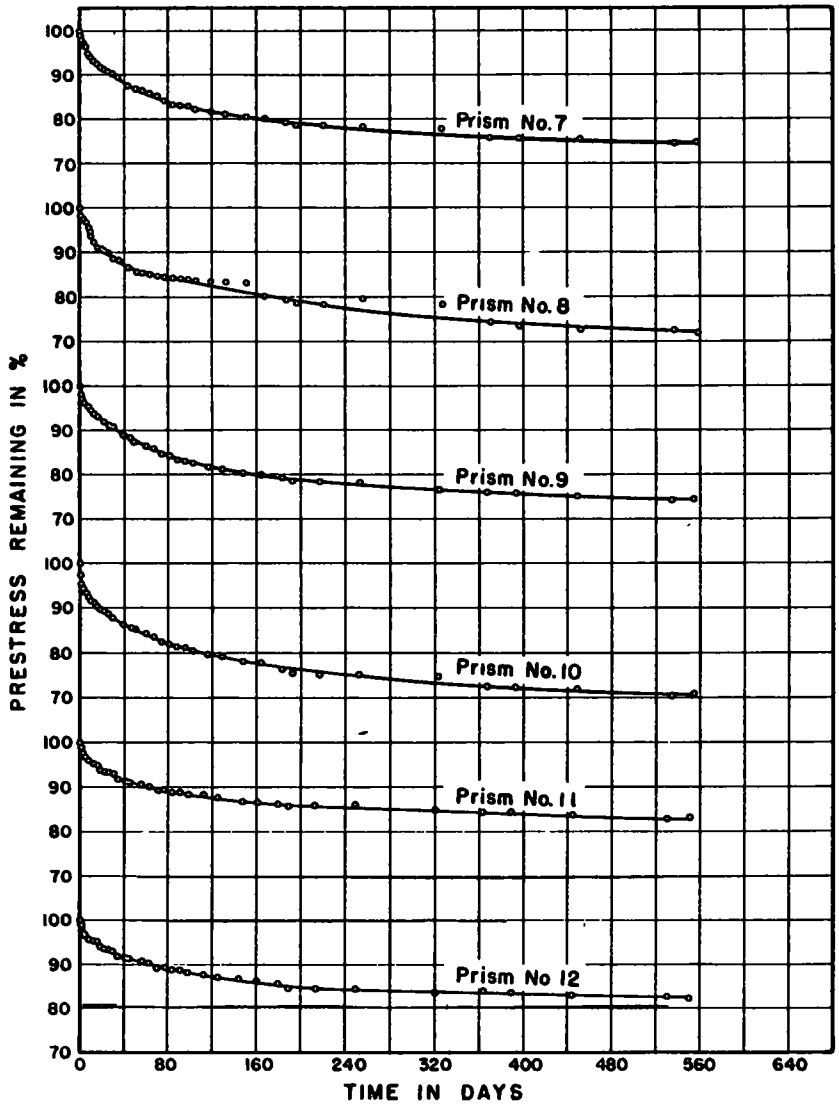

Figure 4. Loss of prestress curves.

18 months, the average values for the different aggregates indicate a 27 percent loss of prestress on prisms from both aggregate A and aggregate B and 17 percent for the normal-weight concrete. Calculations of loss of prestress based on the measured creep and shrinkage of the prisms agree quite well with the pressure cell indications. These calculations yield values for loss of prestress of 23 percent for prisms from both aggregate A and aggregate B and 13 percent for the normal-weight prisms. Comparison of the measured and calculated values indicate losses due to relaxation in the steel of 4 percent for each pair of prisms. A review of the individual prisms indicates relaxation losses ranging from 2.2 to 6.5 percent. The average value of 4 percent is a typical allowance for relaxation loss.

From the slopes of the various curves in Figure 4, it is estimated the ultimate loss of prestress for the normal-weight prisms will be about 20 percent, whereas the curves for the lightweight prisms will probably become asymptotic at a loss of about 30 percent. A large portion of these losses, particularly for the lightweight prisms, can be attributed to the shrinkage of the concrete occurring subsequent to stressing the units. In typical outdoor applications, the loss from this source would likely be reduced by having higher average relative humidities than those prevailing in the storage room housing the test specimens.

The values of loss of prestress measured on the test prisms would require some modification to permit their application in the design of prestressed concrete members. In the test specimens the concrete portions of the prisms are 105 in. long, whereas the length of the stressed steel is approximately 125 in.; the difference between these values being the combined length of the pressure cell, bearing plates, and miscellaneous anchorage hardware. In a typical beam of commercial dimensions, the difference in length between the concrete and the stressed steel is an insignificant percentage of the total length; whereas in the test prisms the steel is 19 percent longer than the concrete.

COMPARISON OF CONSTANT STRESS AND RELAXING STRESS

In the initial phase of this study of time deformations of lightweight concrete, prisms were cast from the same nominal concrete mixtures as were used in the current phase of the study. In the earlier specimens, an almost constant stress of 2,000 psi was maintained on the concrete by periodic retensioning of the stressing steel, whereas in the current study the steel was not retensioned. The time deformations of the specimens subjected to constant stress are shown in Figure 5. With this group of prisms, shrinkage was not measured separately — the curves show the sum of creep and shrinkage. Prisms numbered 1, 2, 3, and 4 are from two slightly different mixtures using aggregate A. Prisms 5 and 6 are from concrete using aggregate B. Inasmuch as details of these tests have been published in an earlier report (1), they will not be repeated here; however, Figure 5 is included because of the additional 3 yr of record not covered in the earlier paper. From the various curves, it is obvious that the time deformation of the prisms still continues, even after 4 yr.

To compare the creep characteristics of the prisms subjected to constant stress with those subjected to a relaxing stress, it is necessary to assume that the shrinkage of the prisms in the first phase was the same as that of the more recent group because shrinkage was not measured separately in the earlier study. With this assumption, the average creep coefficients 18 months after stressing the prisms subjected to constant stress were 0.57 microinches per in. per psi for aggregate A and 0.66 microinches per in. per psi for aggregate B. As mentioned in the preceding discussion of creep measurements, the creep coefficients for prisms in the current study were 0.56 microinches per in. per psi for aggregate A and 0.63 microinches per in. per psi for aggregate B. These values were obtained by using a time-weighted mean stress; therefore, the values should be comparable with those obtained for the constant-stress condition. Good agreement resulted for prisms from aggregate A, and the values for aggregate B prisms are quite similar for the two conditions. The earlier studies did not include specimens of normal-weight concrete, so no comparison is available for this material.

To obtain a visualization of the effect of the diminishing stress intensity, the coefficients for the current study can be computed on the basis of the initial stress level

rather than the mean stress used in computing the values above. On this basis, the average creep coefficients for aggregate A and aggregate B are 0.44 microinches per in. per psi and 0.49 microinches per in. per psi, respectively. At the age of 1½ yr these values are approximately 78 percent as large as the values previously cited. As the specimens become older, an appreciable increase in this difference is anticipated because of the reduced rate of deformation under the diminishing stress intensity. Calculations based on predicted ultimate values of creep in lightweight prisms indicate the coefficient for the relaxing stress condition will ultimately be approximately 55 percent as great as the corresponding value for concrete subjected to constant stress. This predicted value was obtained from the comparison of measurements on the two particular expanded shale aggregates under discussion and would not necessarily be applicable to concrete mixtures from other aggregates.

SIGNIFICANCE OF MEASUREMENTS AS APPLIED TO DESIGN

The recommended practices for the design of prestressed bridge members suggest

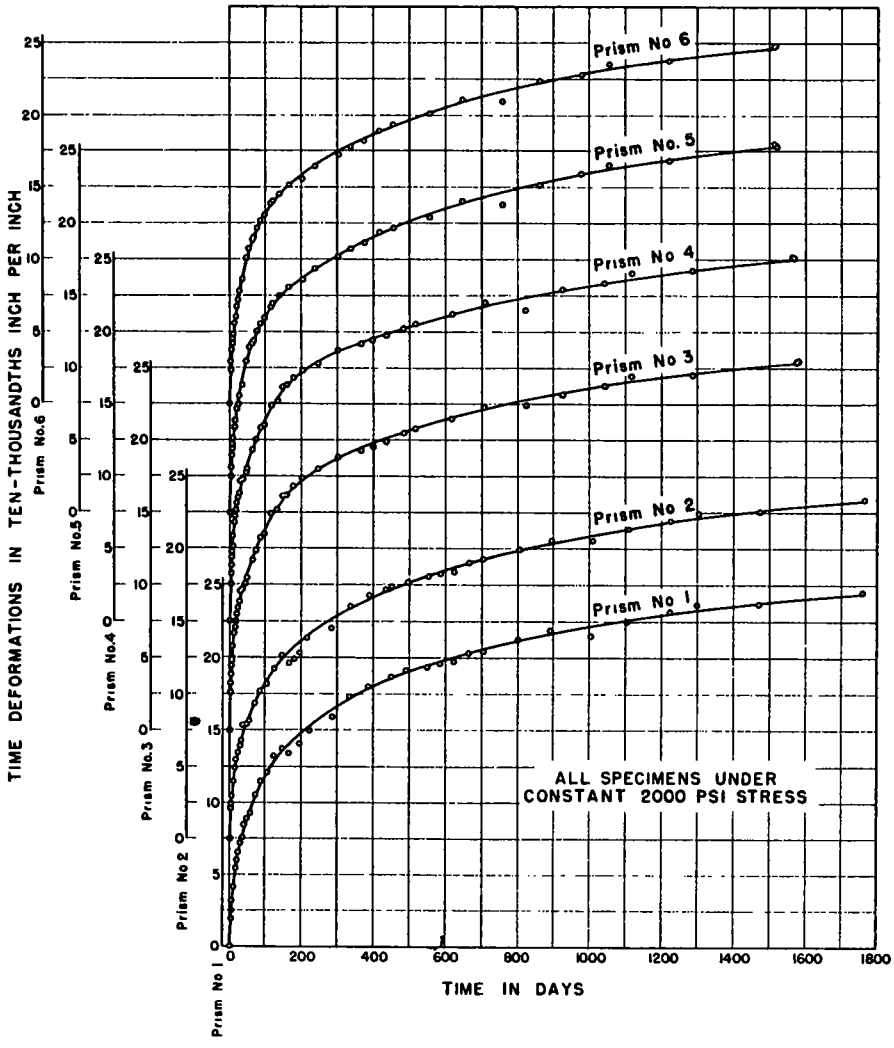

Figure 5. Time deformation curves.

that no tensile stresses be permitted in the concrete when the members are subjected to design loads. Compliance with this recommendation requires that a compressive prestress force of sufficient intensity to completely offset the design tensile flexural stresses be maintained. Because all concrete is subject to some shrinkage and creep after the application of a prestressing force, it is necessary to apply an initial prestress force somewhat larger than the required sustained force to provide for the estimated losses in stress accompanying the time deformations. The total loss of stress is comprised of loss due to shrinkage, loss due to creep, and loss due to relaxation in the prestressing steel. In pretensioned members, there is the additional loss caused by the elastic shortening of the concrete.

Present AASHO specifications permit the use of an assumed total loss in the steel of 25,000 psi for post-tensioned members and 35,000 psi for pretensioned members; or, the losses can be computed if suitable information on the materials is available. These values are for normal-weight concrete. Values for lightweight concretes must be estimated from tests on mixtures from the particular aggregates. For typical stress levels, these assumed losses of stress are similar in magnitude to those computed from equations in the Bureau of Public Roads "Criteria for Prestressed Concrete Bridges" (9). Recommended allowances in other literature on prestressed concrete design yield similar values for loss of prestress.

On this project, the normal-weight concrete specimens show considerably more shrinkage than the design literature anticipates which results in a total loss of prestress exceeding the recommended allowance for post-tensioned members. The ultimate shrinkage of the normal-weight concrete prisms will probably be between 0.0007 in. per in. and 0.00075 in. per in. Roughly 0.0005 in. per in. of this will occur subsequent to stressing, resulting in a stress loss in the steel of about 14,000 psi. The ultimate creep coefficient, based on the initial stress intensity, is estimated at 0.29 microinches per in. per psi. The average end-to-end stress at the centroid of the prestressing steel will vary appreciably among different beam designs, but a value of about 1,000 psi was determined for several beams that were reviewed. For a 1,000-psi concrete stress and the 0.29 creep coefficient, a loss of 8,100 psi in the steel would result, assuming a modulus of elasticity of 28×10^6 psi for the steel. If a relaxation loss of 4 percent is assumed for the steel, this loss would be 6,800 psi. The sum of these values indicates a stress loss of 28,900 psi in post-tensioned members of normal-weight concrete. Using a similar procedure, the calculated loss for pretensioned members is about 41,000 psi. This value includes an allowance for the total shrinkage and the elastic shortening of the concrete in addition to the allowance for creep and relaxation previously discussed. These calculated losses were based on measurements made on normal-weight concrete of a quality commonly used in prestressed members; however, the shrinkage occurring in an outdoor application, where higher relative humidities would be likely to prevail, might be appreciably less than that measured on this project. A smaller amount of shrinkage would, of course, reduce the loss of prestress.

In prior discussions, it was estimated the ultimate shrinkage of concrete using aggregate A will be about 0.0010 in. per in. and the ultimate creep coefficient for this concrete, based on the initial stress, will probably be around 0.49 in. per in. per psi. Due to the tendency of the lightweight prisms to swell during the initial moist curing period, almost all of the shrinkage has occurred subsequent to stressing. Using an estimated average end-to-end stress of 1,000 psi, a 4 percent relaxation loss in the steel, initial steel stress of 170,000 psi, and modulus of elasticity of 28×10^6 psi for the steel, the calculated loss of prestress in the steel is 47,500 psi for post-tensioned members. For pretensioned members, the estimated loss is 61,000 psi. The low modulus of elasticity of the lightweight concrete causes a loss of stress due to the elastic strain that is more than twice as great as that occurring in normal-weight concrete of comparable quality. Fortunately, this is an instantaneous loss that can be provided for by stressing the steel initially to a slightly higher stress level. At the instant the prestress force is released to the concrete, the elastic loss occurs, thus relieving the steel of the initial overstress.

For the concrete specimens using aggregate B, the estimated ultimate shrinkage is

0.0008 in. per in. and the estimated creep coefficient, based on the initial stress, is 0.55 in. per in. per psi. Applying these values to the assumed conditions previously discussed, the estimated loss of prestress would be 44,600 psi for post-tensioned members and for pretensioned members an estimated loss of 57,000 psi results.

Comparing the values in the preceding paragraphs, the estimated loss of prestress for the post-tensioned method is 65 percent higher for aggregate A and 55 percent higher for aggregate B than the comparable normal-weight concrete. For pretensioned members, the estimated losses of prestress for aggregate A and aggregate B concretes exceed the normal-weight mixture by 49 percent and 39 percent, respectively.

SUMMARY

These and previous tests have shown that expanded shale aggregates can be used to produce high quality concrete having adequate strength and workability to be suitable for use in the construction of prestressed concrete bridge members. The 28-day ultimate strength of the lightweight concrete mixtures used in the time deformation studies were in the vicinity of 6,000 psi for nominal cement factors of 9 sacks per cu yd.

For concretes having similar strengths and workability, the use of the expanded shale aggregates permits a reduction in weight of approximately 30 percent. The wet weight of the concrete using aggregate A was 108 pcf, for aggregate B the value was 104 pcf, and for the sand and gravel aggregate concrete, the wet weight was 153 pcf. The reduced weight of expanded shale members would make their transportation and erection more economical. In addition to this obvious factor of economy, the reduction in dead weight would in some instances permit flexibility in design not possible with the normal-weight concretes.

The modulus of elasticity of concretes produced from the expanded shales used in this study are approximately one-half as great as for normal-weight concretes of similar strength. The modulus of elasticity of the lightweight aggregate concretes averaged about 2,200,000 psi, whereas the value for the sand and gravel concrete was about 5,000,000 psi. The low modulus of elasticity is an important consideration in pretensioned members because the elastic shortening contributes directly to the loss of stress in the steel. In post-tensioned members this loss is not involved directly but requires consideration in members having numerous cables in which the loss in stress in first-stressed cables as subsequent cables are tensioned would sometimes be excessive. This loss can be effectively reduced by retensioning some of the earlier cables after all of the cables are stressed. Another factor requiring consideration with respect to the low modulus of elasticity is its effect on the deflection and camber of members cast from this concrete. The elastic deformation as well as the deformations caused by creep would be greater in the lightweight concrete than in normal-weight concrete.

Approximately 19 months after casting, the measured shrinkage was similar for the prisms cast from aggregate B and sand and gravel whereas the shrinkage of the concrete using aggregate A exceeded that of the other mixtures. The present slope of the curves indicates the ultimate shrinkage of the lightweight concretes will exceed that of the normal-weight mixture by approximately 30 percent and 10 percent for aggregate A and aggregate B, respectively. The shrinkage measured on the test prisms is appreciably higher than typical allowances cited in literature on prestressed concrete design. The high shrinkage measured on this project emphasizes the advantages to be realized in using concrete mixtures and curing methods that might reduce the shrinkage.

Eighteen months after stressing, the loss of prestress indicated by the pressure cells averaged 27 percent for each of the lightweight aggregates, whereas the value for the normal-weight concrete was 17.5 percent. Ultimate losses are expected to be around 30 percent for the lightweight prisms and 20 percent for the normal-weight prisms.

At an assumed concrete stress of 1,000 psi in a post-tensioned member, it was estimated the loss of prestress would be about 65 percent higher in aggregate A concrete and 55 percent higher in aggregate B concrete than in the sand and gravel mixture used in this study. For pretensioned concrete, the percentage difference would not be as great although the actual losses would be higher.

The greater loss of prestress occurring in lightweight prestressed members would, of course, be significant in design; however, it does not prohibit the use of expanded shale aggregates in prestressed concrete. The economies made possible by the reduction in weight could in many cases more than offset the added expense of designing for greater losses of prestress.

ACKNOWLEDGMENTS

This project was conducted by the Oregon State Highway Department in cooperation with the U.S. Bureau of Public Roads.

The planning and execution of the project was conducted under the administrative supervision of G. S. Paxson, Assistant State Highway Engineer, Oregon State Highway Department, and under the direct supervision of Roy C. Edgerton, Research Engineer, Oregon State Highway Department. The advice and counsel of these individuals contributed much to the success of the study.

REFERENCES

1. Beecroft, G.W., "Time Deformation Studies on Two Expanded Shale Concretes." HRB Proc., 37:90-105 (1958).
2. Davis, R.E., and Davis, H.E., "Flow of Concrete Under the Action of Sustained Loads." Proc., ACI, 27:837-901 (1931).
3. Guyon, Y., "Prestressed Concrete." Ed. by W.M. Johns, from the translations of A.J. Harris, J.D. Harris and T.O. Lazarides, Wiley, 543 pp., (1953).
4. Jones, T.R., Jr., and Hirsch, T.J., "Creep and Shrinkage in Lightweight Concrete." HRB Proc., 38:74-89 (1959).
5. Lin, T.Y., "Design of Prestressed Concrete Structures." Wiley, 451 pp., (1955).
6. Shideler, J.J., "Lightweight-Aggregate Concrete for Structural Use." Journal, ACI, 29:299-328 (1957).
7. Staley, H.R., and Peabody, D., Jr., "Shrinkage and Plastic Flow of Prestressed Concrete." Proc., ACI, 42:229-244 (1946).
8. Troxell, G.E., and Davis, H.E., "Composition and Properties of Concrete." McGraw-Hill, 434 pp., (1956).
9. "Criteria for Prestressed Concrete Bridges." U.S. Department of Commerce, Bureau of Public Roads, 25 pp., (1955).

Field Testing of Two Prestressed Concrete Girders

ADRIAN PAUW and JOHN E. BREEN, respectively, Professor of Civil Engineering, University of Missouri, Columbia; and Instructor in Civil Engineering, University of Texas, Austin (on leave of absence as Assistant Professor of Civil Engineering, University of Missouri, Columbia, 1959-61).

● THIS PAPER presents the procedures used and the results obtained in a cooperative research project designed to obtain field data to determine the actual behavior during construction and in service of one of the first prestressed concrete structures designed by the Missouri State Highway Department. During the initial planning stage of a pedestrian bridge across the Mark Twain Expressway in metropolitan St. Louis, it was decided to use prestressed, post-tensioned concrete girders. In discussing the design and specifications for the girders, it was suggested that worthwhile technical information could be obtained with a relatively low-cost field observation program.

The program was initiated with the design and manufacture of an instrumentation system which would meet the rugged demands of field service condition and yet provide reasonable accuracy. University of Missouri research personnel supervised the installation of all instrumentation appurtenances in the various elements of the structure, and collected all field data. Measurements were made before, during, and after the post-tensioning operations, before and after all major construction operations, and at appropriate time intervals following completion of the structure. To provide the additional information needed for interpretation of the field measurements, a companion test program was undertaken to measure the actual physical properties of representative samples of the materials used in the construction of this structure.

OBJECTIVES

The objectives of this investigation were to: (a) compare the actual prestress camber of the girder with the camber predicted by the design computations; (b) investigate the distribution of prestressing strains at several sections in the girder; (c) observe the changes in strains and deflections due to creep and shrinkage; (d) evaluate the composite behavior by comparing the observed dead load deflections due to the weight of the slab with the computed deflections; and (e) investigate the effect of differential shrinkage between the girders and the cast-in-situ slab.

INSTRUMENTATION REQUIREMENTS

This research project was primarily conceived as a field study wherein measurements were to be made at regular intervals over a long period of time. To obtain consistent data under these conditions it was considered desirable that the instrumentation used be relatively simple as well as flexible. After a preliminary study it was decided that the following measurements would best fulfill the objectives of the project: (a) concrete strain measurements at several different locations on the girders and in the cast-in-situ walkway slab to provide strain profiles at critical sections, and (b) girder and bridge deflection measurements to provide a record of the actual deflection or camber for correlation with theoretical computed values.

Consideration was given to the use of dynamometers or other instrumentation for determining the loss of tension in the prestressing tendons due to relaxation of the steel and to inelastic strains in the concrete. Although this latter information was felt to be most desirable, the ensuing complexity of the required instrumentation made measurements of this type infeasible. Furthermore, because the tendons were to be grouted soon after post-tensioning, such instrumentation would not have given accurate information on time-dependent losses but would only have reflected the dimensional changes in

the concrete at a particular section. It was therefore decided to estimate the relaxation losses in the tendons by means of a series of companion tests on representative samples under laboratory conditions.

INSTRUMENTATION SELECTION AND LOCATION

Figure 1 shows the completed bridge and its substructure. The bridge is oriented on a north-south axis above the expressway which runs east-west. In all references to the girders, the slab, or the completed bridge, directions will be designated in accordance with this orientation; that is, the east girder, the south end, etc.

On the basis of a preliminary investigation of available strain measuring devices, the basic instrument selected for the measurement of concrete strains was a Whittemore strain meter with a 10-in. gage length reading directly to unit strains of 10 microinches per in. A series of brass inserts were cast into the girders to furnish suitable gage points. The strain-gage points were selected to provide typical strain profiles at the critical sections shown in Figure 2. In general, the stations were placed as close to the end points, the quarter points, and the centerline as was feasible. The occurrence of transverse diaphragms at the quarter points necessitated a slight displacement in the gage point locations. Inserts were installed at each station on the inside faces and on the bottom of each girder at the locations shown in Figure 2. In addition to these inserts, during the concreting of the cast-in-situ walkway slab, strain-gage inserts were installed along the centerline of the walkway in the bottom and in the top surfaces of the slab at each station.

Figure 1. Completed structure.

In selecting a method for measuring the actual deflection or camber at various points along the girders, several schemes were investigated. Because of the small range of deflections anticipated, a system which would give an accuracy of a few thousandths of an inch was desired. Optical instruments available were not adopted because of their lack of sensitivity. After further preliminary study, it was decided that the most feasible method would be to install permanent reference points in the abutments to which a tensioned wire could be attached to serve as a baseline for these measurements. Then brass inserts, similar to those used in the strain measuring program, could be cast into the girder to serve as reference points. The actual deflection measurements would be made by using some mechanical means of determining the change in the distance between the baseline and the reference points on the girders. The system had to be further modified so that it could be used while the girders were still on the ground, before being placed on the abutments.

A baseline system was developed which consisted of a tensioned wire stretched between two fixed reference points. To provide reference points for the readings after the girders were in place on the abutments, special anchorage boxes were cast into the faces of the end piers about 10 in. directly below the center of each girder bearing plate. Four boxes were provided and installed, two in each pier. The position of the reference wire in each anchorage was fixed by passing the wire over a grooved bearing. The two boxes on the south pier were provided with attachments to anchor the wire, and the boxes on the north pier were provided with removable brackets. In setting up the baselines, wires were passed over an additional pulley on the removable brackets and calibrated 50-lb weights were attached to provide constant tension. The No. 23 gage steel music wire used was stressed to about 100,000 psi by the 50-lb weight. The wires were removed between tests and the boxes closed with cover plates.

To provide a reference line for deflection measurements before the girders were placed on the abutments, a temporary baseline system was developed. Two portable, demountable anchorage brackets were designed and manufactured so that they could be mounted on special plug inserts cast into the top surfaces of the girders above the bearing plates. At one end the bracket was provided with a fixed anchorage for the wire, whereas at the other end the bracket was provided with an arm and two additional grooved pulleys from which a 50-lb weight could be suspended. The initial deflection measurements were made using the temporary baseline and inserts spaced along the top surface of the girders. After the girders were installed on the piers, the deflection measurements were transferred to equivalent measurements by using the insert points on the bottom surface of the girder with the permanent baseline system.

Brass inserts were cast into the girders on both the top and bottom surface at the quarter- and center-points as indicated in Figure 2. All deflection measurements were made with the deflection meter shown in Figure 3. The meter incorporated a standard 12-in. Starrett height gage provided with a micrometer adjustment and with

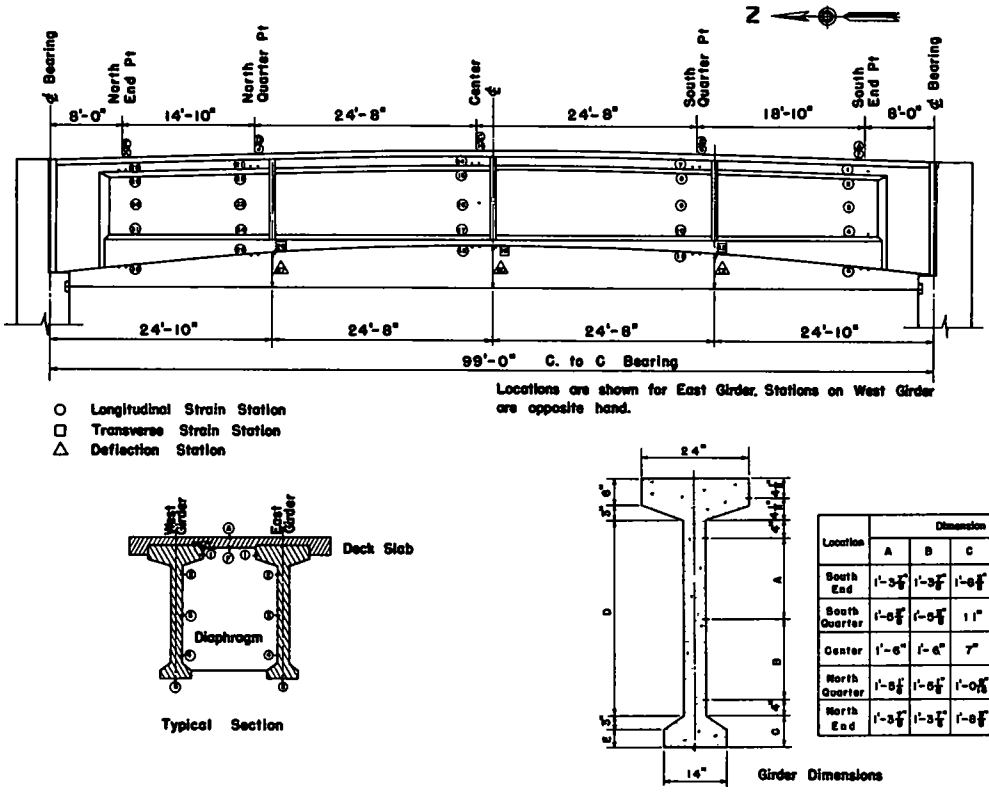

Location	Dimension				
	A	B	C	D	E
South End	1'-3 7/8"	1'-3 7/8"	1'-6 7/8"	3'-3 7/8"	1'-6 7/8"
South Quarter	1'-6 7/8"	1'-6 7/8"	11"	3'-6 7/8"	8"
Center	1'-6"	1'-6"	7"	3'-6"	4"
North Quarter	1'-6 7/8"	1'-6 7/8"	1'-0 7/8"	3'-6 7/8"	9 7/8"
North End	1'-3 7/8"	1'-3 7/8"	1'-6 7/8"	3'-3 7/8"	1'-6 7/8"

Figure 2. Location of gaging stations.

a vernier which permits measurements to be made to an accuracy of 0.001 in. Two modifications were made to make field measurements feasible. A leveling base plate was provided to which the height gage was firmly attached. The base plate had two fixed support points which rested directly in drilled holes in the reference strip, and an adjustable support which permitted leveling of the meter. A level bubble on the base plate indicated when the instrument had been correctly leveled. The second modification was the addition of an extension arm with a vibrating reed. When the movable head of the reed was brought into contact with the baseline wire, the vibration of the reed was damped, giving a sensitive indication of position.

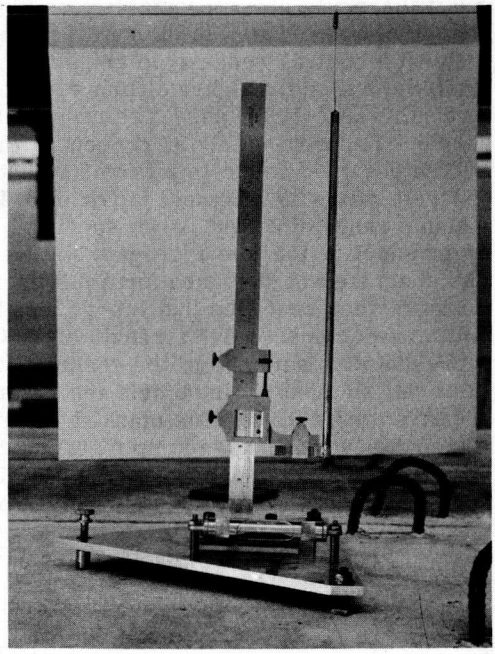

Figure 3. Deflection meter.

Preliminary experimentation and field experience showed that with this measuring system, deflection readings could be reproduced to within 0.002 in., except on unusually windy days when the wire would tend to oscillate. On such days extra care and patience were required, but on only one such day was the wind so severe as to actually interfere with the collection of deflection information. It was necessary to repeat the deflection readings for that date.

A complete description of the instrumentation system and drawings of all the special appurtenances have been given by Pauw and Breen (1).

COMPANION TEST PROGRAMS

A series of companion tests was carried out on representative samples of the materials used in the construction of the actual structure. The purpose of these companion tests was to provide additional information regarding the physical properties of the various materials used.

The post-tensioning system elected by the contractor was the Prescon system. Prescon tendons are manufactured units composed of a number of ¼-in. diameter wires laid in parellel. Positive end anchorage is insured by cold-formed ⅜-in. diameter button or rivet heads on both ends of each wire. All the specimens of the tendon steel furnished by the contractor had button heads formed on the ends, and they were equipped with stressing washers and spreader plates. The specimens were representative samples of the steel used in the main tendons. Information furnished by the contractor indicated that the tendons were manufactured from ¼-in. diameter cold-drawn, high-tensile wire, stress relieved in a lead bath at 600-800 F., and having a guaranteed minimum ultimate tensile strength of 240,000 psi.

The tension test specimens furnished consisted of three single-wire tendons, each of which was 36 in. long when measured between the rivet ends. In the initial tension tests, the specimens were gripped in a 60,000-lb universal testing machine in a manner simulating the way the wires are stressed in the girders; that is, the entire load was transferred to the tendon through bearing on the button heads. All three specimens displayed identical modes of failure, the failure occurring at the throat of the button head formed on the lower end of the wire as placed in the testing machine. The average ultimate strength was 238,300 psi.

Because all the specimens failed by separation of the cold-formed button head, it was decided to retest the specimens using conventional mechanical gripping devices to

see if there was any appreciable loss in ultimate tensile strength associated with this method of anchorage. In the retest procedure, the specimens were gripped mechanically with conical wedge-type grips near the center of the strands. All specimens exhibited a slightly higher ultimate strength in the retest and the average ultimate strength was 247,800 psi. The results indicate that the button-head anchorage device developed approximately 96 percent of the tendon ultimate strength.

The designed concrete mix was selected to meet the specifications for a class B-1 concrete mix with a cement factor of 6.4 sack/cu yd. An air content of 4 percent and a slump range of 2-3 in. were specified. The aggregates selected were Missouri River sand for the fine aggregate and Meramec River gravel for the coarse aggregate. The concrete was designed for a minimum 28-day compressive strength of 5,000 psi. It was further specified that the girders be post-tensioned after the concrete attained a minimum compressive strength of 4,000 psi. During the concreting operations, representative samples of the concrete were obtained for each truck load, and conventional slump and air content tests were made. The results obtained in these tests are given in Table 1. The marked variation in the concrete properties should be noted. Although several of the slump tests indicated greater slumps than permitted by the specifications, the contractor was permitted to complete the casting of this girder at his own risk with acceptance depending on the results of the compressive strength tests.

TABLE 1

CONCRETE PROPERTIES

East Girder Cast October 4, 1957					West Girder Cast October 28, 1957				
Truck	Slump (in.)	Air Content (%)	f'_c (psi)	E_c (psi)	Truck	Slump (in.)	Air Content (%)	f'_c (psi)	E_c (psi)
1	2.0	2.8	4,750	5.33	1	3.5	5.0	5,620	5.23
2		Rejected			2	1.0	3.8	5,690	5.72
3	2.5	5.0	5,580	5.14	3	6.0	7.5	4,950	5.04
4	7.0	7.5	4,600	5.42	4	4.0	7.5	4,630	4.69
5	2.25	4.1	5,720	5.59					
	Average		5,160	5.37		Average		5,190	5.27

Compressive strength tests were performed on standard 6- x 12-in. concrete cylinders as well as on special 3- x 6-in. cylinders. All cylinders were cast on the job site from representative samples of each truck load of ready-mix concrete. Cylinders from each batch were tested at various ages to provide information on the development of compressive strength. These tests indicated that although many of the batches did not reach the specified 5,000-psi compressive strength at 28 days, all attained the 4,000-psi strength specified for post-tensioning. The contractor was permitted to prestress the girders on December 5, 1957. As of that date the east girder was 61 days old and the west girder was 37 days old. The cylinder strength, f'_c, and the secant modulus of elasticity, E_c, at $f'_c/3$ were determined from tests of companion cylinders. The average values of these properties at the time of prestressing are given in Table 1. Because of the wide scatter and of the overlap in the values from the samples for both girders, it was felt that a single average value of E_c of 5.3×10^6 psi for the modulus was reasonable and this value was used to analyze the behavior of the structure.

DESIGN FEATURES

The design of the pedestrian overpass was governed by applicable requirements of

the Missouri State Highway Commission "Standard Specifications," the "Bridge Specifications" of the American Association of State Highway Officials, and the U.S. Bureau of Public Roads "Criteria for Prestressed-Concrete Bridges." The final design dimensions of the girders and of the composite bridge section are shown in Figure 4.

The design specified an initial prestress force for each girder of 424 kips based on a required effective post-tensioning force of 360 kips with the losses assumed equal to 15 percent of the initial force. A temporary increase of the allowable initial unit stress from 160,000 psi to 192,000 psi was permitted to allow temporary overstressing to reduce losses owing to friction and tendon relaxation.

Following award of the contract, the contractor submitted the tendon layout shown in Figure 4, consisting of five cables so arranged as to meet the specifications as to tendon area and the required location of the center of gravity. The upper and lower tendons (Mark A and E) each consisted of twelve ¼-in. diameter wires, each wire having a minimum specified area of 0.0491 sq in. The three interior tendons (Marks B, C, and D) were each made up of ten wires of the same diameter and area. The contractor proposed to use an initial transfer stress of 160,000 psi, corresponding to an initial prestress force of 424 kips; and a working stress after losses of 136,000 psi, corresponding to the specified 360 kip effective post-tensioning force. The order of post-tensioning of the tendons was specified as Mark C, D, B, E, and A.

CONSTRUCTION OPERATIONS

The girders were cast and stressed at a location adjacent to the bridge site. The soffit forms were supported by timber sleepers set in the ground and were adjusted to grade by the use of blocks and wedges. The girders were stressed on December 5, 1957, after the cylinder tests indicated that the girders had reached the necessary

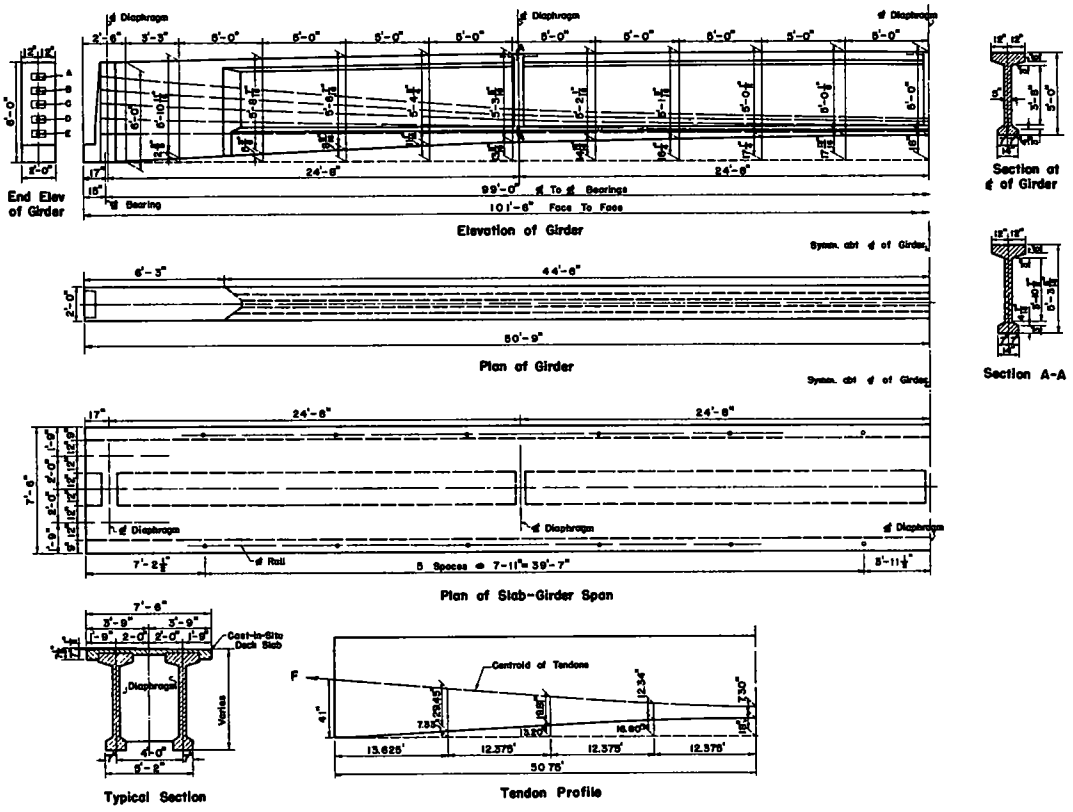

Figure 4. Design dimensions.

4,000-psi minimum compressive strength specified for post-tensioning. Strain and deflection measurements were made after tensioning each cable. Approximately two weeks after tensioning, the tendons were grouted. The girders were raised into place on the piers on January 27, 1958. An auxiliary bracing system was used to increase the lateral stiffness of the girders to permit handling of the long, slender sections with a minimum danger of failure. This bracing system consisted of a set of auxiliary posts and a pair of tensioned cables acting as a double king post truss. It proved quite effective in increasing the lateral resistance of the girders. However it introduced unbalanced strains due to lateral bending. Unfortunately the strain instrumentation was provided on only one side of the girders, and it was therefore not possible to measure the transverse strains which this system might have induced in the girders, thus adding an additional unknown factor.

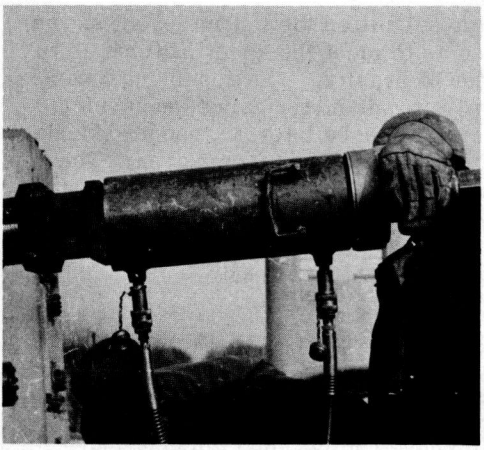

Figure 5. Stressing operation.

After the girders had been set in place on their bearing surfaces, deflection measurements were made to transfer the deflection baseline from the temporary reference line on top of the girders to the permanent baseline installed in the piers. Deflection and strain measurements were continued at regular intervals following erection of the girders.

On April 30, 1958, the deck slab and connecting diaphragms were placed. Prior to the concrete placement temporary shores were installed under each girder at the quarter-points and at the center of the span using sections of tubular scaffolding. The purpose of these shores was to minimize the deflection due to the dead load of the deck slab by developing composite action of the slab with the girders before the total weight of the slab was transferred to the structure. The results of this procedure are discussed in a subsequent section. After completion of the top slab and of the diaphragms which joined the girders together, a hand railing was added and by June 17, 1958, the bridge was completed.

FIELD MEASUREMENTS

At the various stages of construction, complete sets of field measurements were made except when measurements were rendered impossible by the construction procedures. The original readings of the strain and deflection instruments at the respective stations immediately prior to the commencement of the post-tensioning operation has been selected as the arbitrary reference base. Camber is designated by a positive change in elevation and deflection by a negative change. Tensile strain is designated by a positive change and compressive strain by a negative change.

At the time of stressing, the girders rested on the soffit forms and it was not possible to make measurements on the bottom strain gaging stations; hence, strains in the lower fibers could not be referenced to initial measurements before stressing. These measurements were therefore interpreted on the basis of an assumed linear strain distribution in the girder section 53 days after stressing, at which time the bottom strain gaging stations were first accessible. The linear strain distribution was determined from the measured strains at the other longitudinal strain gaging stations at that section on that date. A correction factor was then computed to make the bottom strain reading correspond with this assumed strain distribution. All subsequent strain measurements for the bottom stations were corrected by this same factor. Discussion of the significance of the data obtained is presented in subsequent sections as they pertain to the various subjects under study.

POST-TENSIONING PROCEDURE

The basic objective of post-tensioning is to secure the specified level of prestress in the girder. To accomplish this objective, a means of measuring the actual prestressing force applied as well as a reasonable method of predicting changes in this force and of estimating the prestress level at a given section and at a given time are required.

In the Prescon system, tension is applied to the tendon with a jack which bears on a stressing cage placed between the jack and a special end plate cast into the end of the girder. Then tendon is gripped by an adaptor rod connected to a special stressing washer which bears against the rivet heads formed on the individual wires. When the jack is activated, the stressing washer is forced away from the end bearing block until a desired elongation in the tendon is obtained. Shims are then inserted between the bearing block and the stressing washer. When the jack is released, the force is transmitted to the shims. Figure 5 shows the ram attached to tendon B and the shim plates inserted between the bearing plate and the stressing washer. In this figure the jack has not yet been released to transfer the force to the shim plates. Tendon A, located directly above the ram, is still in its original position flush with the end bearing plate, because it has not yet been stressed. Tendon C, located below the ram, is in its final stressed position, and the shims, which prevent the stressing washer from returning to its original position, can be seen plainly.

In the post-tensioning procedure used for these girders, the tendons were jacked simultaneously at both ends to reduce frictional losses, and shims of proper length were installed prior to release. Ample clearance was available for inserting the shims because the tendons were temporarily overstressed to reduce friction and creep losses. Because only one of the two jacks had been adequately calibrated in the equipment provided for the post-tensioning operation, the tendon stress was controlled by measuring the tendon elongation, and the jack pressure gage readings were observed only as a check for correlation purposes.

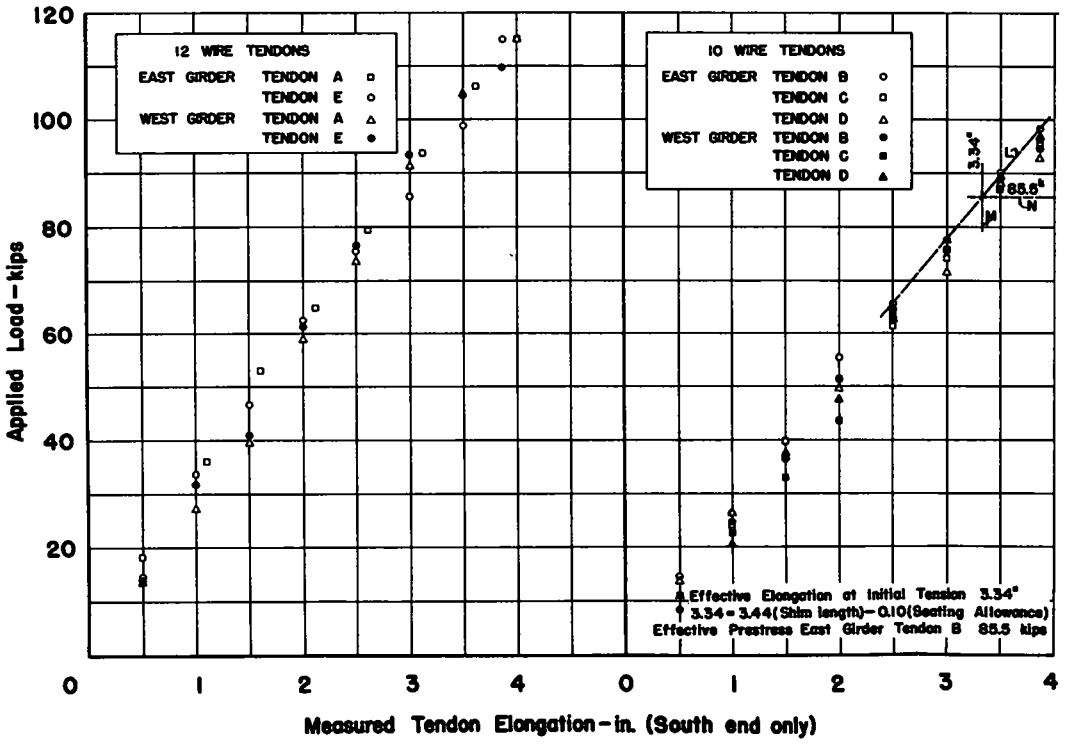

Figure 6. Tendon elongation.

The required length of the shims was calculated on the basis of elastic elongation of the tendons at the desired transfer stress of 160,000 psi. In addition to this the manufacturers recommended that the computed elongation be increased by 0.19 in. to allow for seating of the rivet heads. No allowance on the apparent elongation was made for the effect of elastic compression of the concrete. Based on an average concrete stress of 800 psi, this factor would amount to an additional elongation of 0.18 in. Because shims are used at both ends of the tendon, the net correction is divided by two to give a shim length of 3.44 in. This recommended shim length was modified in the field to correct for initial slack in certain of the tendons.

The initial stressing force, F_i, applied to the tendon was calculated from the field observations of tendon elongations and the corresponding pressure gage readings, and from the jack-calibration data furnished by the contractor. The relationship between the applied force, F, as computed from the pressure gage observations, and the observed tendon elongations, Δ_s, is shown in Figure 6. From these curves the maximum total force applied to the east girder is estimated to have been 516.3 kips corresponding to a stress of 194.7 ksi and the maximum force applied to the west girder, 512.7 kips, corresponding to a stress of 193.4 ksi. These temporary stresses while over-tensioning were slightly more than the 192 ksi allowed by the specifications and considerably higher than the 180 ksi which the contractor had proposed to use.

After holding the over-tensioning force in each tendon for a period of 5 min, shims were inserted and the jacks were then gradually released, transferring the load to the permanent anchorage devices. The initial effective prestress at the anchorage after release of the over-tensioning is designated as F_o and was not measured directly. To estimate its probable value, a semi-graphical method was used based on the tendon characteristics displayed in the initial tensioning and the final tendon elongation determined from the wedges. For example, for tendon B of the east girder, the relationship between the applied prestressing force, F, and the tendon elongation, Δ_s, was obtained for the final stress level in the girder. This relationship is depicted by the dashed line, L, in Figure 6. It was then assumed that on release of the over-tensioning force the tendon force would follow this relationship during the unloading stage. Line M defines the assumed final elongation, Δ_{sf}, of the tendon. This elongation was computed from the known value of the shim length and the manufacturer's suggested value for the tendon seating allowance. In the example, the tendon shim had a length of 3.44 in. and after deducting the 0.10 in. seating correction, Δ_{sf}, is 3.34 in. The effective initial prestress force, F_o, was found to be 85.5 kips as determined by the horizontal line N passing through the intersection of lines L and M. A similar procedure was used for each of the ten tendons. It is recognized that these procedures are somewhat approximate, but in view of the inaccuracies in the initial stress measurement inherent in the system used, a more refined method for estimating the transfer stresses did not appear to be warranted. Computed on this basis, the total effective transfer stress at the jack end, F_o, was 452.4 kips for the east girder, and 450.3 kips for the west girder. Both of these values are approximately 6 percent higher than the design value of 424 kips.

EFFECT OF CABLE FRICTION AND WOBBLE ON THE PRESTRESS FORCE

The tendon forces at the jack were determined from the applied forces and corresponding elongations at the point of jacking. It can be shown, however, that the observed stress at the jack is not applicable throughout the whole length of the tendon. For example, tendon B on the east girder is composed of ten wires, each wire having an area of 0.0491 sq in. In the companion test program the elastic modulus of the wire, E_s, was found to be 28.8×10^3 ksi. Inasmuch as the tendon was stressed simultaneously from both ends, the recorded tendon elongation at one end Δ_s, of 3.875 in. corresponds to the elongation for an effective length, L, of 602 in.; that is, the distance from the point of application of the jack to the centerline of the beam. Solving the elastic deformation equation, it can be shown that an average force of 91.0 kips is required to produce the measured elongation. However, the actual measured initial stress for tendon B, F_i, corresponding to this value was 98.23 kips. Thus it can be

seen that in this particular instance the stress at the jack was about 8 percent greater than the average stress required for the desired elongation.

The difference between the average tendon stress and the stress applied by the jack is the result of tendon friction and the so-called "wobble" effect. Because the tendon is curved, it rubs against the tendon sheath as it is elongated, developing a friction force which is a function of the curvature and the coefficient of friction. Similarly, additional frictional forces are introduced due to small local dislocation of the sheath, which causes the tendon to rub against the sheath when the tendon is tensioned. The force loss due to these dislocations is called the "wobble effect." This problem has been the subject of extensive research (2, 3), and it has been found that the magnitude of the frictional and wobble effects can be approximated by an exponential expression governed by the physical characteristics of the post-tensioning system, and the length and curvature of the tendons.

In the case of a girder where all tendons have the same approximate length so that the length, L, can be assumed constant, the relationship between the applied prestress force, F_i, and the effective force, F_x, at any point a distance x from the point of application of the prestress, can be written as a function of a combined friction-curvature and wobble factor β, thus

$$F_x = F_i e^{-\beta x} \tag{1}$$

It has been shown (2, 3) that for small frictional losses, that is, when β is small, the tendon elongation Δ_S corresponds closely to the elongation computed on the basis of assuming the average tendon force equal to $\frac{F_i + F_L}{2}$ where F_i is the applied force at the jacking end of the tendon and F_L is the reaction at the anchorage end. In the case of a beam simultaneously stressed from both ends, F_i is the force at the jacks and F_L is the force at the assumed point of zero slip; that is, the center of the beam. For this assumption

$$\Delta_S = \frac{F_i + F_L}{2} \frac{L}{E_S A_S} \tag{2}$$

Substituting the observed values of the jacking force, F_i, and the measured elongation, Δ_S, and using the measured values of A_S and E_S, Eq. 2 was solved for F_L. Then using this value for F_x and letting x be equal to one-half the span length, the frictional loss coefficients were computed by solving Eq. 1 for β.

If the girders had not been initially over-tensioned and then released, the tendon force at any section could have been computed directly from Eq. 1, and the distribution of the prestress force along the girder would have been as shown in Figure 7(a). However, the partial release of the over-tensioning force, reduced the initial force, F_i, to the transfer force, F_o. The release of the initial tendon force reversed the direction of the frictional forces along a portion of the tendon adjacent to the jacking end. After release, the tendon force in this region is then defined by

$$F_x = F_o e^{\beta x} \tag{3}$$

As shown in Figure 7(b) for values of x greater than z the force profile developed during over-tensioning remains undisturbed. The value of z can be computed by solving Eq. 1 and Eq. 3 simultaneously for x equal to z. As can be seen from Figure 7(b) and (c), the effective prestressing force at any section a distance x from the point of jacking can be computed as follows:

$$\text{for } x \leq Z \qquad F_x = F_o e^{\beta x} \tag{4}$$

$$\text{for } x \geq z \qquad F_x = F_i e^{-\beta x} \tag{5}$$

Values of the tendon force, F_x, were computed on this basis at the eighth-points

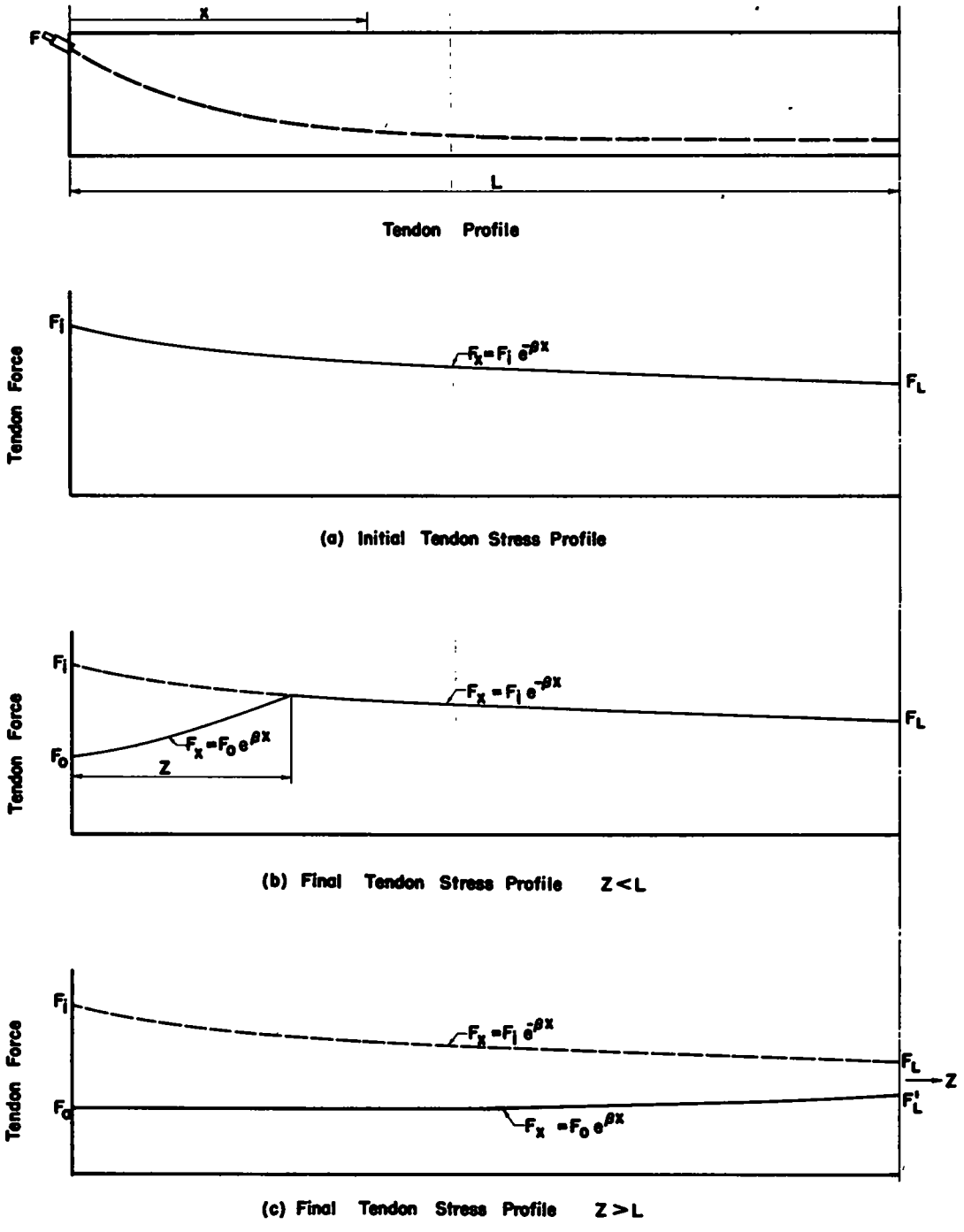

Figure 7. Typical tendon stress profiles.

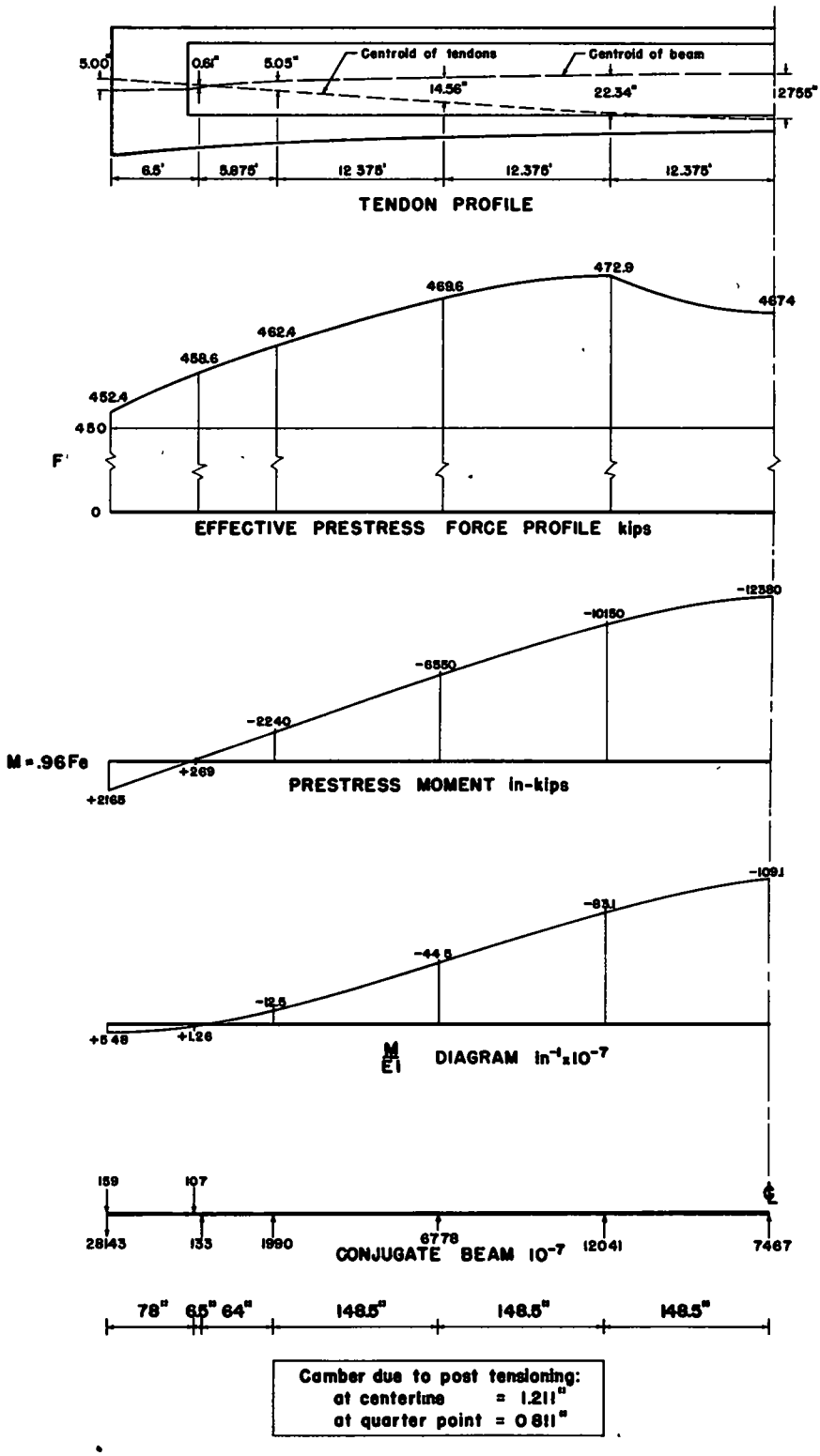

Figure 8. Prestress camber calculations.

and because of the effect of reversed friction, the majority of the tendon force profiles were similar to that shown in Figure 7(b). The combined profile for the east girder may be seen in Figure 8. Computed values of the total tendon force at initial transfer range from 450.3 kips to 472.9 kips as compared to the specified value of 424 kips. This discrepancy points out the need for careful consideration of frictional effects during the post-tensioning operations, because for structures in which the prestress camber is closely balanced by the dead load deflection an error of only 10 percent in the applied prestress force can result in relatively large deflections.

DEFLECTIONS

The girder dead load deflections were computed by the conjugate beam method using the gross section for determination of the moment of inertia, assuming an average modulus of elasticity for the concrete, E_c, of 5.3×10^6 psi and an average unit weight of 150 pcf. The computed centerline deflection was 0.960 in. and the quarter-point deflection, 0.667 in., for the dead load of the girder alone.

The deflection due to the magnitude and eccentricity of the prestressing force was also calculated by the conjugate-beam method. The calculations for the east girder are shown in Figure 8. The calculations are based on an applied prestress moment which was calculated from

$$M_x = 0.96 \; F_x e \qquad (6)$$

in which

e = tendon eccentricity as shown in Figure 8:
F_x = effective prestress force as calculated by Eqs. 4 and 5; and
0.96 = a factor introduced to correct for the loss in prestress due to elastic shortening of the girder when subsequent tendons were stressed. The value of the factor was determined by superposition of strains at the tendon centerlines.

The computations shown in Figure 8 show that the effect of the prestress would result in a 1.211-in. camber at the centerline of the east girder and a 1.196-in. camber in the west girder. The computed camber at the quarter-points was 0.811 in. and 0.800 in., respectively.

The actual computed deflection or camber is the algebraic sum of the computed dead load deflection and the computed prestress camber. The computed net camber is therefore 0.251 in. and 0.236 in. at the centerline of the east and of the west girder, respectively, and 0.144 in. and 0.133 in. at the respective quarter-points. The correlation of these results with the actual measured values is shown in Figure 9. Considering that the total range of the camber and the deflection calculated for the centerline of the east girder is the sum of 1.211 in. and 0.960 in., or a total of 2.171 in., the deviation of the measured value + 0.292 in. from the computed value 0.251 in. represents an error of less than 2 percent. Similar checks showed that the greatest deviation at any point was only 4.8 percent.

In view of this close agreement between the computed and the observed deflections, the procedure outlined is believed to present a satisfactory method for computing elastic deflection or camber in a statically-determinate prestressed concrete beam.

Because time-dependent inelastic phenomena such as creep and shrinkage are very important factors in prestressed concrete, they must be considered in the prediction of the resultant net deflection after a specified time interval. Lin (2) proposes a formula of the form

$$\Delta_t = C_t \, (\Delta F_t + \Delta_{DL}) \qquad (7)$$

in which

Δ_t = deflection at any time, t, after stressing;
C_t = creep coefficient expressing the relationship between the deformation at a particular time, t, and the initial elastic deformation;

Δ_{Ft} = deflection due to the effect of effective tendon force at time, t; and
Δ_{DL} = deflection due to the effect of dead load.

This method assumes that the deflection at a particular time may be expressed as a ratio of the net effect of the tendon force acting at that time and the dead load of the member. From the general nature of creep deformation in concrete it is known that a substantial portion is not generally recoverable (4). In cases in which relatively large losses in the effective tendon force take place gradually, substantial creep effects are developed at a relatively early stage. The proposed formula ignores these effects in computing long-time deformations.

If no cognizance were taken of the effect of the tendon stress losses, the deflections could be predicted by the formula

$$\Delta_t = C_t (\Delta_{F_0} + \Delta_{DL}) \qquad (8)$$

in which Δ_{F_0} is the deflection due to the initial effective tendon force. Obviously this method is in error due to the known loss in camber resulting from tendon stress loss; these values can be regarded, however, as representing the extreme upper limit for residual camber. The previous example can be considered to give the extreme lower limit for deflection of the member. The actual deflection pattern should fall somewhere in between these limits.

If it were possible to express the creep coefficient and the tendon stress losses as time functions, then a theoretically exact solution could be obtained by the use of difference methods. The creep coefficients and the various tendon stress loss components can however, at best, only be determined in an approximate manner. The average of these two limits was therefore used as a reasonable method for predicting the resulting deflections. This approximation results in the expression

$$\Delta_t = C_t \left(\frac{\Delta_{F_0} + \Delta_{F_t}}{2} + \Delta_{DL}\right) \qquad (9)$$

when Eq. 9 is further modified to include the deflection due to loads applied for short-time periods or after most of the creep losses have taken place,

$$\Delta_t = C_t \left(\frac{\Delta_{F_0} + \Delta_{F_t}}{2} + \Delta_{DL}\right) + \Delta_{AL} \qquad (10)$$

in which

Δ_{AL} is the deflection due to short time loads.

In Figure 9 the measured girder deflections are compared to the theoretical values as computed from Eq. 10 using the data for the east girder. The creep coefficients, C_t, were obtained from an assumed creep curve based on the shape of an idealized curve recommended by Lin (2), but modified for an over-all creep coefficient of 3.0 in accordance with normal design assumptions. The mangitudes of the tendon relaxation losses were based on the manufactuer's recommendations, with a maximum value of 4 percent. Tendon stress losses, ΔF_e, due to elastic shortening were based on an assumed average uniform allowance of 4 percent as previously explained, and the stress loss, ΔF_c, due to the effect of concrete creep was calculated from the formula

$$\Delta F_c = (C_t - 1) \frac{f_{c_{ave}} E_s A_s}{E_c} \qquad (11)$$

in which $f_{c_{ave}}$ (the average concrete compressive strength over the entire girder) was determined as 820 psi by averaging the values of the calculated stress profiles. The theoretical deflection values computed on the basis of these assumed tendon stress losses are in good agreement with the measured deflections for the initial 150 days prior to construction of the deck slab and appear to confirm the assumptions in Eq. 8.

The construction operations involved in the casting of the deck slab, removal of the shores, and placement of the hand railing took place over a period of several weeks and for the purpose of simplicity the over-all deflection due to these various operations

is shown as acting at 150 days. The actual schedule consisted of placing of the deck slab on day 146, removal of the shores on day 153, and completion on day 194.

The theoretical deflections due to the weight of the cast-in-situ slab on removel of the shores were computed on the basis of full continuity of the precast girders for the weight of the deck slab only at the time of placement of the deck slab, and for full composite action between the girders and the deck slab at the time of removal of the shores. The observed deflections were of a smaller magnitude than those indicated by the computations.

A further discrepancy in the readings was caused by the construction procedure required in preparing the girders to receive the deck slab. In erecting the form-work for the deck slab and girder-connecting diaphragms, the girders were aligned vertically with crossed guy wires to enable correct placement of the forms. This alignment was performed between the set of readings taken at 139 days and those taken at 146 days. A close inspection of Figure 9 shows that the east girder stations were depressed and the west girder stations were elevated approximately equal amounts during that period. This construction practice resulted in the shifting of a portion of the load from one girder to the other. The effect of such corrections is almost impossible to predict, and interpretation of the data is extremely difficult.

However, it is possible to obtain a qualitative appraisal of the effectiveness of shoring to take advantage of composite action for deflection control. Had the deck slab been carried by the non-composite girders (that is, no shoring) the deflection at the center point would have been 0.337 in. whereas the actual values measured with composite action were less than 0.2 in. However, it is important to note that these data are still inconclusive because of the fact that elevation changes of the deflection stations (which were also the location of the shoring points) occurred with the shores in place. This

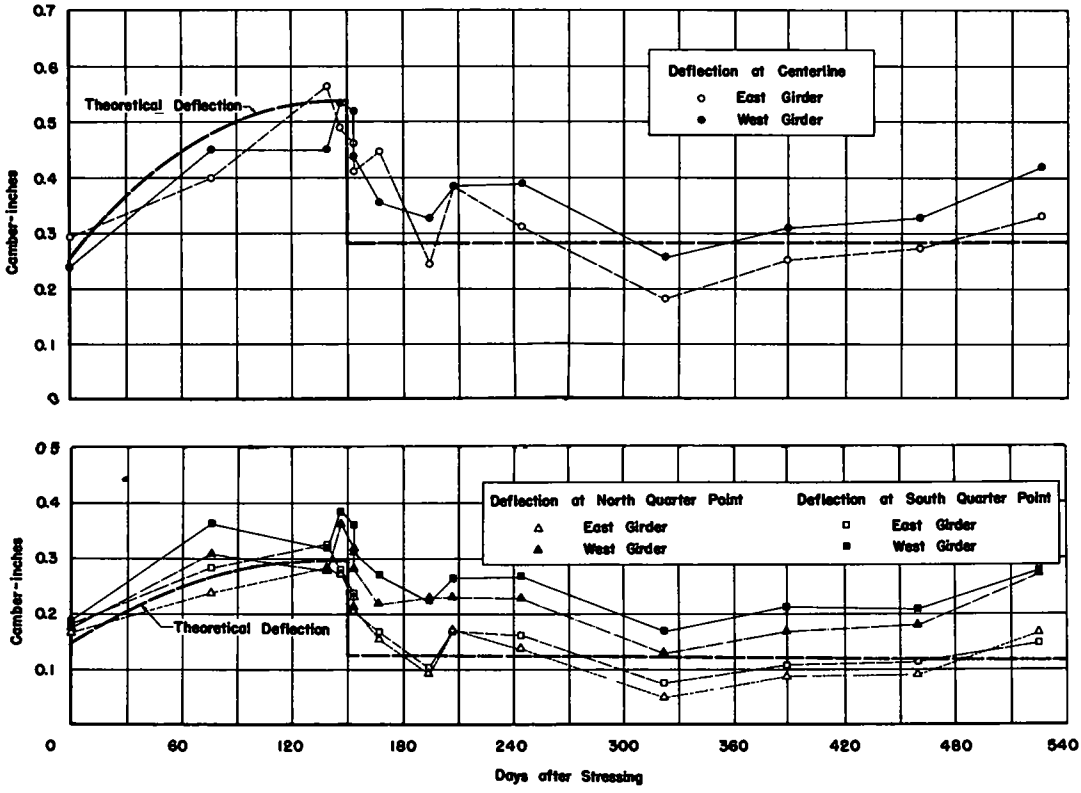

Figure 9. Girder deflections.

indicated that the shores yielded somewhat, thus preventing development of full continuity. Thus it is apparent that if this technique is to be used successfully, careful attention to minor construction details is imperative.

The final variable affecting deflections is the effect of differential shrinkage between the cast-in-situ slab and the original girders. The approximate magnitude of this effect was calculated by assuming that because the girders restrain shrinkage in the slab, tensile stresses will be produced in the slab along the slab-girder junction. Inasmuch as these stresses would be relieved by local cracking, their average value would be one-half of the tensile capacity of concrete. Assuming 250 psi for this value, an effective force equal to this average stress over the slab cross-section was computed and assumed to act at the slab centroid. The resulting moment about the centroid of the composite section was computed, and the shrinkage deflection at the centerline was calculated as 0.088 in. It appears likely that this factor accounts for at least a portion of the deflection noted in the period between 153 and 322 days after stressing.

CONCRETE STRAIN MEASUREMENT

Because it was possible to measure the concrete strains at several sections of the girders after the stressing of each tendon was completed, additional information as to the behavior of the members during the post-tensioning operation was obtained. The theoretical stress distributions were computed on the assumption that the girder behavior was in accordance with the generally accepted elastic theory. These computed stresses were then transformed into equivalent strains using $E_c = 5,300,000$ psi as found in the companion test program. Values were calculated for the stress and strains with:

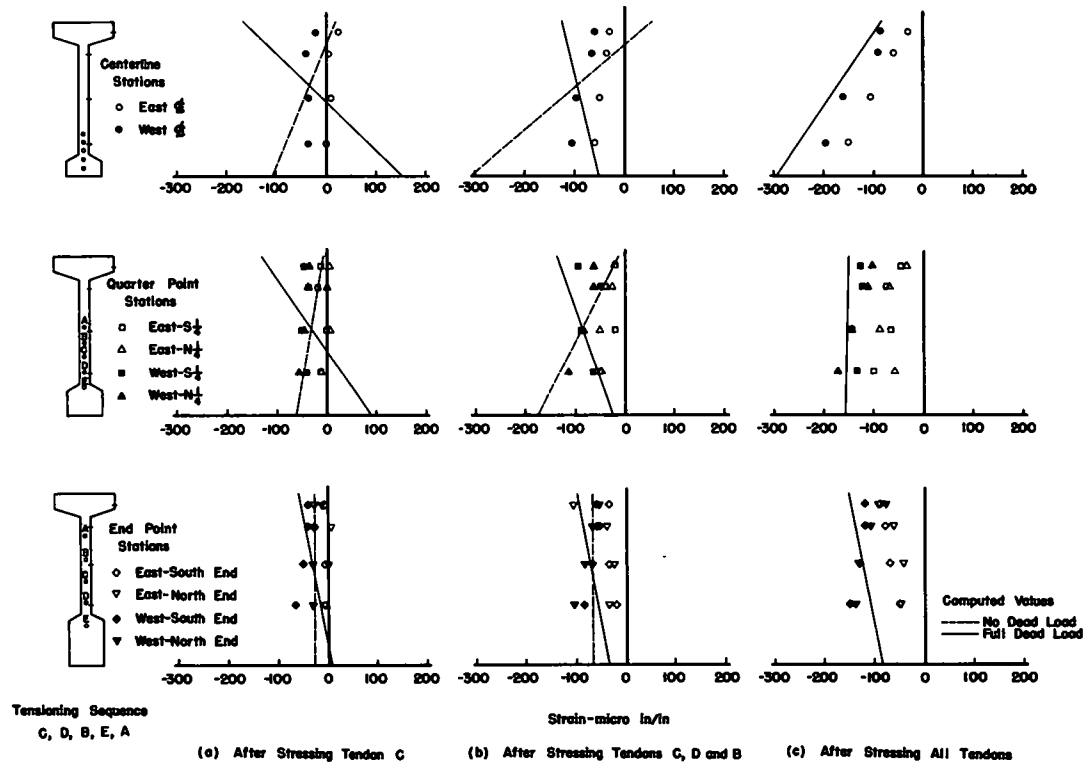

Figure 10. Prestress strain profiles.

1. Tendon C stressed — no dead load acting;
2. Tendon C stressed — full dead load acting;
3. Tendons B, C, and D stressed — no dead load acting;
4. Tendons B, C, and D stressed — full dead load acting; and
5. Tendons A, B, C, D, and E stressed — full dead load acting.

The computed strain profiles are shown in Figure 10 together with the corresponding measured strains.

It is apparent that the measured strains for the west girder are in much better general agreement with the theoretical strain profiles than the measured strains for the east girder. A slight lateral bowing of the east girder was noted during the post-tensioning operation, and it is possible that the resulting secondary strains modified the values of the principal longitudinal strains. Another possible explanation for the discrepancy is that in some way the effective prestress force applied to the west girder was greater than the force applied to the east girder. The stressing procedures were identical in nature; discrepancies noted were minor and the observed vertical movements of both girders were in reasonably good agreement. It should be observed that, in general, the measured strain profiles after partial stressing of the girders fell between the computed strain profile for the case of zero dead load and the profile based on the full dead load acting. Thus, it appears that an increasing portion of the dead load was effective for each prestress increment, even though the exact amount could not be ascertained. It should be noted that no significant tensile stresses due to dead load were developed during the stressing operation because the soffit forms provided partial support until the full dead load was transferred to the stressed tendons.

After completion of the prestressing, further strain measurements were taken before and after all major construction operations and on an intermittent time schedule after final completion of the bridge. Typical examples of the observed strain profiles are shown in Figures 11, 12, and 13. These measurements confirm Navier's hypothesis

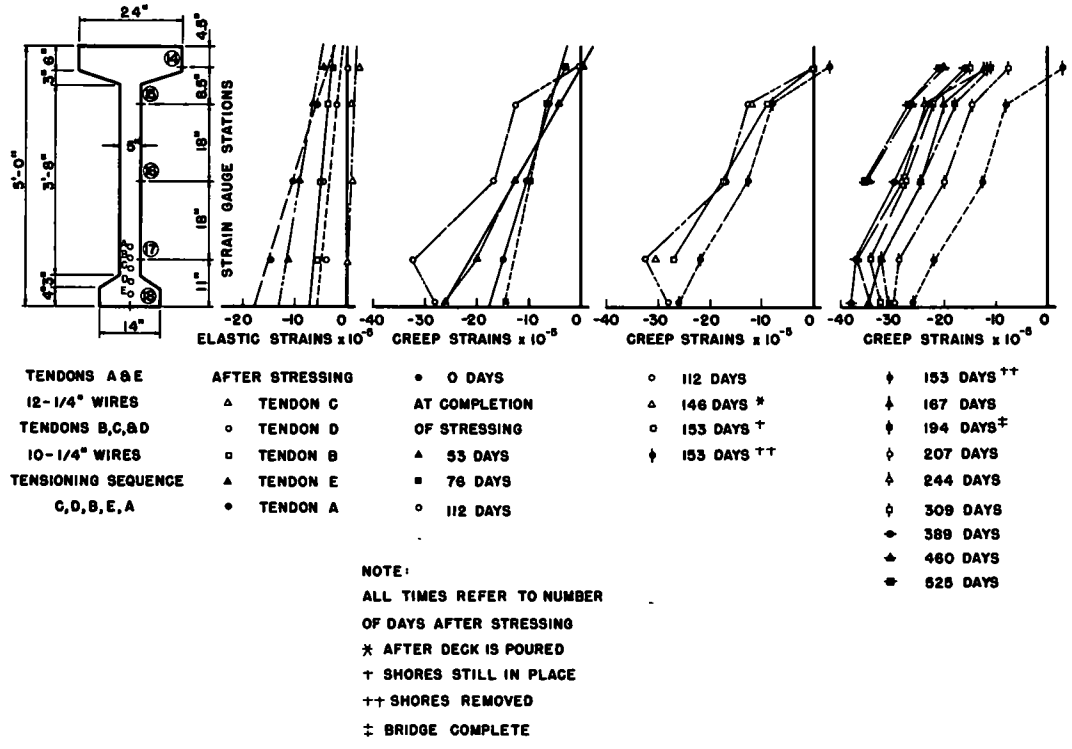

Figure 11. Strain profile at center of east girder.

because it can be seen that the observed strain distributions were reasonably linear and remained linear even after considerable inelastic deformation.

In general, the longitudinal strain measurements subsequent to post-tensioning reflected principally the effect of creep and shrinkage and, to a lesser extent, the effect of the composite action. Because the stress and, hence, the strains produced by placement of the deck slab and of the hand railing were of a comparatively small magnitude, it was difficult to correlate in anything more than a general way the observed readings with the computed data. Although the girder strains were relatively unaffected by the placement of the slab, and all stations showed the influence of a positive bending moment on removal of the shores, there apparently was an almost immediate strain recovery following this construction operation because the strain readings returned to the same general pattern that they had been following. It may be concluded that for materials subjected to appreciable inelastic deformations, the effects of additional small elastic deformations are quickly suppressed by the inelastic effects so that it becomes almost impossible to separate the effects of the elastic and inelastic properties.

The longitudinal strain measurements also tend to emphasize the reduction of the inelastic effects of creep and shrinkage with time. It may be observed that the major portion of the inelastic changes took place during the first year after stressing and that subsequent changes were a great deal smaller. This result is in accordance with accepted theories of creep and shrinkage.

STRAIN MEASUREMENTS IN THE DECK SLAB

The inclusion of strain gaging stations in the deck slab provided an opportunity to evaluate the effectiveness of composite action between the girders and the slab and also to observe the magnitude of differential shrinkage present. The variation of the longitudinal strains along the centerline of the bottom surface of the cast-in-situ slab

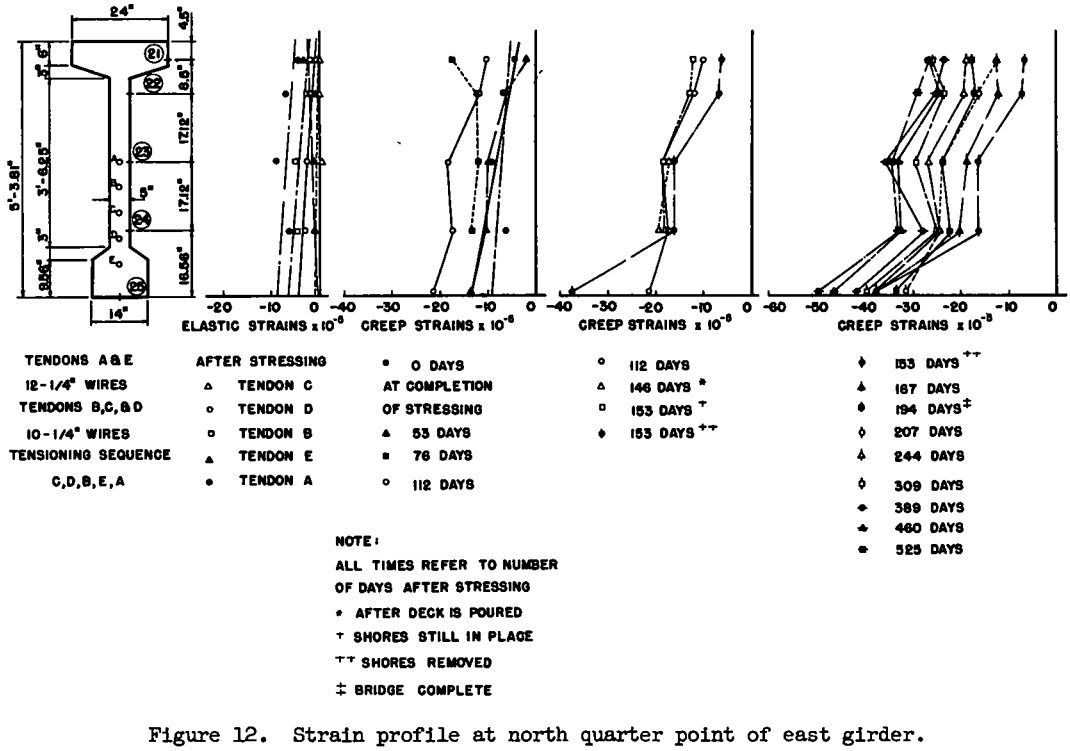

Figure 12. Strain profile at north quarter point of east girder.

are plotted in Figure 14. It should be noted that immediately on removal of the shores (153 days after stressing of the main girders and 7 days after pouring of the cast-in-situ slab) all of the stations along the centerline of the lower surface of the deck slab indicated tensile strain. At the corresponding points on the top surface, the slab was subjected to compression. According to conventional elastic theory, all stations should have registered compressive strain on removal of the temporary shores, because the centroid of the composite section lies below the bottom surface of the deck slab. This discrepancy may be due to localized bending in the longitudinal direction coupled with larger localized transverse bending of the slab due to unequal deflection of the two girders on removal of the shores. However, because no positive explanation was noted, the applicability of conventional composite action theory in this case is therefore questionable.

The effects of shrinkage of the cast-in-situ slab became immediately apparent, however, because subsequent readings at all stations indicated compressive strains which grew in magnitude with a diminishing time relationship. It is extremely interesting to note that the magnitude of the observed strains after 500 days is in very close agreement with the predicted value of 195 microinches per in. which was obtained from a series of shrinkage tests on prisms cast from the same concrete as the deck slab (1).

GENERAL SUMMARY

This report describes a program for a field study of the behavior of a prestressed concrete pedestrian overpass. The purpose of this study was to develop information which might be useful in the design and construction of future prestressed concrete structures. The field study was accompanied by a companion test program to determine the physical characteristics of the materials used in the actual construction. The results of the test on the samples of steel used in the tendons indicated substantial agreement with the elastic properties claimed by the manufacturer. However, field measurements and tests on samples of the concrete used in the girders indicated sizeable differences in the quality of the concrete used in various parts of the girder. These differences made the correlation of observed and theoretical values, influenced by such factors as the modulus of elasticity, extremely difficult.

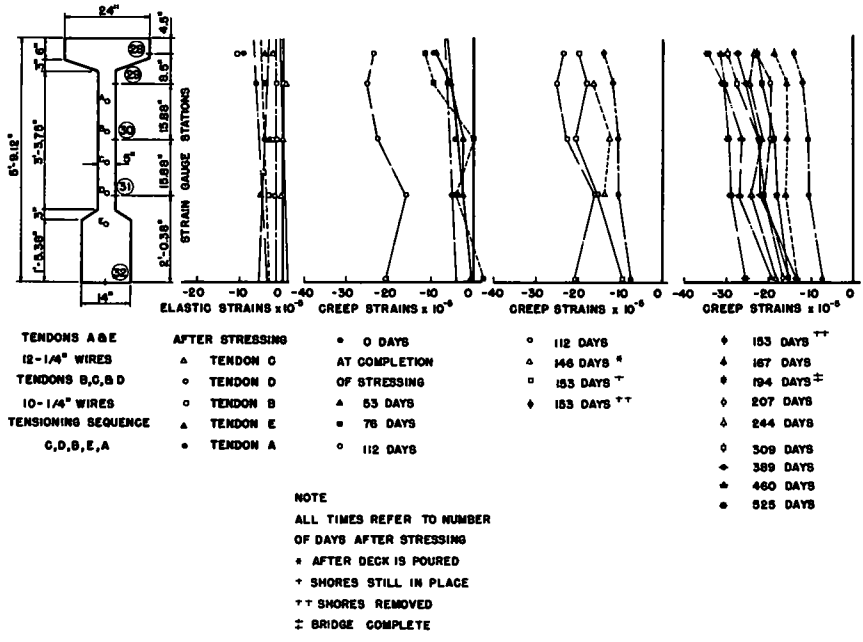

Figure 13. Strain profile at north end of east girder.

Jack pressure and tendon elongation measurements made during the post-tensioning operation indicate that the girders may have been slightly overstressed, due to the fact

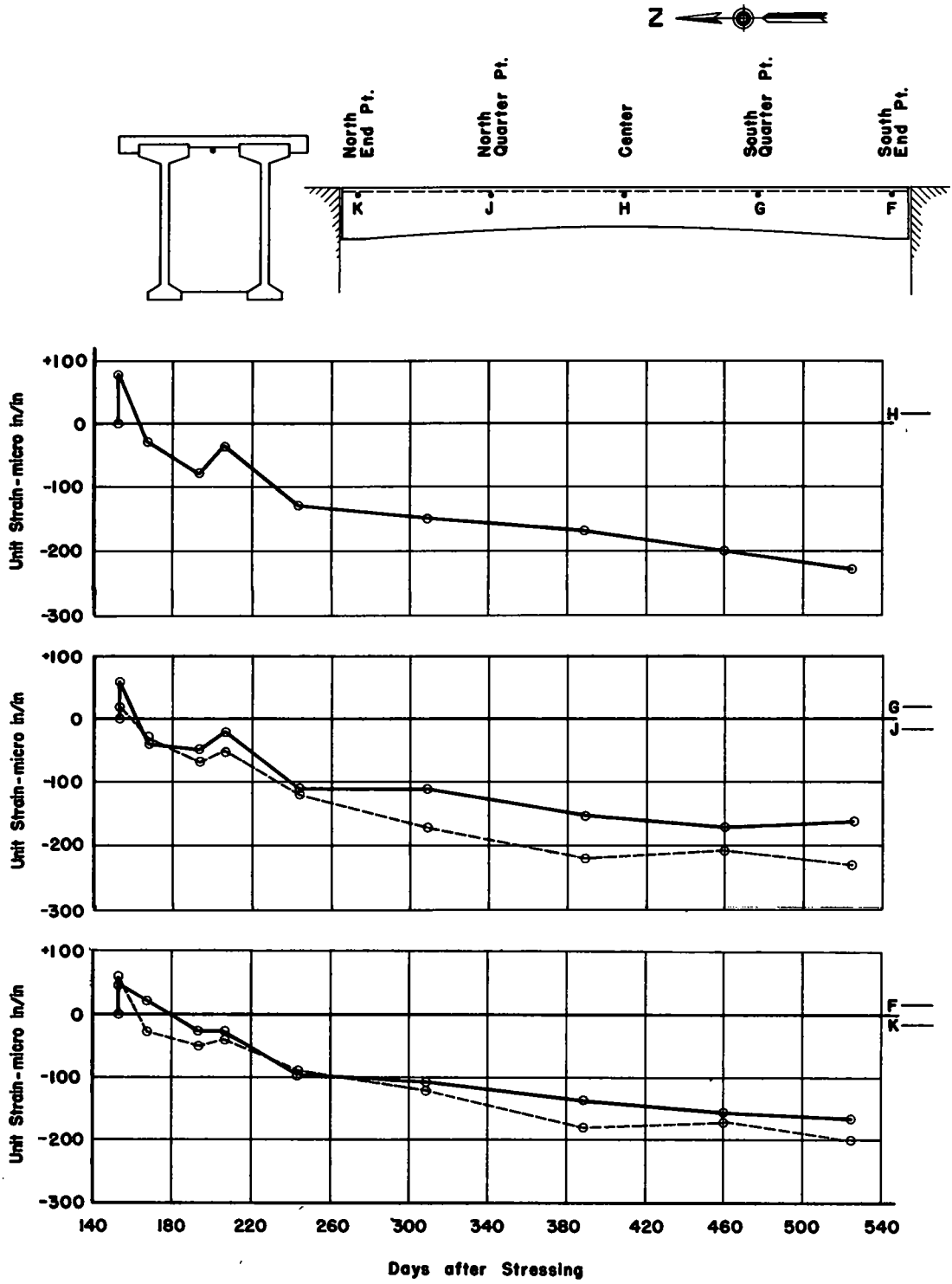

Figure 14. Strains in bottom of deck slab.

that the frictional characteristics of the tendons were not considered. The magnitude of the prestressing force was controlled by measurement of tendon elongation; the observed force, based on the hydraulic jack calibration, was used for reference purposes only. The analysis of the observed strains and deflections during the post-tensioning operation was found to be complicated by the uncertainty involved in the transfer of the girder dead load from the soffit form to the tendons. It is significant to note, however, that no appreciable tensile strains were measured at any section of the girder during the post-tensioning operation. Even though small tensile strains were noted after the stressing of the first tendon, these strains were reversed on the application of additional prestress.

The deflection measurements during the period in which the cast-in-situ slab was placed, revealed that the construction procedure used introduced strains and deflections which were not considered in the design assumptions. The assumption made was that continuity would be developed for the dead load of the slab only. However, in setting up the slab and diaphragm forms and prior to the placing of the deck slab, the girders were realigned by means of crossed wires to permit leveling of the forms. This construction practice resulted in the shifting of a portion of the load from one girder to the other girder. Furthermore, the deflection profiles indicated that the girder elevations decreased at the support points between the time of placing of the concrete and the removal of the shores. This decrease indicated that the shores yielded under the load of the cast-in-situ slab, and hence, a loss of continuity occurred.

Development of composite action between the cast-in-situ deck slab and the precast girders was confirmed by the observed deflection measurements. The measured deflections were in much closer agreement with the predicted values for composite action than they would have been had no composite action been assumed. The effectiveness in reducing the dead load deflections and in equalizing small discrepancies in initial camber of the prestressed girders by shoring the girders before placing of the deck slab was established. Finally, the time-dependent behavior of the structure was found to be predictable from a consideration of the material properties and the applied loads. With proper assessment of the tendon losses, due to such factors as elastic shortening, shrinkage, creep of the concrete, and relaxation of the steel, the deflection of a structure at any given time may be estimated by

$$\Delta_t = C_t \left(\frac{\Delta_{F_0} + \Delta_{F_t}}{2} + \Delta_{DL} \right) + \Delta_{AL} \qquad (10)$$

The deflection components used in Eq. 10 may be calculated by the conjugate beam method. Using the measured values of the prestress force and the elastic modulus, and with the moment of inertia based on the gross concrete section, the deflections predicted by Eq. 10 were found to be in good agreement with the observed values. The effect on the deflection of the differential shrinkage between the concrete in the girders and that in the cast-in-situ slab was found to be one of the most difficult variables to assess. An approximate method for evaluating this factor was developed, and although the measured deflections tended to confirm the theory, it was not conclusively proven.

CONCLUSIONS AND RECOMMENDATIONS

Although the test program was extremely limited in nature, because in effect it involved only the use of a single test specimen, the following conclusions are believed to be warranted:

1. The over-all behavior of the structure was found to be in reasonable agreement with the design assumptions used in general elastic theory.
2. The actual effective tendon force was approximately 10 percent higher than the design value due to the effect of tendon wobble and friction.
3. The assumption that the tendon losses may be approximated as 15 percent of the initial prestress force was confirmed by a comparison of the measured deflection with the calculated values based on the actual properties of the materials used in the structure.

4. The technique of providing temporary shores for the girders during the placing and curing of the cast-in-situ slab was found to be effective in developing composite action before transfer of the slab dead load and in equalizing minor differences in the camber of the precast girders. However, it was noted that careful attention to construction details is required to insure that the designer's assumptions will be fully justified.

ACKNOWLEDGMENTS

The work reported herein was supported by the Missouri State Highway Commission and by the Bureau of Public Roads under a cooperative research agreement. The assistance of the personnel of District 6 of the Missouri State Highway Department in facilitating the field operations was greatly appreciated. Also the assistance of James M. Belling, Malise J. Graham, and Phillip H. Huff, graduate research assistants, in the performance of the testing and in the reduction of the data is gratefully acknowledged.

REFERENCES

1. Pauw, A., and Breen, J. E., "Field Testing and Analysis of Two Prestressed Concrete Girders." Bull. 46, Univ. of Missouri, Engineering Experiment Station (1959).
2. Lin, T. Y., "Prestressed Concrete Structures." Wiley (1955).
3. Cooley, E. H., "Friction in Post Tensioned Prestressing Systems." Research Report I, Cement and Concrete Association, London (1953).
4. Troxell, C. E., and Davis, H. E., "Composition and Properties of Concrete." McGraw-Hill (1956).

THE NATIONAL ACADEMY OF SCIENCES—NATIONAL RESEARCH COUNCIL is a private, nonprofit organization of scientists, dedicated to the furtherance of science and to its use for the general welfare. The ACADEMY itself was established in 1863 under a congressional charter signed by President Lincoln. Empowered to provide for all activities appropriate to academies of science, it was also required by its charter to act as an adviser to the federal government in scientific matters. This provision accounts for the close ties that have always existed between the ACADEMY and the government, although the ACADEMY is not a governmental agency.

The NATIONAL RESEARCH COUNCIL was established by the ACADEMY in 1916, at the request of President Wilson, to enable scientists generally to associate their efforts with those of the limited membership of the ACADEMY in service to the nation, to society, and to science at home and abroad. Members of the NATIONAL RESEARCH COUNCIL receive their appointments from the president of the ACADEMY. They include representatives nominated by the major scientific and technical societies, representatives of the federal government, and a number of members at large. In addition, several thousand scientists and engineers take part in the activities of the research council through membership on its various boards and committees.

Receiving funds from both public and private sources, by contribution, grant, or contract, the ACADEMY and its RESEARCH COUNCIL thus work to stimulate research and its applications, to survey the broad possibilities of science, to promote effective utilization of the scientific and technical resources of the country, to serve the government, and to further the general interests of science.

The HIGHWAY RESEARCH BOARD was organized November 11, 1920, as an agency of the Division of Engineering and Industrial Research, one of the eight functional divisions of the NATIONAL RESEARCH COUNCIL. The BOARD is a cooperative organization of the highway technologists of America operating under the auspices of the ACADEMY–COUNCIL and with the support of the several highway departments, the Bureau of Public Roads, and many other organizations interested in the development of highway transportation. The purposes of the BOARD are to encourage research and to provide a national clearinghouse and correlation service for research activities and information on highway administration and technology.